Alma Mater Studiorum - Università di Bologna

DOTTORATO DI RICERCA IN

CHIMICA

Ciclo 35

Settore Concorsuale: 03/A1 - CHIMICA ANALITICA

Settore Scientifico Disciplinare: CHIM/01 - CHIMICA ANALITICA

ANALYTICAL APPROACHES FOR THE MEASUREMENT OF SULFIDE IN BIOLOGICAL AND PHARMACEUTICAL FIELDS

Presentata da: Nan Zhang

Coordinatore Dottorato

Luca Prodi

Supervisore

Pierluigi Reschiglian

Co-supervisore

Daniele Fabbri

Esame finale anno 2023

Table of Contents

Abstract

Hydrogen sulfide (H_2S) is a widely recognized gasotransmitter, with key roles in physiological and pathological processes. The accurate quantification of H_2S and reactive sulfur species (RSS) may hold important implications for the diagnosis and prognosis of various diseases. However, H_2S species quantification in biological matrices is still a challenge. Among the sulfide detection methods, monobromobimane (MBB) derivatization coupled with reversed phase high-performance liquid chromatography (RP-HPLC) is one of the most reported. However, it is characterized by a complex preparation and time-consuming process, which may alter the actual H_2S level. Moreover, quantitative validation has still not been described based on a survey of previously published works. In this study, we developed and validated an improved analytical protocol for the MBB RP-HPLC method. Main parameters like MBB concentration, temperature, reaction time, and sample handling were optimized, and the calibration method was further validated using leave-one-out cross-validation (CV) and tested in a clinical setting. The method shows high sensitivity and allows the quantification of H_2S species, with a limit of detection (LOD) of 0.5 µM and a limit of quantification (LOQ) of 0.9 µM. Additionally, this model was successfully applied in measurements of H_2S levels in the serum of patients subjected to inhalation with vapors rich in H_2S.

In addition, a properly procedure was established for H_2S release with the modified MBB HPLC-FLD method. The proposed analytical approach demonstrated the slow-release kinetics of H_2S from the multilayer Silk-Fibroin scaffolds with the combination of different H_2S donor's concentration with respect to the weight of PLGA nanofiber.

In the end, some efforts were made on sulfide measurements by using size exclusion chromatography fluorescence/ultraviolet detection and inductively coupled plasma-mass spectrometry (SEC-FLD/UV-ICP/MS). It's intended as a preliminary study in order to define the feasibility of a separation-detection-quantification platform to analyze biological samples and quantify sulfur species.

Keywords: **Hydrogen sulfide pool; Biomarkers; High performance liquid chromatography with fluorescence; Monobromobimane; Sulfur species; Method validation; Silk Fibroin scaffold; GYY4137; SEC-FLD/UV-ICP/MS;**

Chapter 1. Optimization and validation of a monobromobimane (MBB) derivatization and RP HPLC-FLD detection method for sulfur species measurement in human serum after sulfur inhalation treatment

1.1 Introduction

1.1.1 General physical and chemical characteristics of H_2S

Hydrogen sulfide (H_2S) is investigated and characterized as a colorless, flammable, water-soluble gas with the rotten egg smell. It is heavier than air (d = 1.19) with a molecular weight of 34.08 and burns in air with a blue flame emission. H_2S is slightly soluble in aqueous solution at ambient temperature, one gram of H_2S will dissolve in 242 mL of H_2O at 20 ℃, and it can yield as different species, such as hydrosulfide anion (HS^-) and sulfide anion (S^{2-}). By this means, H_2S acts as a weak diprotic acid with two dissociation constants, pK_a^{H2S} of 7.04 and pK_a^{HS-} of 11.96, respectively. The indicated equations determine the relative ratios of protonation forms at actual pH values [1, 2]. See equations (1)-(4) in **Figure 1.1**. In addition, H_2S is highly soluble in water (~80 mM) when temperature is raised to 37 °C and it can easily penetrate the lipid bilayer of biological membranes with two-fold higher concentration than water without a transporter. The partition coefficients (Kp) were found to be around 1.9 – 2.1 fold in liposome membranes relative to water [3].

$$H_2S \overset{pK_a^{H_2S} = 7.04}{\rightleftharpoons} H^+ + HS^- \quad (1)$$

$$K_a^{H_2S} = [HS^-][H^+]/[H_2S] \quad (2)$$

$$HS^- \overset{pK_a^{HS-} = 11.96}{\rightleftharpoons} S^{2-} + H^+ \quad (3)$$

$$K_a^{HS-} = [S^{2-}][H^+]/[HS^-] \quad (4)$$

Figure 1.1 Dissociation forms of volatile H_2S at different pH conditions.

Currently, it's been widely known that the stability of undissociated form of H_2S is the greatest under acidic conditions, and it exists as the volatile H_2S. Conversely, since the physiological pH level in blood is about 7.4, approximately one-third of H_2S exists as the volatile H_2S and two-thirds as the HS^-. When at pH conditions higher than 7.4, similarly, H_2S is primarily found

in the form of HS^- in biological systems, but gaseous H_2S and sulfide anion S^{2-} are still present, respectively, at low and at negligible concentration levels as the dissociation of HS^- to S^{2-} occurs almost exclusively at very high pH values. Thus, sometimes, it is considered that S^{2-}, nearly does not exist in commonly aqueous alkaline solutions of inorganic polysulfides, sodium hydrosulfide (NaHS) and sodium sulfide (Na_2S) reagents, which were widely utilized as a source of exogenous sulfide in a few published research literatures.

In this present study, term of 'H_2S species' mentioned is collectively used to refer to all three species forms including the diprotonated (H_2S), monoanion (HS^-) and dianion (S^{2-}) that disperse in aqueous solution. Generally, the term H_2S species is used in the case of biological samples and H_2S in the case of gas samples. What's more, it is not possible to separate the effects of gaseous H_2S and HS^- on physiological functions and signaling processes since these species coexist at physiological conditions in cells and in circulation [4]. Definition and interconversion of these compounds will be introduced in detail in the next section.

1.1.2 Toxicity of H_2S: Is H_2S a foe or friend?

Historically, it's been three hundred years since the first description of hydrogen sulfide toxicity by Ramazzini, in 1713 [5]. But for more than a century, H_2S has been previously regarded as a toxic gas in earlier studies, and it was a potential industrial and environmental health hazard. Until the 1990s, the explosive research on H_2S was focused on mechanisms of H_2S toxicity and most studies about toxic effects of this molecule have been further investigated. In addition, several studies devoted to the toxicity of H_2S to humans have been published in the last decades [6-8]. Besides, in the view of Milby et al. [9], the majority of the data presented in previous reviews continues to be valid, but some issues deserve further clarification. So, elucidation of some controversial issues related to H_2S poisoning has been discussed and it indicated that the determination of sulfide in biological specimen can be useful in corroborating a diagnosis of H_2S toxicity utilizing urine, blood, and tissue analyses. However, it should be noted that the extent of toxicity for this molecule is mostly driven by the sulfide concentration levels. That means degree of damage having more to do with exposure concentration of H_2S which would result in various physiological responses to humans. It is extremely toxic and quickly causes death to humans in elevated concentrations (> 500 ppm (~15 mM)). Even long-term exposure

to H_2S in lower concentrations (> 50 ppm) can cause adverse effects, such as conjunctivitis. But if exposure is transient, as usually happens in the oil patch, recovery may be equally rapid and apparently complete in functional terms. **Table 1.1** shows approximate thresholds for the major physiological effects to human exposure to H_2S.

Table 1.1 Toxic effects of H_2S exposure to human with increasing concentration in air.

H_2S concentration in air (ppm)	**Physiological responses**
0.01-0.3	Odor threshold
1 – 5	Moderate offensive odor
10	Obvious unpleasant odor
20	Odor very strong
20 – 50	Conjunctives and lung irritation
100 – 150	Eye irritation, olfactory paralysis, odor disappears
200 – 300	Pulmonary edema may occur
500 – 1000	Loss of consciousness, cessation of respiration and death

Due to the physiological effects occurring with the accumulation of H_2S in humans, it is, therefore, significant to understand the pathways involved in H_2S metabolism and detoxification. So far, the metabolism of H_2S can be divided into three main pathways, including oxidation to sulfate, methylation, and reaction with metallo- or disulfide-containing proteins. Apart from complexation of H_2S with methemoglobin to form sulfmethemoglobin has been found to apparently detoxification. The third metabolic pathway is largely responsible for the toxic character of H_2S which contains the reactions of H_2S with essential metalloproteins. Collectively, metabolic pathways primarily contributed to the toxicity profile of H_2S were shown in **Figure 1.2**.

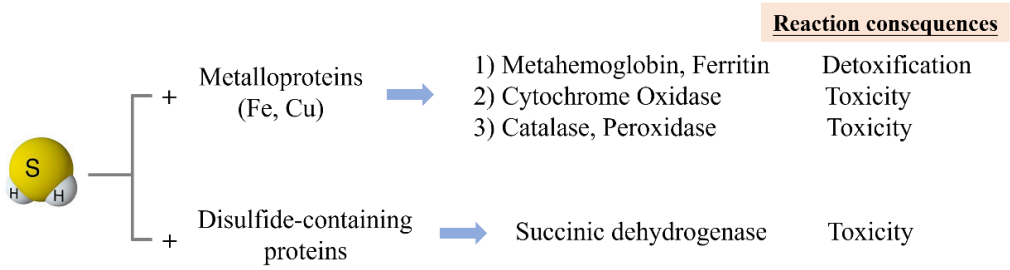

Figure 1.2 Metabolic pathways primarily responsible for the toxicity profile of H_2S.

As we all know, H_2S has been proved to play a similar manner to hydrogen cyanide (HCN), causing anoxia at the cellular level attributed to the toxicity of H_2S. The primary mechanism

for the toxic action of H_2S is the ability to direct inhibition of the activity of a kind of metal-containing enzyme in the mitochondrial respiratory chain, namely cytochrome c oxidase [6, 10, 11]. Meantime, the small molecular H_2S has the potential to reduce disulfide bridges in proteins. This reaction has been proposed as a basic mechanism for H_2S inhibition of succinic dehydrogenase, then toxicity reaction consequences occurred, whereas the toxic consequences of inhibition of enzymes like catalase and peroxidase have not been completely explored. In addition, it's necessary to mention that Truong and co-workers [7] reported that the molecular mechanism of H_2S cytotoxicity also involves the formation of reactive sulfur species (RSS), which depletes glutathione (GSH) and activates oxygen to form reactive oxygen species (ROS). It's demonstrated as another important mechanism contributing to H_2S-induced cytotoxicity.

1.1.3 Generation of endogenous H_2S through enzymatic and non-enzymatic pathways

Endogenous H_2S is synthesized and degraded by mammalian tissues at relatively high rates [12], and is detectable in blood circulation [13]. It is endogenously produced by mammalian cells mostly via enzymatic pathways, while only a small part is produced by non-enzymatic pathways [14]. H_2S is mainly formed as a byproduct in mammalian cells from sulfur-containing amino acids (SAAs), like methionine, cysteine or homocysteine, which are the main precursors for the enzymatic generation of H_2S via the trans-sulfuration pathway enzymes. The enzymatic reactions were catalyzed by three main enzymes, cystathionine β-synthase (CBS), cystathionine γ-lyase (CSE), and 3-mercaptopyruvate sulfur transferase (3-MST). Therein, enzymes of CBS and CSE contributed to the majority of the endogenous produced H_2S in mammalian tissues and may also produce RSS metabolites besides H_2S. Then, after the conversion of methionine to homocysteine, CBS is required to form cystathionine from homocysteine whereupon CSE converts cystathionine to L-cysteine, the latter being the key substrate in the generation of H_2S as shown in **Figure 1.3**. Among these three enzymes, homocysteine is converted into cystathionine and cysteine in turn by sulfur transfer under the catalysis of CBS and CSE. Cysteine and thiols are catalyzed by CBS via β-substitution. Different from CBS, CSE catalyzes three kinds of reactions, including the *α,β*-cleavage of cysteine, the α,γ-cleavage of homocysteine, and the γ-substitution of homocysteine through a second mole of homocysteine. In addition to this enzymatic pathway of H_2S generation, a non-enzymatic mechanism for H_2S

release from the sulfur-containing amino acids, specifically cysteine and homocysteine, catalyzed by iron (Fe^{3+}) and Vitamin B6, has been recently characterized and may contribute to sulfide homeostasis under certain physiological conditions [15].

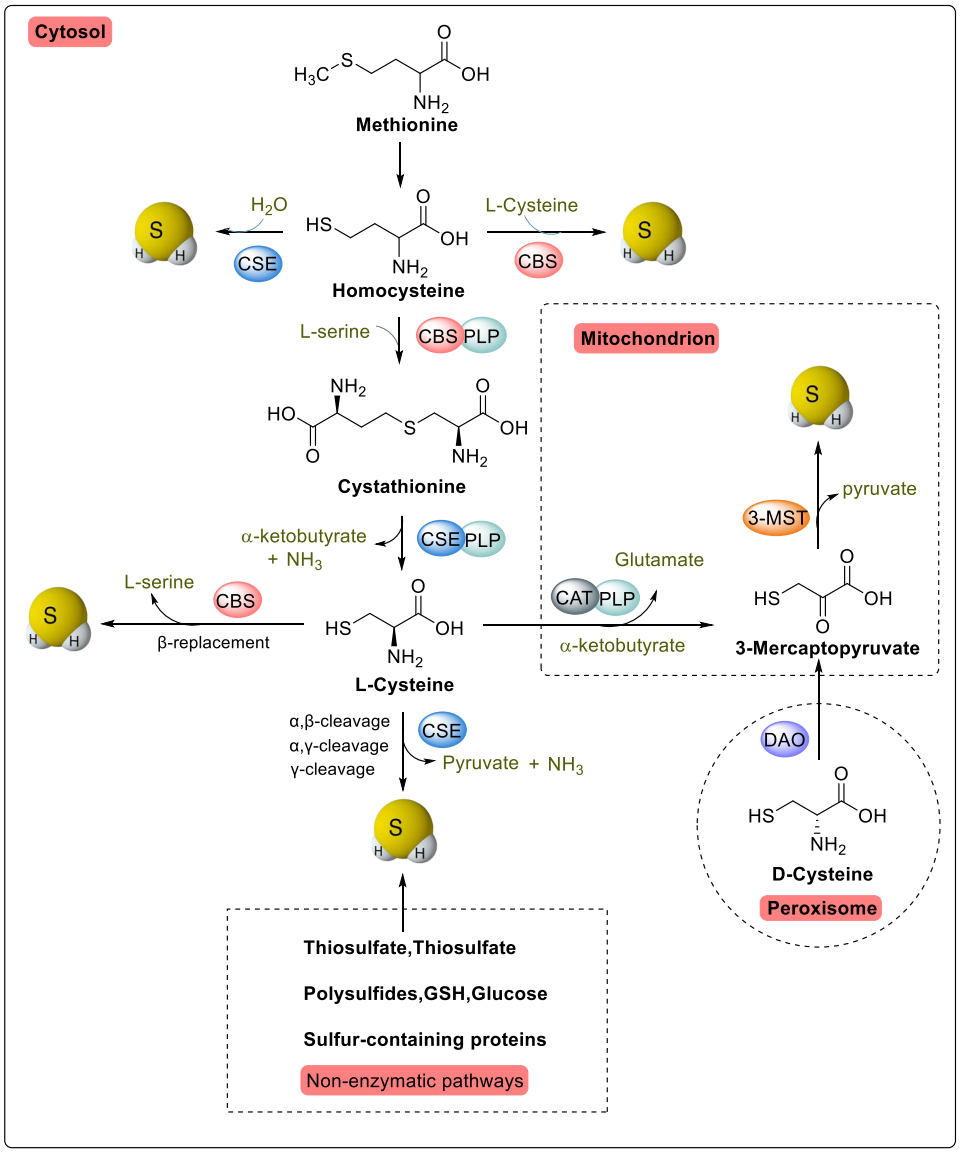

Figure 1.3 Endogenous production of H_2S in mammalian tissues through enzymic and non-enzymic pathways.

The enzymatic activities of CSE and CBS, while miscellaneous in terms of substrates and yields, require the pyridoxal phosphate (PLP) cofactor form of Vitamin B6 (VitB6) in *α,β*-elimination or *β*-replacement of SAAs thiol group to generate H_2S, through the trans-sulfuration pathway [16]. Notably, PLP is not required for 3-MST function, it is involved its upstream enzyme cysteine aminotransferase (CAT) to transfer cysteine into 3-mercaptopyruvate, which serves as substrate for 3-MST to finally produce eventual H_2S [17]. Thus, enzymatic production of H_2S

from SAAs in mammalian tissues is partly dependent on PLP, and a small portion of endogenous H_2S is derived via nonenzymatic reduction. Additionally, in the presence of reducing equivalents such as NADPH and NADH, reactive sulfur species in persulfides, thiosulfate and polysulfides, also glucose, GSH, sulfur-containing proteins are reduced into H_2S and other metabolites. Of particular note, in contrast to enzymatic synthesis pathways, endogenous production of H_2S through non-enzymatic processes in mammalian cells is not well understood to date. Specifically, D-Amino acid oxidase (DAO) can also produce achiral α-keto acids, including 3-mercaptopyruvate (3-MP), from D-amino acids, some of which are found in mammalian tissues by Kimura's group recently [18]. DAO is localized to peroxisomes, whereas 3-MST is mainly found in mitochondria. Metabolite exchanges between peroxisome and mitochondria can import 3-MP into mitochondria where it is further catalyzed into H_2S by 3-MST. Mitochondria and peroxisomes, which are essential cellular organelles in mammals, exchange various metabolites as well as enzymes via a specific form of vesicular trafficking, and are usually in close proximity to each other or have physical contact. So, 3-MST along with DAO can produce H_2S by the interaction of both organelles [18, 19]. Worthy to mention, as H_2S is an endogenous compound, a lot of preclinical animal studies are required for specific exogenous sulfide delivery systems before progression into human studies. Furthermore, synthetically developed H_2S-releasing compounds are another alternative as exploitation of 'sulfide–precursors' or 'prodrugs' that induce production of H_2S through metabolic pathway.

1.1.4 Metabolism of endogenous H_2S

Much has been discovered about the way in which H_2S is generated, but less is known about the metabolism of H_2S (see **Figure 1.4**). After synthesis by trans-sulfuration from L-cysteine, various metabolic pathways participate in the regulation of H_2S concentration in the cell. Significant pathways for H_2S metabolism include sulfide is oxidized in the mitochondrion by sulfide quinone oxidoreductase (SQR) to generate persulfide. Subsequently, persulfide is further oxidized to sulfite by ethylmalonic encephalopathy 1 protein (ETHE1) [16]. In addition, Olson and co-workers [20] proved that H_2S (or polysulfides) interact/react with superoxide dismutase (SOD) cysteines to affect catalytic activity. Thus, SOD oxidizes H_2S directly to produce polysulfides contribute to sulfide metabolism. Furthermore, H_2S reacts with

methemoglobin molecules containing metals or disulfides to form sulfhemoglobin and with proteins in the tissues in the form of bound sulfur pool, which might also eliminate H_2S and act as a metabolic sink for H_2S [14].

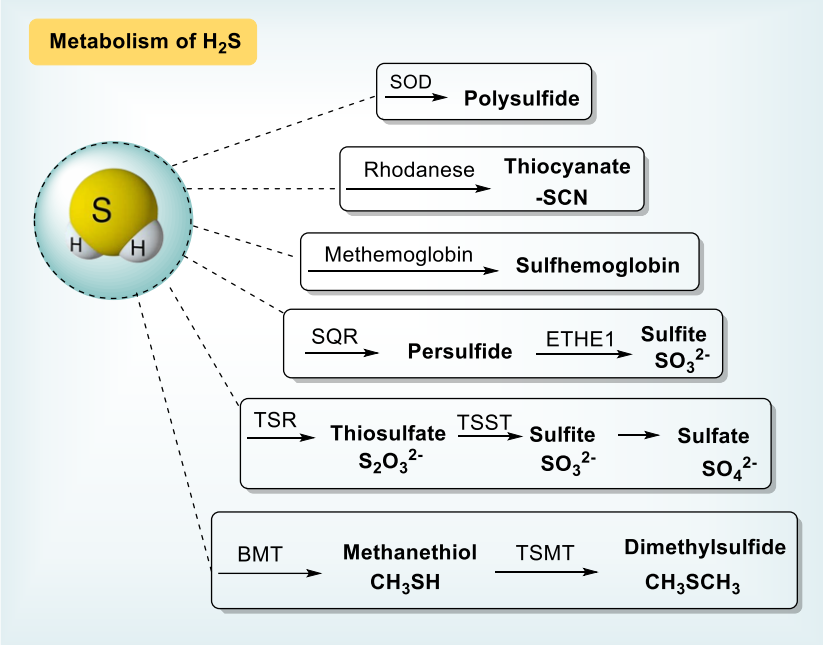

Figure 1.4 Metabolism of endogenous H_2S.

Besides, H_2S can further metabolize into thiosulfate ($S_2O_3^{2-}$) catalyzed by thiosulfate reductase (TSR) enzymes, then thiosulfate can rapidly oxidize to sulfite (SO_3^{2-}) through thiosulfate sulfurtransferase (TSST) and is subsequently converted to sulfate (SO_4^{2-}). Ultimately, H_2S is metabolized in mitochondria mainly in the form of thiosulfate or sulfate. In addition to the above oxidation pathway metabolism, H_2S can also undergo methylation by bisulfide methyltransferase (BMT) and thiol-S-methyltransferase (TSMT) to yield methanethiol (CH_3SH) and dimethylsulfide (CH_3SCH_3), and it is also as a substrate for rhodanese, accounting for the formation of thiocyanate (SCN^-). Multiple chemical and biochemical catabolic fates are probably still to be discovered and should be understood well.

1.1.5 (Patho-)physiological effects of H_2S in various biological systems

As mentioned above in paragraph 1.1.2, for many decades, H_2S has historically been regarded as a poisonous molecule and environmental hazard [6]. Besides, H_2S is an ancient metabolite with novel regulatory roles and many reviews focused on this topic over several years. Some approaches, in a few cases such as the use of chemical agents that actively remove sulfide from its sites of action to therapy were developed in preventing some of the adverse effect caused by

sulfide. However, it was not until the late 1900s that H_2S was discovered to be the third important gasotransmitter along with carbon monoxide (CO) and nitric oxide (NO) [21]. As a byproduct of the trans-sulfuration pathway, H_2S is gradually known for its pathophysiological roles in various tissues and organs and chemical signaling mechanisms of H_2S have received significant attention. So far, a growing body of evidence has gradually confirmed that H_2S can be an endogenously produced gaseous signaling thiol metabolite and plays an important role in various physiological and pathological processes recently [22-25]. Therein, three main signaling pathways nowadays included, thus, formation of persulfide and polysulfide, cross-reactivity with NO, and reactions with different metalloenzymes which has been mentioned in paragraph 1.1.2 [26]. In this paragraph, physiological roles and pathological considerations of H_2S will be mainly emphasized and thoroughly discussed. In **Figure 1.5**, it shows some representative roles played by H_2S in major organ systems in human.

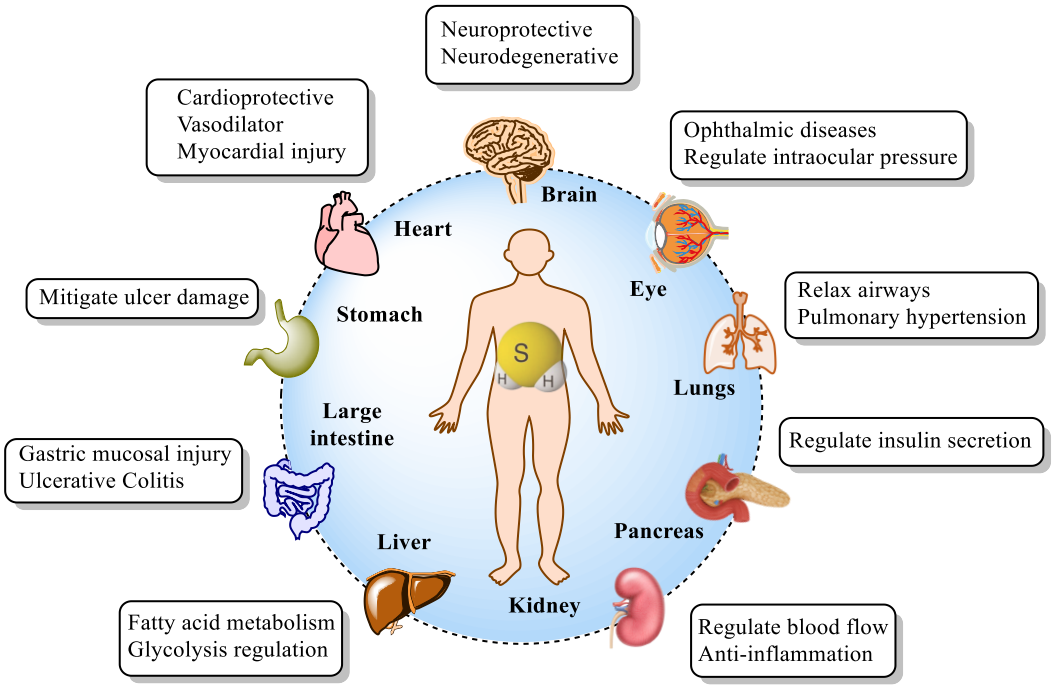

Figure 1.5 A schematic diagram showing some physiological and pathological roles of H_2S in major organ systems in human.

In previous survey, an outline of major milestones in H_2S research related to its neuroprotective potential mechanism in brain has been given by Kumar's group [27]. In addition, reviews accomplished by Kimura et al. [28-30] mainly focused on the physiological roles of H_2S and H_2S-derived polysulfides as signaling molecules and contribution to the discovery of these molecules and their metabolic pathways and mechanisms of action. Yang et al. [31] analyzed

the relationship between H_2S and some chronic diseases, including hypoxic pulmonary hypertension, myocardial infarction, ischemic perfusion kidney injury, diabetes, and chronic intestinal diseases. Furthermore, Aroca et al. [32] discussed the topic of H_2S: From a toxic molecule to a key molecule of cell life. The authors aim to highlight the importance of its crosstalk with other signaling molecules (like NO, CO, H_2O_2) and its participation of H_2S in many physiological and pathological processes in animals. Its fine regulation for the proper function of the cell and its survival were both described.

Some fundamental biological functions of H_2S also received substantial research interest in the last decades [33]. For example, neuromodulation [27, 34-39], insulin release [40-42], and the roles as a regulator in endocrine system [41, 42], renal physiology [43, 44], a modulator of gastrointestinal mobility [45-48], a regulator of reduction of IOP in glaucoma [49], and as an inhibitor of cancer cell growth [14, 50-53]. Moreover, H_2S is involved in the regulation of bone cell differentiation and was shown to play an anabolic role in various bone wasting conditions [54].

The functional role of H_2S at physiologically relevant concentrations in brain was gradually uncovered in early 1990s. The study by Awata et al. [55] in 1995 provided the enzymatic mechanisms for this endogenous H_2S in rat brain, in which activities of CBS and CSE in six different brain regions were detected though the activity of CBS was >30-fold greater than that of CSE. Abe et al. [37] reported that H_2S is expressed largely by the activity of CBS and CES in the hippocampus and cerebellum and it's present in a relative high level in the brain. These observations made it possible role of H_2S as an endogenous neuromodulator. The seminal studies by Kimura's group in the late 1990s [37] ushered in a new era of biological signaling mediated by H_2S. Kimura et al. [34] briefly reviewed recent progress in the study of H_2S as a novel physiologically active neuromodulator/transmitter in the brain based on the uncovered evidences that the brain contains relatively high concentrations of endogenous H_2S (50–160 μM).

It also should be emphasized that as the third gasotransmitter other than NO and CO, H_2S plays important physiological roles as a vasorelaxant exerting beneficial cardiovascular (CV) effects including cytoprotection [56-58], inflammation and anti-inflammation[59-63], angiogenesis

[64], vasodilation [26, 65, 66] and anti-atherogenic effect [67]. Stein et al. [68] especially presented the redox chemistry of H_2S and the main physiological actions it may cause, and several examples highlighting the cytoprotective functions of H_2S within the context of cardiovascular disease are also reported. Olson et al. examined the actions of H_2S derived from NaHS on isolated blood vessels and measured plasma H_2S concentration in trout. In the cardiovascular system as a gasotransmitter of H_2S [69-71], including those involved with smooth muscle relaxation [65, 72-74]. Liu et al. [75] reviewed in detail the effects of H_2S, especially in disease situations, and also the various underlying mechanisms on the cardiovascular system. Besides, atherosclerosis is a chronic progressive disease manifesting in clinical cardiovascular disease (CVD). It is a complex process involving endothelial dysfunction and vascular inflammation, among others. Noteworthy, Olas et al. [76] described how hydrogen sulfide may be used as therapeutic agent in the CVD. Cheung et al. [67] have shown that H_2S protects against atherosclerosis by CSE gene activation for the first time by reducing plasma lipid accumulation, inhibiting oxidative stress and plaque formation, and suppressing inflammation in vascular tissues via nuclear factor-kappa B (NF-kB) pathway. In the study,it provided direct evidence that H_2S is an important mediator in attenuating atherosclerosis formation, and up-regulation of CSE/H_2S pathway would be a potential target for therapeutic intervention against its formation. Calvert et al. [77] evaluated potential mechanisms of H_2S-mediated cardioprotection using an in vivo model of pharmacological preconditioning and reported H_2S mediates cardioprotection through nuclear factor erythroid 2-related factor 2 (Nrf2) signaling. Elrod et al. [58, 78] reported that hydrogen sulfide attenuates myocardial ischemia-reperfusion injury by preservation of mitochondrial function. The findings demonstrate that H_2S may be of value in cytoprotection during the evolution of myocardial infarction and that either administration of H_2S or the modulation of endogenous production may be of clinical benefit in ischemic disorders.

Ali et al. [79] revealed H_2S can be an early biomarker for metabolic response to acute myocardial infarction (AMI) by establishing a comparative metabolomics approach. In their work, a total of 68 metabolites were identified in serum samples from patients and healthy controls using GC/MS. Such an untargeted metabolomics approach provided greater coverage

of the metabolome and nineteen marker metabolites were identified in patients, all of them are considered as potential biomarkers. These findings indicate that metabolite profiling techniques can develop a detailed picture of the metabolic changes that occur in response to the disease. Hence, this can provide an opportunity to develop predictive biomarkers that will potentially allow for an earlier medical intervention.

Recently, there was suggestion that H_2S might play a role in gastrointestinal physiology. However, it has been demonstrated to play a role in maintaining the integrity of the gastrointestinal mucosa, inhibiting motility, and suppressing inflammation. This is leading to new avenues for therapeutics, in much the same way that knowledge of the surprising physiological roles of NO has and that of CO will do. Additionally, H_2S serves as a regulator of organ development and tissues homeostasis. An abnormal level is also found to be associated with ophthalmic diseases. Under physiological states, H_2S plays a critical role in regulation of intraocular pressure (IOP), protect retinal cells, inhibit oxidative stress and alleviate inflammation by modulating the function of intra or extracellular proteins in ocular tissues [49].

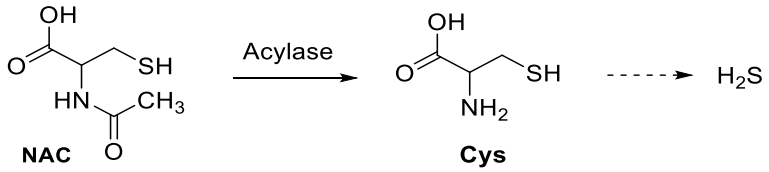

Figure 1.6 N-acetylcysteine (NAC) is converted to Cysteine (Cys) through a deacetylation reaction catalysed by acylase.

Recently, Citi et al. [59] reported the usefulness of some H_2S-donors for the function of acute lung anti-inflammatory and antiviral roles of H_2S. Worthy of mention, some preliminary clinical results suggested an inverse relationship between endogenous H_2S levels and severity of COVID-19. In the paper, the pharmacological basis for a potential beneficial role of H_2S against COVID-19 and the potential repurposing of H_2S donor drugs in the management of this disease are discussed. For example, N-acetylcysteine (NAC) is a renowned pharmacological antioxidant substance acting as a source of cysteine thereby promoting endogenous GSH biosynthesis as well as generation of sulfane sulfur species when desulfurated to H_2S shown in **Figure 1.6**. Furthermore, NAC can be as an antioxidant and disulphide breaking agent [80, 81]. Bourgonje et al. [82] revealed the possibility of increasing endogenous H_2S levels upon NAC

administration of high doses to many COVID-19 cases, and it has been demonstrating remarkable clinical improvement.

Based on various physiological functions played mentioned above, the mounting evidence of an significant part of the H_2S system in preclinical studies and in therapeutic applications has stimulated investigation of the correlations between H_2S normal/abnormal levels and the onset and the prognosis of certain diseases, including cardiovascular diseases [69, 83, 84], SARS-CoV-2 [85-87], diabetes [88, 89], osteoporosis [90]. Additionally, H_2S has been reported to participate in the pathogenesis of a variety of disorders, including chronic obstructive pulmonary disease (COPD) [91, 92], hypertension [93-96], hyperglycemia [97], colonic diseases [98] such as ulcerative colitis (UC) [99], aging and age-related pathologies [100, 101], Alzheimer disease (AD) and Down syndrome [102-104], Parkinson's Disease (PD) [105, 106], depressive disorders [107] etc..

The study conducted by Chen et al. [108] demonstrated that in patients with stable COPD, serum H_2S levels have been found to be significantly increased as compared to age-matched control subjects or those with acute exacerbation of COPD (AECOPD). What's more, serum H_2S levels were negatively correlated with the severity of airway obstruction in patients with stable COPD, whereas they were positively correlated with the lung function in all patients with COPD and healthy controls. It's suggested that endogenous H_2S may participate in the development of airway obstruction in COPD.

Data provided by Stefan et al. [99] supported a possible role of sulfide in the pathogenesis of ulcerative colitis (UC) and confirm the role of butyrate in the regulation of colonic proliferation and in the treatment of UC, due to sulfide-induced hyperproliferation was be in a reversed state when samples were co-incubated in the combination with sulfide and butyrate. Moreover, H_2S has a toxicity on the same order as cyanide, Jimmy et al. [109] and other investigators have carried out studies suggesting that excessive sulfide production may play a pathogenic role in UC. Suarez et al. [110] studied the ability of bismuth subsalicylate (BSS), a compound that binds H_2S, to reduce the amount of H_2S releasing in the colon. It's demonstrating a treatment that reduces colonic H_2S levels could be clinically useful in the treatment of flatus odor and of UC.

Perridon et al. [100]. discussed the known, assumed and hypothetical effects and roles of H_2S on the aging process comprehensively. The actions of H_2S on the hallmarks of aging and on several age-related pathologies were also reviewed. Taken together, all previous studies demonstrated that H_2S may have anti-aging properties by altering intercellular communication. Eto et al. [111] showed that the levels of H_2S are severely decreased in the brains of Alzheimer's disease (AD) patients compared with the brains of the age-matched normal individuals. The authors also confirmed findings that S-adenosyl-L-methionine (SAM), a CBS activator, is much reduced in AD brain while one of the two CBS substrates, homocysteine, is increased in the serum of AD patients. These observations suggest that CBS activity is reduced in AD brains and the decrease in H_2S maybe involved in some aspects of the cognitive decline in AD.

Though acknowledging the challenges ahead, research on H_2S physiological implications and pharmacotherapy of H_2S is entering an exponential exploration era [112]. Therefore, evaluation for the varied pathophysiological roles and effects ascribed to H_2S in various biological systems always based on examination of the extensive chemical attributes of H_2S species which have been mentioned in previous paragraph 1.1.1. Meanwhile, further studies are needed to understand the full impact of H_2S on body system as it may represent a unique target for therapeutic intervention. Thereby, commonly used method for H_2S measurement were firstly discussed and shown in **Table 1.5** in next paragraph 1.2, it indicates a whiff exploration that blossomed for many novel technologies have been developed to detect endogenous H_2S species generation, and various H_2S-releasing compounds have been developed to assist therapeutic intervention of wide spectrum of diseases related to abnormal levels of H_2S production.

1.1.6 Chemical nature of general reactive sulfur species (RSS)

Sulfur is a multivalent and nonmetallic chemical element which the atomic number is 16 and it is a crucial biologically active element due to its unique properties and wide range of accessible oxidation states. Generally, the term 'reactive sulfur species' (RSS) is used to refer collectively to reactive sulfur chemotypes (including organic and inorganic) that, can react with, oxidize or reduce other molecules under physiological conditions [4, 113]. Noteworthy, in addition to reactive cysteine species in proteins, inorganic sulfur-containing species are also classified as RSS. In the light of their significant roles in redox homeostasis, cell signaling, and metabolic

regulation, RSS are viewed indispensable to life. Nevertheless, divergent from reactive oxygen and nitrogen species (ROS, RNS), whose roles in cellular signal mediating and in number of physiological and pathological processes have been extensively studied in previous works, the role of RSS in cellular signaling, redox homeostasis, and mammalian metabolism has only recently drawn attention among scientific community. In a special issue, Iciek et al. [114] reviewed the RSS in and (Patho)-physiological conditions and in therapy which provided some selected meaningful cases and new information about this unusual element, sulfur, and its compounds investigation.

Of particular interest, H_2S molecule is one of the prototypical inorganic RSS, which is part of a relatively stable reactive intermediate sulfur species with a half-life on the order of minutes time-scale [115]. Moreover, it shows low reactivity toward disulfides, such as cystine and glutathione disulfide (GSSG) compounds [116]. Noticeable, H_2S represents merely a portion of sulfur-containing small molecules that contribute to bioavailable designated RSS, which represent oxidized sulfide species including a group of reactive molecules with other molecules contained in acid-labile sulfide (ALS) and bound sulfane sulfur (BSS) [117].

Complementary works from Mishanina and co-workers [118] also hypothesis that sulfide oxidation pathways are a main source of RSS with signaling potential. It is proposed that the canonical mitochondrial and the heme-dependent sulfide oxidation pathways are important sources of RSS and that enzyme-catalyzed trans-persulfidation reactions are an important mechanism for ensuring target specificity of reversible post-translational persulfide modification. Meantime, RSS likely serve as important biological redox mediators through participation in different nucleophilic-electrophilic reactions, such as with thiols (RSH) being nucleophilic, disulfides (RSSR, also known as the form of oxidized thiol) being electrophilic, and persulfides (RSSH) being either electrophilic or nucleophilic upon deprotonation (RSS^-), where R represents an anion or organic group here. Specifically, a sulfhydryl group (-SH) consists of a sulfur atom (S) with two lone pairs, bonded to hydrogen (H) also called “thiol group”.

As indicated above, due to the electron-rich or electron-deficient properties, most RSS are known to be unstable and reactive in biology. The sticking point to the versatility of sulfur in

metabolism lies in its ability to cycle through various valence states. This is well reflected by the fact that the sulfur atom can accept or donate electrons and exist in a wide range of biologically relevant oxidation states range from −2, as in H_2S, to +6, as in sulfate (SO_4^{2-}).

Chemically, H_2S has reductive and nucleophilic properties that contributing to its physiological effects. It is well known that nucleophiles are electron rich and owns the potential to react to decrease the electron density, then become neutral or have a tendency to be negatively charged. H_2S bioavailability is regulated through its conversion into different chemical forms, or pools due to the strong reducing potential of H_2S and its affinity for thiol groups in proteins [119, 120]. By means of elucidation of the redox biology of H_2S, it will increase understanding of its role in human physiology and enable potential therapeutic role in pathologies where oxidative stress is central to the disease process. Xie et al. [121] discussed the current understanding of the mechanism of antioxidant effects of H_2S based on recent reports. Obviously, there should be multiple targets and signaling pathways involved to inhibit mitochondria ROS production and achieve cellular redox homeostasis. Additionally, Benchoam et al. [122] and Cuevasanta et al. [123] reviewed H_2S and persulfides oxidation by biologically relevant oxidizing species. It is indicated that H_2S/HS^- species can react with metal centers and oxidized thiol products such as disulfides (RSSR) and sulfenic acids (RSOH), thus leading to the formation of persulfides ($RSSH/RSS^-$) with the latter one. Nevertheless, Kelsall et al. [124] demonstrated the thermodynamics of sulfur/water system in the form of a potential-pH diagram, and calculated from reported critically assessed standard Gibbs energies of formation of the species considered, the results shows that only the –2 (sulphide), 0 (elemental sulfur) and +6 (sulphate) oxidation states are truly stable in water under ambient conditions. Therefore, the sulfur atoms of most sulfur compounds in biological tissues are existing as reduced divalent (−2) or fully oxidized hexavalent states (+6) forms.

Some representative structures of compounds were shown in **Table 1.2**. It's well known that oxidation of H_2S can lead to various products, including sulfite (SO_3^{2-}), sulfate (SO_4^{2-}), thiosulfate ($S_2O_3^{2-}$), persulfides (RSS^-), organic and inorganic polysulfides (RSS_nSR, HSS_nS^-), and elemental sulfur (S_8). All these mentioned sulfur compounds play an important role in various biochemical and chemical biological processes [118, 125].

Table 1.2 Chemical structures of some common biologically relevant RSS: the range of sulfur oxidation states between −2 and +6. (n = 2-7)

Oxidation states of sulfur (S)	RSS	Chemical structure
−2	Hydrogen sulfide	
	Thiol	
	Iron-sulfur cluster	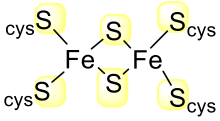
−1	Hydrogen disulfide	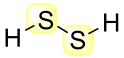
	Polysulfane	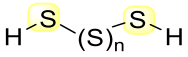
	Hydropolysulfide	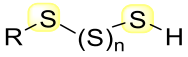
	Polysulfide	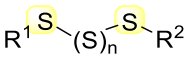
0	Elemental sulfur	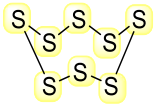
	Polysulfane	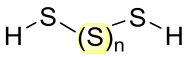
	Hydropolysulfide	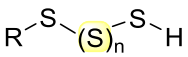
	Polysulfide	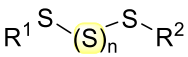
+1	Thiosulfinate	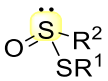
+2	Sulfinic acid	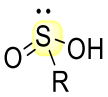
+3	Thiosulfonate	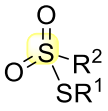
+4	Sulfonic acid	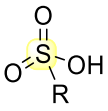

+5	Thiosulfate	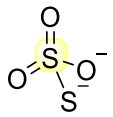
+6	Sulfate	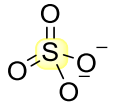

Generally, sulfide oxidation pathways are considered to be primarily mechanisms for disposing of excess sulfide and generate a series of RSS that could modify target proteins. They are existing as compounds containing sulfur-bonded sulfur, including mainly persulfides (RS-SH) and polysulfide (RS-S_n-SR), these mentioned two types of RSS are the most studied and have been identified in mammalian and other biological systems with possible involvement in various cellular functions. Although the enhanced reactivity in comparison to H_2S makes such species more versatile signaling agents, it also makes understanding their reactivity more challenging.

Of special interest, Bailey et al. [126] applied a combination of nuclear magnetic resonance (NMR) and UV-Vis spectroscopy techniques to investigate the spectroscopic properties and reactivity of three isolated organic persulfides, and reported a simple model for persulfide reactivity, including their multifaceted roles, such as nucleophiles, electrophiles, and sulfide donors. Additionally, the observed results indicated that persulfides can only release H_2S following reduction by another species, including another persulfide, which supports the general hypothesis that persulfides may play considerable roles for sulfide storage and transport, whereas free H_2S/HS^- is prone to reaction with other reactive biological species. Therefore, the reactions of isolated persulfides provided critical insights into the interplay between H_2S and persulfide reactivity.

As mentioned above, sulfide metabolites, such as persulfide and polysulfide, which belong to RSS have recently been appreciated for various physiological significance and determined as important signaling agents themselves associated with many biological activities and functions [127, 128]. Furthermore, the diverse redox landscape of RSS provides simple ways in which key chemical properties of RSS such as nucleophilicity, electrophilicity, pK_a, and bond strengths can be modulated by interactions with other redox-active systems, thus making RSS

ideal for many roles in biological signaling. Emerging evidence suggests that these chemical intermediates or derivatives molecules may have similar or divergent regulatory roles compared with H_2S species (H_2S, HS^-, S^{2-}) in mediating various biological functions. Unfortunately, our understanding of these diverse RSS metabolites and how they contribute to all kinds of pathophysiology phenomena remains poorly understood, thereby further research is required to figure out the definition and classification of kinds of terms refer to sulfur-related species used in scientific community.

1.1.7 Storage and release of H_2S species: Sulfide pools interconversion

1.1.7.1 Labile sulfur species (LSS)

Presently, various terms have been used to illustrate various labile sulfur species in the literature. So, it's necessary to do more clear clarification and identification of these terms. Sulfur compounds can be present in two distinct forms in biological tissues, that is stable and labile forms. Sulfur atoms which stay in 0, −2 and +6 states are stable, and compounds containing the sulfur atoms in such states will be not liberated by simple chemical treatment, such as in treatment of acid condition or reducing agents. Such a sulfur is generally defined as stable sulfur, such as methionine, cysteine, and sulfuric acid etc. Additionally, methionine and cysteine are sulfur-containing amino acids and are present in the unbound state and as constituents of proteins and peptides. On the other hand, unstable forms of sulfur-containing compounds such as acid-labile sulfur, sulfane sulfur and protein-associated sulfur belong to labile sulfur species, as classified in **Figure 1.7**. These miscellaneous forms of sulfur compounds have the

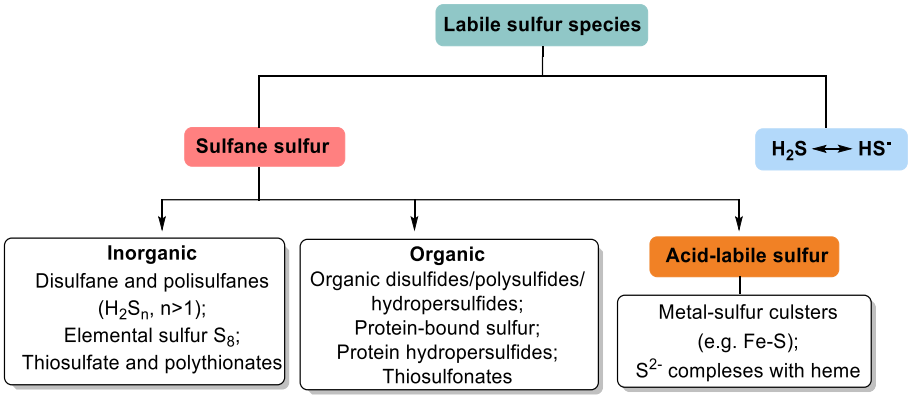

Figure 1.7 Classification of labile sulfur species.

potential to be liberated as H_2S by simple chemical treatment such as under acid conditions or reducing agent treatment. Consequently, the determination of these inorganic sulfide is the basis

for the measurement of labile sulfur [129].

Sulfane sulfur atoms are previously also defined as divalent sulfur atoms bonded only to other sulfur in 1991, except that they may bear ionizable hydrogen at some pH values [117]. As reported, there are four enzymes involved in the generation or utilization of sulfane sulfur: cystathionase, 3-mercaptopyruvate sulfurtransferase, rhodanese and glutathione-dependent thiosulfate reductase. For better understanding the relationship among "sulfane sulfur", "bound sulfur" and "acid-labile sulfur" and "free sulfide", a diagram was carried out by giving some representative compounds (see **Figure 1.8**).

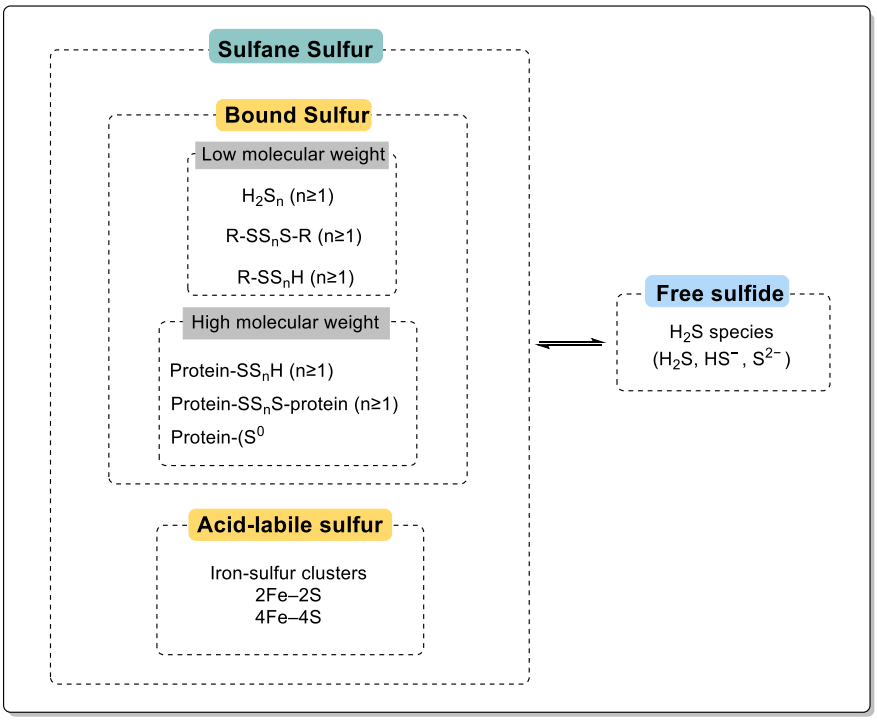

Figure 1.8 A relationship between sulfane sulfur compounds and H_2S species (where R represents an anion or organic group).

1.1.7.2 Free sulfide (H_2S species)

In aqueous solutions, H_2S is a weak acid and quickly reach the equilibrium of $H_2S/HS^-/S^{2-}$ species. Nevertheless, changes of pH value can readily alter the equilibrium of $H_2S/HS^-/S^{2-}$ species. In this study, sodium sulfide was chosen as the H_2S donor, main equilibrium forms of H_2S/HS^- released from Na_2S in aqueous was presented in **Figure 1.9**. It is also worth mentioning that during the uncatalyzed oxidation of H_2S in aerobic solutions, a mixture of unstable intermediates and reaction products will be formed, such as polysulfanes, sulfite, thiosulfate and elemental sulfur etc. However, it's considered to be the conversion of sulfide to

hydrosulfide instead during the studies which will place particular emphasis on. And only after the special treatment with an acid milieu, sulfide salts can convert to volatile H_2S [130].

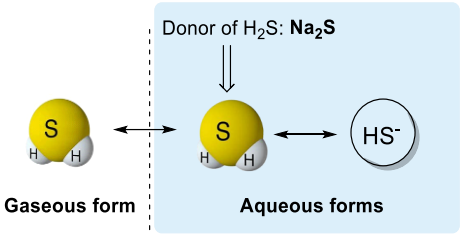

Figure 1.9 Free sulfide: equilibrium forms of H_2S/HS^- provided by Na_2S in aqueous solutions.

1.1.7.3 Acid-labile sulfur (ALS)

As aforementioned in paragraph 1.1.4 (metabolism of endogenous H_2S), the metabolic origin of labile sulfur is cysteine-sulfur. A set of mitochondrial reactions of cysteine appears to function for the formation of labile sulfur, including acid-labile sulfur in iron–sulfur clusters. This might be related to the fact that, in eukaryotes, most iron–sulfur proteins are located in mitochondria [131]. Also, it must be noted that as a component of non-heme iron–sulfur proteins, acid-labile sulfur functions in electron transfer in the mitochondrial electron-transfer system and in enzyme activity [132].

Generally, iron-sulfur clusters (Fe-S) are composed of iron atoms and an equal number of inorganic sulfides with cysteinyl-S iron coordination [133]. Rhombic 2Fe–2S cluster and cubic 4Fe–4S cluster [Fe_4S_4] are the commonly types of acid-labile biological Fe-S clusters [134]. The structures were described as in **Figure 1.10**.

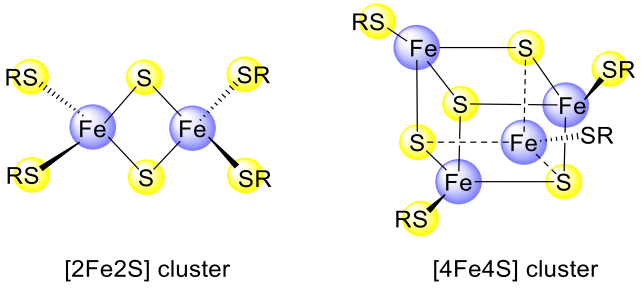

Figure 1.10 Structure of common acid-labile biological Fe-S clusters: rhombic 2Fe–2S cluster [Fe_2S_2] and cubic 4Fe–4S cluster [Fe_4S_4].

1.1.7.4 Bound sulfur species (BSS)

In 1993, sulfur atoms releasable as a hydrogen sulfide ion (HS^-) by reducing agents, such as dithiothreitol (DTT) and tris(2-carboxyethyl) phosphine (TCEP) was defined as “bound sulfur”. In other words, bound sulfur refers to a sulfur atom that exists in a zero to divalent form (0 to

−2) [135]. Currently, bound sulfur species are representing both small-molecular-weight thiols and protein-associated thiols bound with sulfur atoms normally having an oxidation state 0 or −1. BSS can be further regarded as sulfur atoms covalently BSS pools, and predominantly including persulfides and polysulfides, which can subsequently liberate H_2S/HS^- under reducing conditions by adding reducing reagents. It's also worth mentioning that some literatures name "bound sulfur species" as "bound sulfane sulfur", which both represent as a compound containing sulfur-bonded sulfur [130]. Kimura et al. reviewed the release mechanism of H_2S and interpreted how bound sulfane sulfur is referred to a store pool of H_2S. It's demonstrated that H_2S can be stored as bound sulfane sulfur, which in turn may release H_2S when cells receive certain physiological signals in biological processes.

Based on those above-described mainstream classification and definition found in the literature, accordingly, it can be designated that acid-labile sulfide and bound sulfane sulfur pools are the two main stored biochemical sources of H_2S species, which act as sulfide buffering regulators by releasing H_2S via different chemical reactions. Conversion of various biochemical forms of reactive sulfur species was shown in **Figure 1.11**.

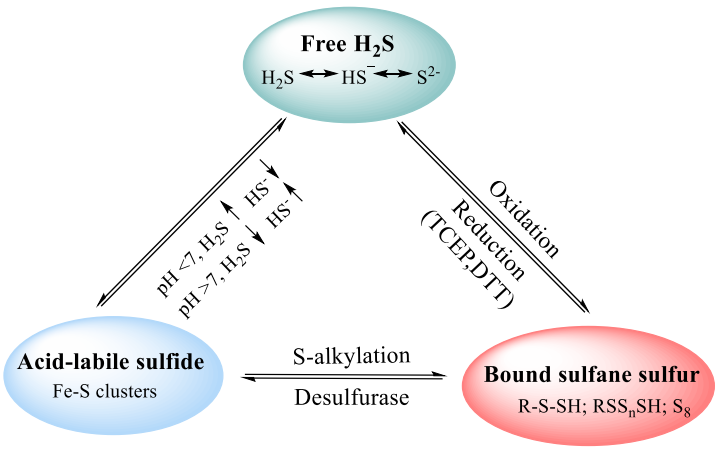

Figure 1.11 Interconversion of various biochemical forms of labile sulfur species: free hydrogen sulfide (H_2S species: H_2S, HS^-, S^{2-}), acid-labile sulfide (Fe-S clusters), and bound sulfane sulfur.

Therein, undissociated form of H_2S can hydrolyze to the forms of dissociated. H_2S end up to being in various forms of gas H_2S (≈ 20%), hydrosulfide anion (HS^-, ≈ 80%), and sulfide anion (S^{2-}, < 0.1%) [136] with different proportions at a physiological pH 7.4 and 37 °C. But at pH 3.8, HS^- becomes negligible (0.06%) and solutions can be considered 100% H_2S. In addition, iron–sulfur proteins are ubiquitous in living things and there are more than 120 distinct classes of proteins and enzymes. Whereas acid-labile sulfide consists of iron-sulfur clusters contained

in iron-sulfur proteins which are non-heme iron proteins (such as ferredoxin, glutaredoxin and enzymes like succinate dehydrogenase, ribonucleotide reductase) [137], which can release H_2S below a pH of 5.4. Other sulfane sulfur species including hydropolysulfides (RS_n-SH), thiosulfonates (RSO_2SR^-), where R represents an anion or organic group; thiosulfate ($S_2O_3^{2-}$), polythionates ($S_n(SO_3)_2^{2-}$)) and elemental sulfur (S_8) and peptide-protein bound (e.g., haemoglobin, myoglobin, neuroglobin), which can release H_2S under reducing conditions. The structures of these compounds can be found in **Table 1.3**. Therein, sulfide which can be liberated from proteins by treatment with reducing agent DTT appears to include persulfide and elemental sulfur. And it's suggested that there existing three main forms of bound sulfur containing in normal human serum. That is elemental sulfur bound to hydrophobic sites on protein molecules (S), reduced sulfur bound to protein as a trisulfide (R–SSS–R), and protein persulfide (R–SSH). And all these sulfur species play a significant role in the synthesis of S-proteins and S-amino acids by microbial action and have been established to trigger sulfide-triggered biological events [138-141].

In the previous content, reduction reagents were referred several times, Getz et al. did a comparison in properties of DTT and TCEP in biochemistry. Structures of these two compounds were illustrated in **Figure 1.12**. It was indicated that TCEP is highly advantageous over DTT, and the spin labels in TCEP are two to four times more stable than in DTT although the choice of reductant varies when it's in different applications. What's more, Burn et al. proposed the mechanism of selective reduction of disulfides by TCEP in water (see **Figure 1.13**) and indicated the cleavage of the disulfide bond appears to be the rate-determining step (RDS) [142, 143].

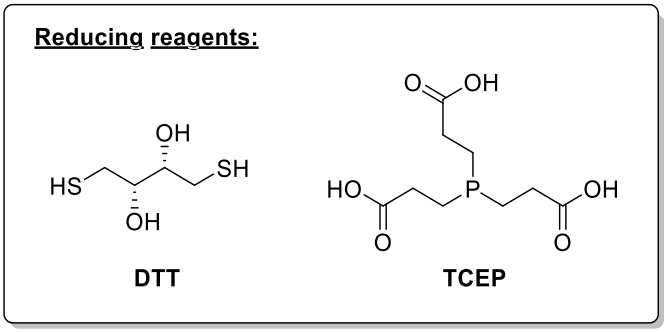

Figure 1.12. Sulfhydryl reducing agents DTT and TCEP.

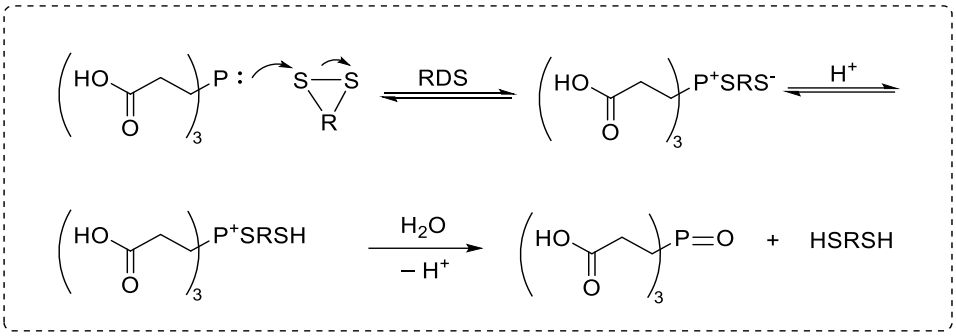

Figure 1.13 Reduction mechanism of disulfides by TCEP in H_2O.

Recently, the clinical relevance of sulfide pools has been demonstrated by Rajpal et al. [144] indicating that plasma H_2S metabolite bioavailability can be a predictive indicator for cardiovascular disease. These results emphasized the importance of cellular redox state for regulating H_2S bioavailability, and hints a role played by bound sulfane sulfur (BSS) in cardiovascular health. Simultaneously, in conjunction with their clinical study and data observations, a significant decrease in the levels of acid-labile and bound sulfane sulfide in plasma samples of subjects of vascular disease including CVD and peripheral arterial disease (PAD) were obtained [144].

Structures of general sulfane sulfur compounds have been demonstrated extensively in literature. Several examples of the structure of biological sulfane sulfur compounds were listed in the **Table 1.3**. Of particular attention, there exist three forms of sulfane sulfur atoms associated with proteins. One form is a sulfur atom bound to protein as a persulfide, the second is protein polysulfide and the third is protein-associated elemental sulfur. Hannestad et al. [145] detected significant amounts of protein-associated sulfur in the brain, heart, kidney, liver, skeletal muscle and spleen of rats, but it was negligibly low in blood plasma and erythrocytes. To some extent, these results suggested that the transport function of serum albumin for sulfur did not occur. Nevertheless, more evidence should be obtained by developing more advanced detection methods with higher selective and sensitivity for better explaining the essence inside. As shown below in **Figure 1.14**. A schematic diagram was clearly illustrated to show how bound sulfane as a main sulfur store source of H_2S and as a signaling molecule when cells receive certain physiological signals. That is H_2S produced by enzymatic (enzymes such as CBS, CSE, 3MST) and non-enzymatic pathways then functions as a signal molecule which can be monitored by various established techniques based on different theories. Afterwards, it can

be stored as bound sulfane sulfur, which in turn may release H_2S.

Table 1.3 Examples of biological sulfane sulfur compound structure.

General sulfane sulfur compounds	**Structure of biological sulfane sulfur**	
Thiosulfate	Thiosulfate	SSO_3^{2-}
Persulfide	Thioysteine (cysteine persulfide)	Cys-S-S^-
	Thiocysteamine (cysteamine persulfide)	$CH_2S\text{-}S^-$ $CH_2\text{-}NH_2$
	Glutathione persulfide	GS-S^-
	Protein persulfide	Protein-S-S^-
Thiosulfonate	Thiotaurine	$CH_2\text{-}SO_2\text{-}S^-$ $CH_2\text{-}NH_2$
Polysulfide	Thiocystine	Cys-S-S_n-S-Cys(n≥1)
	Protein polysulfide	Protein–S(–S)S_n (n≥1)
polythionate	Tetrathionate	$^-O_3S\text{-}S_n\text{-}SO_3^-$ (n≥1)
Elemental sulfur (S^0)	Protein associated sulfur	Protein–(S^0

The determinate sulfide levels with versatile methods as a monitor of physiological response can be achieved, such as diagnosis and prognosis roles in human subjects in comparison with normal sulfide concentration. Reversely, the corresponding physiological or pathological effects could be predicted in this way.

At present, the determination of stored sulfur compounds is important for the study of their structures, metabolism and function because of the high reactivity of sulfur. These labile sulfur compounds are determined after conversion to sulfide or sulfide derivatives. So far, many kinds of techniques have been used for the analysis of labile sulfur species, as discussed in the paragraph 1.2. However, the values reported are not always in a good agreement. The discrepancy among reports seems to be derived from the instability of sulfide, such as its property of high volatility and great susceptibility to oxidation. Therefore, precautions are necessary to suppress errors arising from the nature of sulfide itself and further studies are

needed for developing novel, better and stable methods.

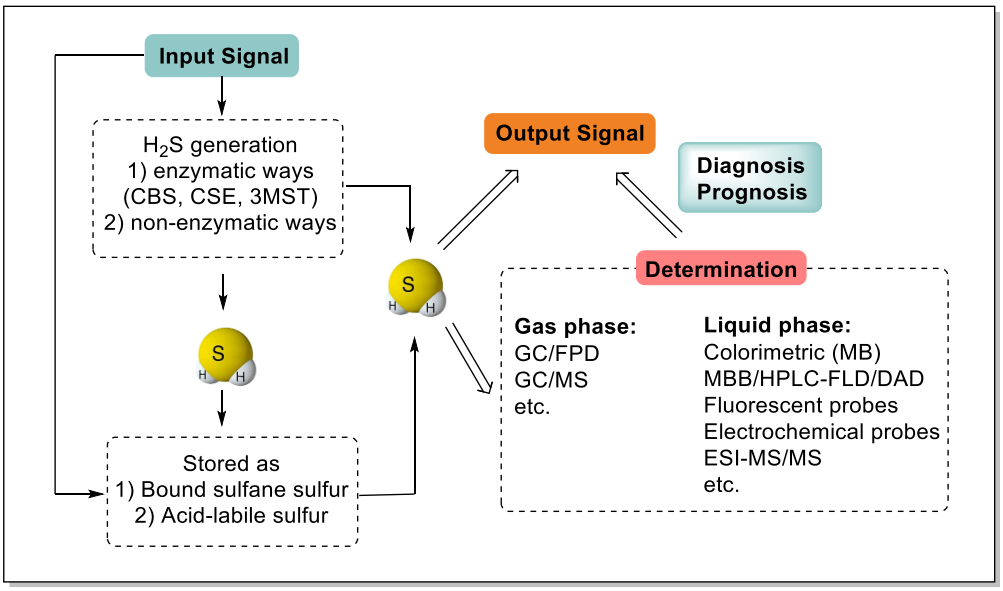

Figure 1.14 Schematic diagram to show how bound sulfane as a sulfur store source of H_2S which is regarded as a signalling molecule.

1.1.8 Versatile methods for sulfide determination in biological fields

Currently, there are numerous research endeavors as well as clinical trials investigating the therapeutic manipulation potential of H_2S, owing to its vast involvement in various physiological processes [146]. The monitoring of H_2S and the study on pathological and pharmacology mechanisms of H_2S require detection methods with high selectivity, sensitivity and precision. However, the deficiency of appropriate methods for H_2S detection and quantification makes the accurate measurement of H_2S challenge. It is also rare to have a consensus for the determination of the actual amount of bioavailable H_2S associated with normal or pathophysiological processes. Thus, H_2S species quantification in biological matrices remains a critical challenge also in medicine. Next, we will discuss the investigations currently completed by scientists with kinds of analytical methods on the related topic of H_2S measurements in different biological specimens. These methodologies will help to elucidate the practicality of using the H_2S as a monitor of physiological response in human subjects.

As shown in **Table 1.4**, from the standpoints of pros and cons, a survey was carried out to summarize most frequently used analytical methods. This may be of importance in practical application when face the choice of techniques. Indeed, recently, the detection of sulfide, particularly hydrogen sulfide, has long been the focus of the analytical community. A large

number of analytical protocols for determination of sulfide has been established and performed to scrutinize H_2S levels in different biological samples (such as cells, blood and tissues).

Table 1.4 Advantages and disadvantages of commonly used analytical methods for H_2S measurement in biological tissues.

Method	Advantages	Disadvantages	Reference
GC-FPD/IC	Highly Sensitive and selective (ppb)	Complex sample preparation; difficult to determine different forms;	[147-149]
GC/MS	High sensitivity and selectivity; Rapid response time	Complex sample preparation; Difficult to achieve quantification Easy to decompose;	[149-152]
GC/Chemiluminescence detection method	Sensitive detection (nM – pM)	Detects total sulfur; Limited throughput;	[153]
Direct spectrophotometric methods	Low background	Micromolar (μM) detection limit; Protein absorption interference	[154, 155]
Fluorescence sensor	High sensitivity; Real-time measurement	Slow response time; Photoexcitation cause damage to samples	[156-167]
Methylene blue method	Easy handling; Performed in most studies; Relative low cost and high performance;	Limited sensitivity and selectivity; Methylene blue dimer and trimer formation; Strong acid chemical pre-treatment; Interference of other colored substances;	[168-172]
Electrochemical sensor	High sensitivity; Real-time measure in a wide range of samples; Easy to setup and use; Reproductivity;	Prone to fouling; Limited throughput; Need to calibrate and pre-treatment before measuring; Limited detection of various forms;	[173-177]
MBB derivatization method (HPLC/FLD or LC-MS/MS)	From moderate to high sensitivity range (nM – pM); Stable derivatives; High throughput; Capable of determining multiple biological pools; Ease of handling;	Need dark and hypoxic conditions; Require RP-HPLC instrumentation (compare to portable sensors); Time-consuming;	[144, 178-187]

These methods include gas chromatography (GC) with flame photometric or sulfur chemiluminescence detection [149, 153, 188, 189], ion chromatography (IC), direct spectrophotometric determination [169] or spectrophotometry after derivatization [154, 155], and the use of sulfide-sensitive fluorescent sensors [157, 165]; colorimetric analysis monitoring methylene blue formation [168-172] and other colorimetric sensors [163, 190], use of potentiometry with a sulfide ion-specific electrode [174] or a polarographic electrode sensors [177], high performance liquid chromatography with fluorescence detection (HPLC-FLD) or mass spectrometry (MS) analysis of the monobromobimane (MBB) derivative of sulfide [178, 181, 182], an isomer of MBB was also shown to have high sensitivity for the quantification of H_2S in blood [184].

In addition, several works focused on detection techniques have determined the levels of per/polysulfides in biological systems. Among the new methods for the detection of sulfur biological pools the use of green-fluorescent-protein (GFP)-based probes [191] and a resonance synchronous spectroscopy-based method (RS2) [192] have been reported. Notably, GFP-probes can detect real-time polysulfides levels in live cells and subcellular organelles, with minimal interference due to reactive oxygen species (ROS) scavenging, while the RS2 method can detect intracellular polysulfides and persulfides by comparison of species-specific RS2 spectra and intensities at physiological pH.

It is well established that many of sulfur-rich RSS are in a dynamic equilibrium and rapidly interconvert and this interconversion is particularly prevalent for polysulfides, as polysulfide interconversion is significantly faster than the electrophilic labeling, which means that such systems are under Curtin–Hammett control. Interestingly, works from Nagy and coworkers using complementary analytical methods confirmed experimentally that the electrophilic labeling of polysulfides is indeed under Curtin–Hammett control. For example, when cysteine and glutathione hydropolysulfides were generated in situ and quenched with alkylating agents such as monobromobimane (MBB), N-ethylmaleimide (NEM), and iodoacetamide (IAM), only short polysulfide adducts were observed with NEM labeling whereas longer chain adducts were formed with IAM or MBB [125, 193]. Also, for hydropolysulfides, alkylation with NEM is based on nucleophilic addition, but IAM is nucleophilic substitution, as shown in **Figure 1.15**.

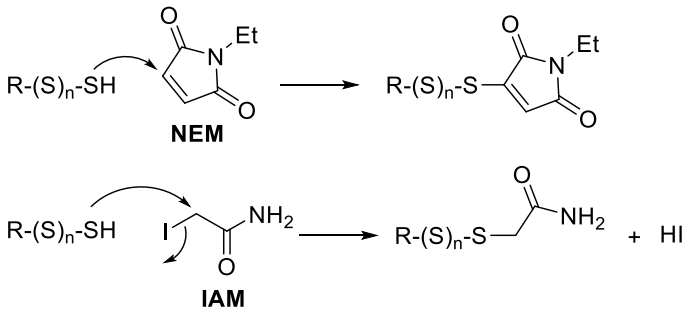

Figure 1.15 Alkylation with NEM (nucleophilic addition) and IAM (nucleophilic substitution).

As described in paragraph 1.1.2, because of the toxicity of H_2S in ppm level and the extensive formation in the atmosphere that may cause industrial and environmental problems, there also exist a need for a rapid, simple and practical method for the poisonous H_2S determination in the environment. Therefore, some of these analytical techniques were originally developed for the determination of sulfide in air and water samples and were then further optimized to be applied for biological sources. Therefore, it can be said that the determination of inorganic sulfide in the environmental air and water should be the basis of labile sulfur measurement in biological samples. As stated above in paragraph 1.1.7, since most labile sulfur is liberated as inorganic sulfide which can be present as H_2S, HS^- or S^{2-} (denoted as H_2S species in this thesis) in the aqueous phase and as H_2S in the gas phase. Therefore, in essence, the assay methods used for sulfur species detection is the determination of inorganic sulfide eventually.

Lawrence et al. and many investigators reviewed analytical strategies for the detection of sulfide these years [1, 129, 178, 194, 195]. Most of reviewers detailed the need for sulfide measurements and describe the basis of many of the current approaches to sulfide detection. The collation of information from a broad range of sources, covering the major approaches, has been achieved and the salient points of each technique presented and critically appraised. Commonly, the quantification of H_2S species existing in various biological matrices encounters several difficulties and limitations due to the nature of gaseous of the small molecule, particularly its volatility, redox lability, and most importantly, its low steady-state concentration [141]. Depending on the chemistries of the methods used, marked differences in H_2S levels in physiological fluids, spanning from nanomolar to hundreds of micromolar level, have been reported in some literature [1, 182, 196, 197]. Moreover, the methods most often employed for H_2S measurements are associated with substantial artifacts [198, 199] and various

complications can arise, depending on the sample sources analyzed, e.g., quantitation of steady-state H_2S levels in tissues [130].

Table 1.5 Summarization of various methods for H_2S species determination in biological samples.

Detection methods	Source	Sulfur species type	Detection Limit	Reference
Methylene blue method	Gas H_2S	H_2S	1.0 μM	Fogo et al. 1949 [168]
	Sodium sulfide	H_2S, HS^-, S^2	2 – 80 μM	Lewis et al. 1965[169]
	Rat brain	H_2S, HS^-, S^{2-}	9.0 μM	Ishigami et al. 2009 [171]
Sulfide ion-selective electrodes	Rumen and Blood	Free and acid-labile sulfide	1.0 μM	Khan et al. 1980 [173]
	Biological media	H_2S	< 100 nM	Brown et al.2019 [175]
Polarographic method	Whole blood	Free H_2S, total sulfide	Free H_2S: 14 nM Total sulfide: 0.1 μM	Wintner et al. 2010 [185]
	Rat vascular tissue	Free H_2S	10 nM	Doeller et al. 2005 [200]
Fluorescence probes	In cardiac tissues	H_2S, HS^-, S^{2-}	15 nmol min^{-1} g^{-1} (protein)	Chen et al. 2012 [157]
	H_2S formation from E.coil Cysteine	H_2S, HS^-, S^{2-}	53 nM	Pose et al. 2022 [201]
	Sodium sulfide	H_2S, HS^-, S^{2-}	92 nM	Kaushik et al. 2015 [202]
Chemiluminescence detection method	Rat brain microdialysate	H_2S, HS^-, S^{2-}	0.3 μM	Fang et al. 2019 [188]
Gas chromatography method	Multiple tissues from mouse	Free and acid-labile sulfide	2 nM	Levitt et al. 2011 [149]
	Rat liver and heart tissues	Acid-labile H_2S	112 – 274 nmol/g	Ubuka et al. 2001 [147]
	Blood	S^{2-}	35 – 80 μM/L	Hyspler et al. 2002 [151]
	Blood	H_2S, HS^-, S^{2-}	0.01 μg/g	Kage et al. 1988 [203]
Gas Dialysis/Ion Chromatograph	Human and rat brain tissue	H_2S, HS^-, S^{2-}	100 μM	Goodwin et al. 1989 [204]
Microdistillation/Ion chromatography	Gut contents and whole blood	H_2S	2.5 μM	Richardson et al. 2000 [205]
Microfluidic method	Human blood plasma	H_2S, HS^-, S^{2-}	70 – 125μM	Karunya et al. 2019 [206]

Above, most of these techniques do not have enough capacities for effectively distinguishing thiols in cells and are often limited to measure H_2S. In addition, these methods have some limitations, such as long reaction time, complex preparation process, low specificity, low sensitivity and inconsistent reported results. Likewise, due to the variety of experimental methods used, highly variable results with respect to determination of the absolute concentration of sulfide have been yielded. Therefore, these currently available protocols are largely resulting in little consensus for detection and quantification of H_2S in complex samples. The need for highly specific, highly selective, reproducible and accurate H_2S measurements seems imperative to untangle the non-resolved disadvantages of the current methods.

Methods to detect the various forms of H_2S are critically reviewed and compared in the literature [207]. H_2S presents complex biological effects in various body systems and the conundrum is coming up. Thus, how does this small molecule exert such widely differing effects? Does different level of H_2S exert different effects on the cell? Answering to the conundrum might be the absolute concentrations of H_2S achieved locally at the site of interest. Based on the previous conundrum put forward, it's learned that accurate and reliable measurement of biological hydrogen sulfide can provide critical information associated with various pathophysiological functions. According to the literature survey, in **Table 1.5**, it is now clearly showing that a wide range of different levels of sulfur species have been reported when using various methods for H_2S species determination in biological specimens. In the subdivided paragraphs of this section, many representative examples with different analytical protocols applied in determination of sulfur species especially for H_2S species, will be discussed and addressed thoroughly.

GC-FPD (Gas chromatography-flame photometric detector)

Determination of hydrogen sulfide and acid-labile sulfur in animal tissues by combining gas chromatography with flame photometric detector (GC-FPD) and ion chromatography (IC) method was employed by Ubuka et al. [147]. Trapping H_2S in alkaline solution was determined by GC-FPD as H_2S or by IC as sulfate after oxidation with hydrogen peroxide. Acid-labile sulfur of fresh rat liver and heart tissues ranged in 112 – 274 nmol/g. But free H_2S was not detected by using this method without acidification with H_3PO_4. Na_2S was used as the standard

material. Standardization of Na_2S was performed by IC after oxidation to sulfate with H_2O_2. Determination of acid-labile sulfur in rat tissues was performed by direct and indirect methods, respectively. In the direct method, tissue homogenate or sample solution placed in a gas equilibration vial was acidified with H_3PO_4, and the headspace gas was subjected to GC. In the indirect method, tissue homogenate was acidified with H_3PO_4 and the H_2S liberated was transferred to a 0.1 M sodium hydroxide (NaOH) solution using a gas transfer system with nitrogen as the carrier gas.

GC-MS (Gas chromatography/mass spectrometry)

Gas chromatography is sensitive enough to measure physiological sulfide levels, but it potentially liberates loosely bound sulfide because of irreversible sulfide binding or shifts in phase transition equilibria. Measure free H_2S, can also measure labile sulfur by adding extra acid [149]. Furthermore, a simple and sensitive method by using gas chromatography with an electron capture detector (GC/ECD) and gas chromatography with mass spectrometry (GC/MS) for quantitative determination of thiosulfate in human blood and urine was devised by Kage and co-workers, which the part of GC/MS was used to identify the disulfide. Advantages of this method are that deproteinization and column treatment are not required, the analytical technique is simple and expeditious, whole blood can be analyzed with the limit of detection reached as low as 0.003 μmol/mL [150]. Hyspler et al. introduced an optimized and validated analytical method for sulphide anions quantitative determination in whole blood using GC–MS technique in selected ion monitoring (SIM) mode. Whereas the limit of quantification was determined as a lower limit of the linearity range and was found to be 3 μmol/L [151]. This approach makes it possible to analyze large numbers of samples in short periods of time. Kage et al. also applied GC/MS to the analysis of sulfide in blood. In the method, the ‘‘extractive alkylation’’ technique was employed by using an alkylating agent pentafluorobenzyl bromide (PFBBr). After dealing with derivitization and centrifugation, the organic phase containing sulfide derivate was analyzed by GC/MS with the detection limit determined as 0.01μg/g. Another case applied with GC/MS method for sulfide determination, the calibration ranged is from 0.2 to 4 μM for sulfide baseline determination in blood and plasma from swine and mice, and from 0.2 to 100 μM for spiking experiments. The signal to noise ratio was at least 5 for the lowest calibration

concentration 0.2 μM (LOD) [152].

GC-CL (Gas chromatography with chemiluminescence detection)

Vitvitsky et al. [153] described the application of GC coupled to sulfur chemiluminescence detector (SCD) to measure the rates of H_2S production and degradation by tissue homogenates at physiologically relevant concentrations of substrates. Analysis of H_2S levels detection relies on the equilibration of H_2S between the liquid sample and gas phases in a hermetically sealed sample chamber. H_2S present in the gas phase is measured following GC separation and detected using a 355 sulfur chemiluminescence detector. In this method, H_2S in biological samples separated from other sulfur compounds provides sensitivity of detection to around 0.5 pmol. But parameters such as column type, injection volume, injection mode, and gas flow rate, will affect the amount of sample that reaches the detector, subsquently affect the sensitivity of the method.

Spectrophotometric methods

Kovatsis et al. [154] reported the results on the feasibility of determining H_2S in atmosphere by an indirect atomic absorption spectroscopy (AAS) method. ln this developed method, definite amounts $Pb(CH_3COO)_2$ solution is added to the test sample for trapping H_2S and the excess reagent is measured by AAS. It appeared to offer a simple system for handling large numbers of samples followed saving operation time. Systematic investigation of the various parameters involved was undertaken in the article. In comparison with the colorimetric and GC methods, the proposed method is easier and timesaving whereas it requires a special vacuum-sampler.

Guenther et al. [155] described a direct ultraviolet spectrophotometric technique to determine total dissolved sulfide ($H_2S + HS^- + S^{2-}$ + reactive polysulfides) in natural waters through direct ultraviolet detection of the HS^- ion which was determined with low background absorption and a limit of detection <1 μM. An optimal pH range of 8.0 – 9.0 where HS^- is >95% of total sulfide decide the dominance of HS^- in UV absorption. The spectrum of a 50 μM total sulfide solution at pH 8 shows a well-defined peak at 230 nm. Also, simplicity and speed of data acquisition can be seen as the advantages of this method.

Alberti et al. [208] described an optical sensor named as ELL-CC for sulphide and thiol

detection by using the reaction between the Ellman's reagent (5,50-dithiobis(2nitrobenzoic acid)) and a generic thiol (RSH). UV-vis spectra and images of the ELL-CC sensors in a working range from 0 to 58 mM of sulphide solutions were studied. Specifically, the relationship between the analyte content and the change in the UV-vis spectrum of the sensor was obtained by employing a partial least squares regression (PLS). Notably, the main cations present in real matrices, such as Na^+, K^+, Ca^{2+} and Mg^{2+}, do not have interferences in the development of the yellow color of the ELL-CC sensor.

MB method (Methylene blue method)

Since in 1883, the original distribution of methylene blue (MB) method by Fischer, and the optimization of this method by Fogo and coworkers [168]. MB method has been developed for derivatization–spectrometric determination of sulfide and is seen as the gold standards for many years in the field of environmental measurements of H_2S. As shown in **Figure 1.16** is the chemical principle of MB method.

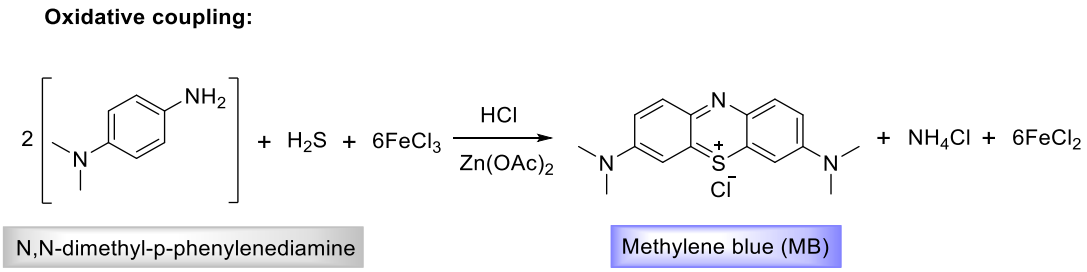

Figure 1.16 Detection of sulfide with the methylene blue method.

The MB method is based on the incubation of sulfide with *N, N*-dimethyl-p-phenylenediamine, in a ferric chloride catalyzed reaction with a 1:2 stoichiometric ratio in a strongly acidic medium to synthesize the methylene blue dye, which is detected spectrophotometrically. Also, the blue color of methylene blue is measured at 670 or 650 nm. A separate center well contained H_2S trapping agents such as alkaline zinc acetate ($Zn(OAc)_2$). It is a convenient method for environmental samples like wastewater. However, the extreme acid conditions used in the reaction system become a problem when applied in biochemical samples. It will result in H_2S releasing from acid-labile sulfides, such as iron-sulfur clusters, and could has the potential to change equilibria, thus promote conversion of HS^- to H_2S [129].

Though MB method are often not sensitive for biological samples which containing relatively

a small amount of H_2S, this method always gave accurate results on appropriate samples. Simultaneously, owing to the strongly acidic conditions used in the method, sulfide may be determined even in the presence of many metals. In the last 10 years, the MB method and the sulfide-sensitive electrode are the most reported method for measuring the H_2S concentration. Biological source of H_2S levels in the blood or plasma of several species, including rat, human, or mouse were reported by using these two methods. However, this method can be highly problematic, making it inappropriate for measuring biological levels of hydrogen sulfide. Key problems include methylene blue dimer and trimer formation, interference of other colored substances, and strong acid chemical pretreatment (pros and cons) [168]. Siegel et al. [169] examined interfering substances and found that by adding 1.0 mM thiosulfate, according to the investigation, 20% inhibition of MB formation will be observed. And these titrations or colorimetric methods, however, lack sensitivity and do not lend themselves easily to the analysis of biological samples.

Fluorescence sensors

Fluorescent probes for measurement of sulfide have greatly evolved in the last couple of years. It holds great potential among the currently developed detection methods because of their high sensitivity, selectivity, and biocompatibility. Feng et al. [158] and Kumar et al. [160] discussed published fluorescent probes for H_2S detection and quantification and divided those probes into three main categories. As indicated in **Figure 1.17**. That is, probes which react with H_2S through a nucleophilic reaction, undergo selective reduction of H_2S, and probes which trap H_2S with a coordinated metal. Furthermore, the authors critically appraised the performance against some key criteria for biological applications. As followed, some cases were exemplified to know more about the present fluorescent sensors for H_2S detection.

Hartman et al. [159] developed a novel fluorescent turn-on chemo-dosimeter based on 8-aminopyrene-1,3,6-trisulfonate (APTS) for direct determination of H_2S species in biological fluids. This reported method can detect H_2S directly in serum without additives. And HS^- was easily quantifiable by fluorescence when its concentration was between 2 and 100 μM.

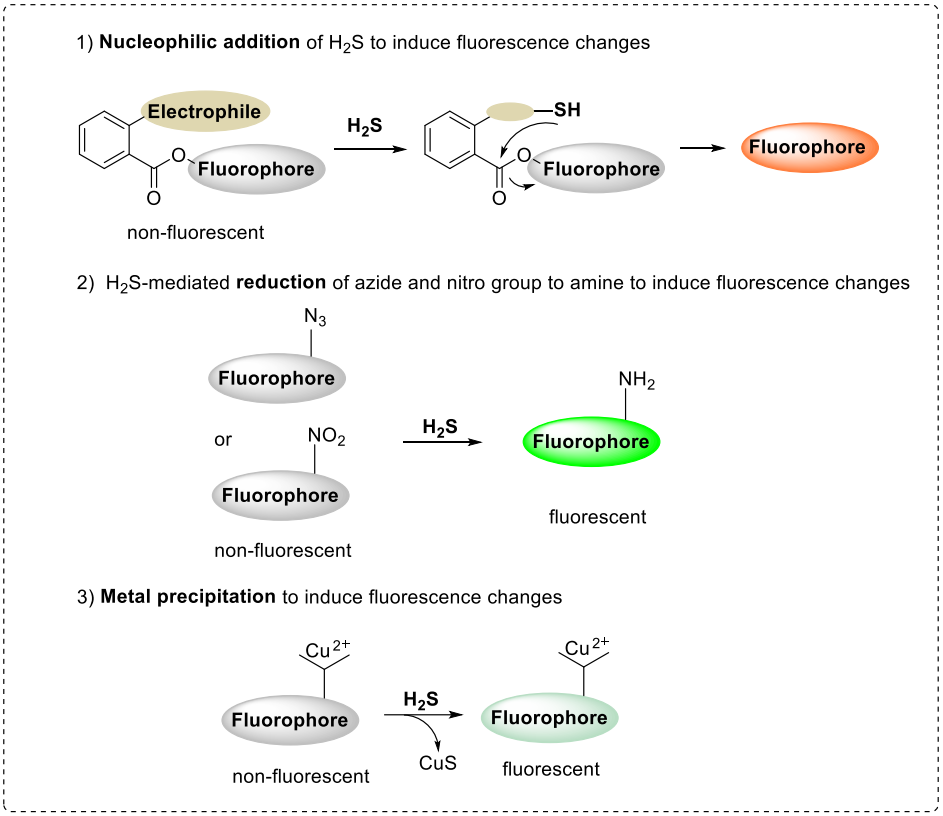

Figure 1.17 Three categories of fluorescent probes for H_2S detection.

Jose et al. [156] discussed the recent developments in the detection of gasotransmitters, H_2S, CO and NO via fluorescent nanoprobes based on different mechanisms such as fluorescence enhancement and quenching. Whereas it should be noted that fluorescent nanoprobes for gaseous signaling molecule are very less as compared to the large number of sensors built from small molecules that work under various detection mechanisms. Peng et al. [164] introduced applications of a series of 2-pyridyl disulfide based fluorescent probes (WSP1, WSP2, WSP3, WSP4 and WSP5) for H_2S detection. The strategy is based on the dual-nucleophilicity of hydrogen sulfide and a H_2S-mediated tandem nucleophilic substitution-cyclization reaction is used to induce the fluorescence change. High sensitivity and selectivity were showed for H_2S and other RSS, such as cysteine and GSH. Zhou et al. [209] systematically evaluated four commercially available probes (WSP-1, WSP-5, CAY), considering their detection range, sensitivity, selectivity, and performance in different environments. Furthermore, their capacity for endogenous H_2S imaging in live cells was demonstrated. Compare with other analytical methods have been reported but are limited for various reasons. Yet, a major challenge exists with the regard to interference by other thiol species. Kaushik et al. [202] reported a new

Alizarin Red S based fluorescent probe (ARS-Zn(II)) for the detection of H_2S in aqueous buffer solution. The calculated detection limit of ARS-Zn(II) with H_2S was reached lower as 92 nM. Chen et al. [157] reported and evaluated a coumarin-based fluorescence chemoprobe (C-6Az and C-7Az) for the selective and sensitive detection of H_2S in degassed PBS buffers and fetal bovine serum. And in situ visualization of endogenous H_2S was achieved in cardiac tissues of normal rats and atherosclerosis (AS) rats using two-photon confocal fluorescence imaging which is the first study for H_2S detection in cardiac tissues. Luo et al. [163] summarized the optical probes based on nanomaterials for the detection of H_2S in biosystems in recent five years, the nanoprobes published in previous literature, Au NRs-FSN and PPF-AgNPs were discussed in practical use for H_2S detection in serum samples with a LOD range of 0.5 – 10 μM. Montoya et al. [210] developed a selective colorimetric probes for H_2S based on nucleophilic aromatic substitution, and the efficacy of the probes was demonstrated in serum with sub-micromolar detection limits as low as 380 nM. Peng et al. [211] reported the synthesis of a novel reduction-sensitive fluorescence chemoprobe, dansyl azide (DNS-Az), and introduced its application in the determination of H_2S in a serum and whole blood with a LOD of 1 μm in buffer/Tween and 5 μm in bovine serum. The unprecedented fast response by DNS-Az to sulfide allows for the detection of transient changes in H_2S levels without sample pretreatment. This method is very important considering the fast metabolism and volatile nature of H_2S in biological systems. The result (31.9±9.4 μm) determined in mice blood was very close to the previously reported serum concentration of H_2S (34.1 μM) [212]. Karunya et al. [206] proposed microfluidic device with Dansyl-Azide (DNS-Az) probe enables rapid and accurate estimation of a key gasotransmitter H_2S in human blood plasma. The device can be used for detecting sulfide in plasma in the range 33 μM to 330 μM (i.e. the smallest and highest concentrations, respectively). The endogenous sulfide levels in plasma of healthy individuals were found to vary between individuals in the range of 70 μM to 125 μM, which agrees well with the values reported in literature. Qian et al. [165] reported the development of two highly sulphide-selective fluorescent probes (SFP-1 and SFP-2), and demonstrated the utility of the probes in quantification of enzymatic H_2S biogenesis and live-cell monitoring of free sulfide. From the viewpoint of probe design, properties like nucleophilicity and reducing capacity, Li et al. [161]

established a near-infrared fluorescent probe HCB-BT, which containing a hemicyanidin conjugated with benzothiazole unit though unsaturated olefinic bond as fluorophore and a 2,4-dinitrobenzenesulfonate unit as recognition group to detecting the sulfide. It has been successfully applied to detect endogenous H_2S in living cells and mice. This might help uncover more physiological and pathological mysteries related to hydrogen sulfide.

Electrochemical sensors

A variety of electrochemical methods using potentiometry, voltammetry, and amperometry have been used to measure sulfide species recently. Xu and co-workers [177] discussed up-to-date literature on the electrochemical sensors for detection of hydrogen sulfide. Herein, ion selective electrodes and polarographic sulfide sensors applied in biological milieu for potential therapeutic use will be addressed. Khan et al. [173] released a rapid and accurate method for measurement of sulfide sulfur levels in rumen and blood with a sulfide-specific ion electrode. Owing to the rapid oxidation of sulfide, antioxidation and reducing agents containing in buffers with high pH were used for an accurate determination of this form of sulfur, meantime, A Johnson-Nishita apparatus was used for blood sulfide liberation in an acid medium, then measured by using the sulfide ion electrode. Lindell et al. [174] introduced a method for the determination of sulphide in blood using an ion-selective electrode also with a wash-bottle reactor. This method involves liberation of blood sulphide by addition of acid and subsequent trapping of the volatilized H_2S gas in NaOH solution with a detection limit of 10 μg/L. The applicability of the method was studied in 12 clinical cases involved in H_2S poisoning with the range of 40 – 600 μg/L. Brown et al. [175] described the development of a direct amperometric sensor based on the oxidation of H_2S/HS^- at a glassy carbon electrode. It's the first time a series of electropolymerized films were reported, which is good for H_2S permselective behavior but against common biological interferences. Simultaneously, the anti-biofouling ability of film-modified electrodes with high selective was evaluated in simulated fluids. The optimized electrode was able to achieve a LOD of <100 nM. By using a micro sulfide ion electrode for studying and analyzing, Velázquez-Moyado et al. [176] described the changes of H_2S level in the stomach for the first time. This electrode has a sensibility of 0.01–100 μM of H_2S and this study provides the basis for a real-time analysis of the H_2S changes in-vivo in the healthy and

wound stomach. Based on membrane on probe allow passage of free H_2S, while keeping out ionic species, Wintner et al. [185] employed an amperometric sensor for determination of dissolved H_2S/HS^- levels. In this study, a comparison of sulphide levels in vitro measured by amperometric detection and by the MBB derivatization method was carried out. It indicated that sulfide measurements between the two methods also showed a good correlation when sodium sulfide was added to fresh plasma or into a normoxic solution of 5% HAS (human serum albumin) in HEPES ((4-(2-hydroxyethyl)-1-piperazineethanesulfonic acid).

Chemiluminescence detection

Chemiluminescence (CL) detection methods have the characteristics of simple equipment and high sensitivity. A strong CL intensity was found in the luminol/H_2O_2 system catalyzed by horseradish peroxidase (HRP). The presence of H_2S can cause the deactivation of the HRP, resulting in the reduction of the CL intensity of the luminol/H_2O_2 system. Fang et al. [188] reported a simple but sensitive CL sensor for H_2S detection based on the HRP-catalyzed luminol–H_2O_2 CL system. The proposed method was applied to detect H_2S in rat brain microdialysate with a detection limit of 0.30 μM. But there still some disadvantages for CL method. For example, although many CL methods have been reported for sulfide detection, nearly all methods detect the total amount of compounds containing sulfide.

IC (Ion Chromatograph)

Gas Dialysis/Ion Chromatograph

Sulfide can be separated from other anions by ion chromatography (IC). A continuous flow gas dialysis pretreatment and quantitation by IC with electrochemical detection analytical technique has been successfully described by Goodwin et al. [204] and utilized to the determination of H_2S in brain tissue homogenates both in rats and humans with a detection range of 100 μM. The sulfide levels were determined selectively and without any interference from other blood components. Meantime, two case studies of human hydrogen sulfide inhalation fatalities are presented in the study. And significantly elevated sulfide levels were observed in both cases by employing the described method. A detection limit of 0.02 μg/g tissue of S^{2-} was determined in tissue homogenates of brain after employing the described protocol.

Microdistillation/Ion chromatography

Richardson et al. introduced a new method for the determination of H_2S in gastrointestinal contents and whole blood by microdistillation/ion chromatography. This method can overcome some problems, such as the volatile nature of the compound, and the viscosity and turbidity of the samples. The limit of detection of the method was determined as 2.5 μM [205].

Monobromobimane derivatization method

In principle, monobromobimane assay reaction with the thiol-specific species derivatization fluorescent agent monobromobimane (MBB) to sulfide-dibimane (SDB) through a nucleophilic reaction can also be classified as a fluorescent sensor case for H_2S species detection. Sor far, sulfide levels have been determined by the combined MBB derivatization method with HPLC–FLD and/or LC-MS/MS techniques. For addressing this type of method, most reported works with MBB method for RSS measurement were summarized and discussed in parapraph 1.3. Taken together, based on the literature survey, a detection limit range of commonly employed measuring assays were shown in **Figure 1.18**.

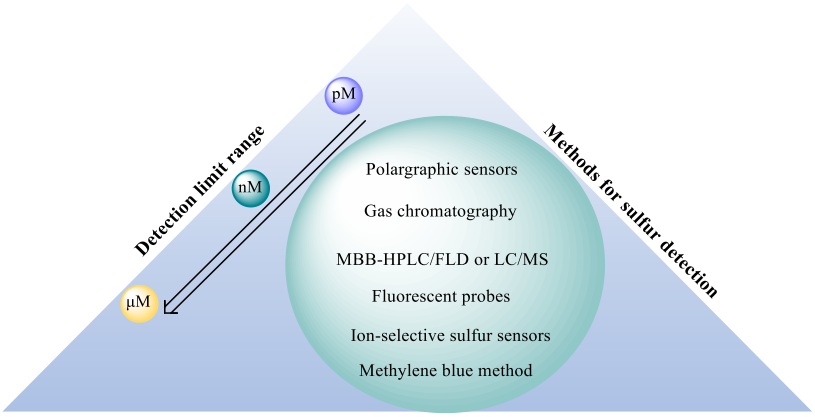

Figure 1.18 Range of limit of detection with commonly used sulfur measuring assays.

1.1.9 Monobromobimane (MBB) derivatization-based method coupled with HPLC-FLD and mass spectrometry for sulfur species measurement in biological samples

1.1.9.1 Application history of the MBB-derivatized method in biological contexts

Fahey et al. [213] and Newton et al. [214] were the first to report the use of MBB as a fluorescent probe for detection and quantitation of biological thiols in 1981. Subsequently, in 1984 Shea et al. [215] have modified the Fahey procedure and achieved the measurement of thiosulfate in plasma and urine by precolumn derivatization with MBB. Afterwards, Cotgreave

et al. [216] described quantitative determinations of cysteine and glutathione present in mixed disulfides with protein and in soluble low molecular weight disulfides and the estimates of intraprotein disulfides in a number of test biological systems. Untill 1995, Kosower et al. [217] described the use of four bromobimanes for fluorescent labeling of biochemical and biological systems and introduced these four commercially available compounds, MBB, dBBr, qBBr and SBBr which are the short form names. In the report, it noted that the *syn* series is generally fluorescent, while the anti-series is phosphorescent. And the latter have not yet been utilized for studies of biological systems. Therefore, in this present study, emphasis will be placed on *syn* series, especially on the fluorescent reaction involved in MBB reagent. The molecular formulas of the representative four bromobimanes were shown in **Figure 1.19**.

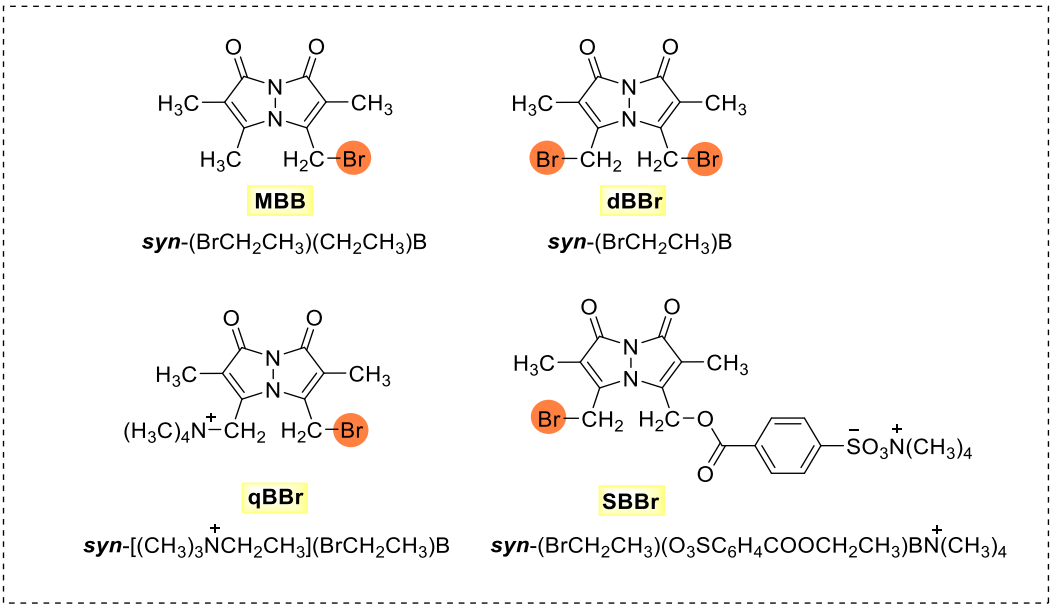

Figure 1.19 Four commercially available bromobimanes for fluorescent labeling of biochemical and biological systems.

As discussed in paragraph 1.1.6. RSS in the reduced state (–2 valence of sulfur), such as H_2S and thiols, are good nucleophiles, especially when deprotonated (HS^-, RS^-). Likewise, in 1995, as indicated in **Figure 1.20**, Newton et al. [218] was concerned with MBB and SBBr, then described the reaction of these reagents with thiols (RSH) to form the corresponding S-labeled products, MB-SR and SB-SR, which are stable and suitable for quantitative determination. In the chapter, main study of the investigator was focused on refinements and extensions of the MBB derivatization methodology. But different from MBB, SBBr is an anionic reagent that does not enter cells.

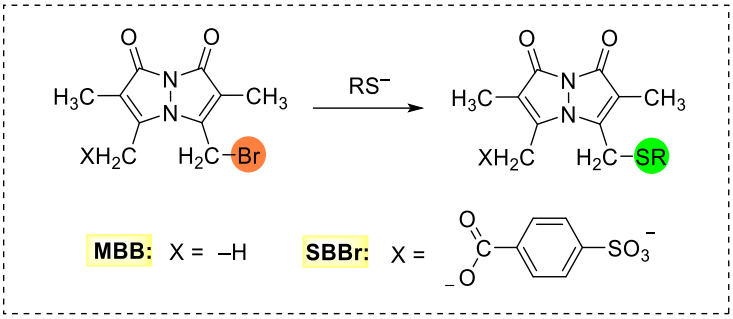

Figure 1.20 Reaction of MBB and SBBr with thiols (RSH) access to MB-SR and SB-SR.

Nowadays, it's well known that MBB is a fluorescent cell-permeable alkylating agent that reacts with extra- and intracellular sulfide pools and sulfhydryl-containing biomolecules. It can be used as an alkylating agent and rapidly derivatized with free H_2S chemical forms under moderate conditions [214]. The alkylation of sulfide is explained by the following steps illustrated at **Figure 1.21**. The reaction one is a bimolecular reaction between sulfide and MBB to give the intermediate sulfide-monobimane species (SMB). Afterwards, SMB is the target of the next nucleophilic attack by a second MBB molecule to yield the stable product sulfide-dibimane (SDB). The first step is critical as there are many parameters that must be tightly controlled to achieve reproducible results. The resultant product of this reaction, sulfide-dibimane (SDB), is fluorescent and stable and can be separated and quantitated. This allows for an accurate determination of absolute H_2S species present levels in various biological media [183, 185]. As a conclusion, the two key steps of the MBB derivatization method are selective and highly controlled alkylation of the target sulfur-mediated molecule. In this thesis, after conversion of H_2S species in human serum to the MBB derivative, followed by HPLC separation and fluorescent quantitation of the alkylated product can be achieved.

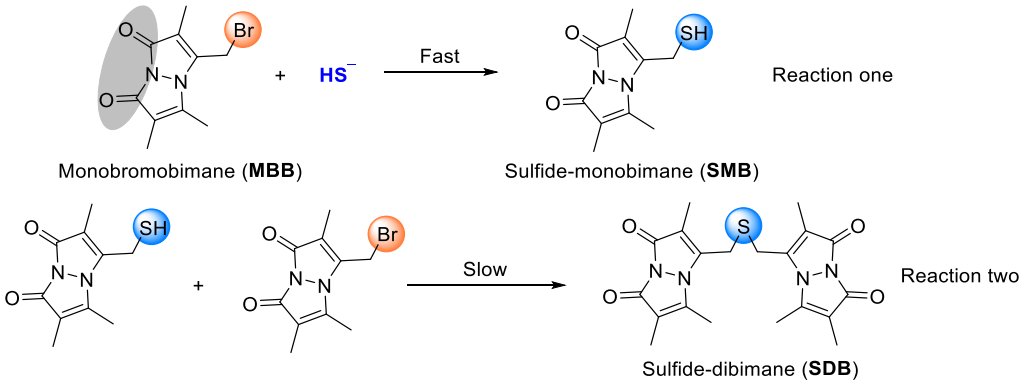

Figure 1.21 Chemical reaction principle of MBB and H_2S in aqueous solution.

Importantly, it's noteworthy that optical parameters are significant chromatographic conditions during method development for characterization of compounds. The derivatized product SDB has fluorescence which the excitation wavelengths at 390 nm, emission wavelengths at 475 nm, respectively. The maximum absorption is in the near UV (λmax =390 nm), it has no significant difference from the absorption of the MBB reagent (λmax = 396 nm) [217] [219].

Table 1.6 List of representative sulfur compounds and their predicted reaction with bromobimane (" + " indicates positive reaction, " – " indicates no reaction will occur)

Sulfur species	Molecular formula	Reaction with MBB
Hydrosulfide	HS^-	+
Sulfite	SO_3^{2-}	+
Thiosulfate	$S_2O_3^{2-}$	+
Per/Polysulfides	HSS_n^-/ RSS_n^-	+
Cysteine	$C_3H_7NO_2S$	+
Glutathione	$C_{10}H_{17}N_3O_6S$	+
Organic thiols	R-SH	+
Polythionates	$S_nO_6^{2-}$	–
Elemental sulfur	S^0	–
Sulfonate	$R\text{-}SO_3^-$	–
Sulfate	SO_4^{2-}	–

Due to the membrane permeability characteristic of MBB, It is frequently used as a suitable fluorescent alkylating agent, which selectively reacts with free sulfhydryl-containing biomolecules [214], and resulting in the liable H_2S rapidly derivatizing under gentle conditions [220]. Hence, the MBB method is highly sensitive and selective with the low limit of detection. Furthermore, attribute to its high sensitivity for most biological applications, the MBB method has found wide application ranging from clinical to studies investigating sulfide metabolism pathways [18]. Whereas, in the current study, only a few works using chemical derivatization with MBB in conjunction with high performance liquid chromatography-fluorescence detection/mass spectrometry (HPLC-FLD/MS) have been reported to make it suitable to quantify different sulfide pools in biological samples [179, 182], (see **Figure 1.22**). Therefore, the development of a quantitative MBB-sulfur derivatization involved method for simultaneous product separation and analysis in various biological samples with high accuracy and selectivity is still a matter of challenge. At present, some representative sulfur compounds find in literature

and their predicted reaction with bromobimane were summarized, as shown in **Table 1.6**.

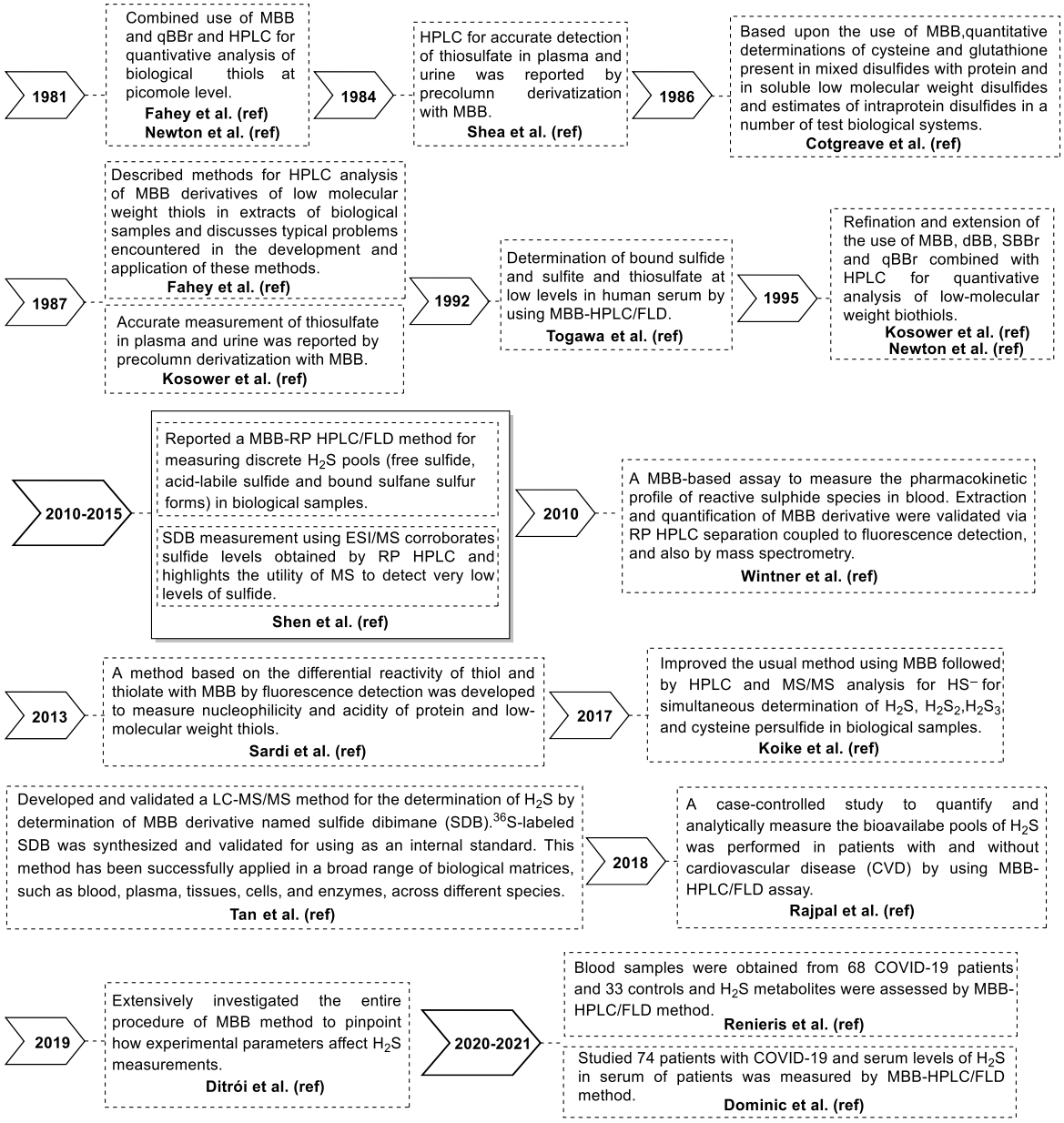

Figure 1.22 Major milestones in MBB-Sulfur mediated derivatization investigation and application.

1.1.9.2 Measurement of reactive sulfur species (RSS) able to convert into H_2S species by using MBB derivatization and hyphenation with spectrofluorimetry and/or mass spectrometry (MS)

As H_2S species can be generated from RSS like persulfide/polysulfide degradation, much of the reported biological activity associated with H_2S may indeed be that of sulfides. That is, H_2S may act primarily as a biomarker for the biologically relevance of per/polysulfide species etc. As it is expected that these divalent (−2) RSS are especially nucleophilic, most concentrations of reactive persulfides and polysulfides in biological samples were measured by the reaction with thio-specific derivatization agents. Additionally, mostly because of the low molecular weight and simple chemical structures of H_2S species and some other sulfur species it is not suitable for their direct quantification by spectrofluorimetry and/or MS. So, the target molecules always widely undertaken chemical derivatization step before determination. Following, the derivatized fluorescent products can be effectively separated by HPLC with relevant gradient elution programme and accurately quantified by fluorescent detector, diode array detector (DAD) and/or MS. This kind of assay procedure was established to measure various biological sulfide pools and it was refined and extended in few works to improve its reliability and reproducibility. Herein, the MBB derivatization method will be emphasized and introduced as one of the most frequently used method to measure reactive sulphide species, especially in H_2S species determination. This kind of MBB derivatization-based methods can be extensively applied and obtain unique developments during the quantitative analysis of available blood sulphide, particularly in sources from biological matrices. For example, the investigation released by Togawa and colleagues in 1992 [221], by using HPLC separation after conversion to MBB derivatives, a sensitive and specific method was established to detect bound sulfide, bound sulfite and thiosulfate in human serum with the determination results of low limits 0.5, 0.2, and 0.05 μM, respectively. These separated products were detected fluorometrically with excitation set at 396 nm emission at 476 nm and the maximum absorption in the near UV (λmax =390 nm). In this method, by addition of DTT, sulfide liberated from serum samples under the reducing condition was measured to be 1.30 ± 0.60 μM. On the contrary, without DTT treatment, no sulfide was observed, indicating that sulfide was bound to serum proteins, presumably as the persulfide. Noteworthy, this developed method was applied to the detection of the available

HS^- in normal human serum samples, which may include ionically bound HS^- in addition to the free H_2S, that is H_2S species.

Shen group applied for a patent successfully on measurement of biologically labile hydrogen sulfide pools [222]. Thereafter, starting from 2010 to 2015, they conducted a series of investigations and explorations on this topic of quantification of H_2S species, focusing on MBB derivatization method which is suitable for H_2S biological pools determination. Thus, H_2S species existing in biological medium would be rapidly derivatized with excess MBB resulting in forming a stable SDB product that can be subsequently quantified and identified by HPLC-FLD and/or ESI/MS. The resultant fluorescent SDB is analyzed by RP-HPLC using fluorescence detection with the limit of detection for SDB (2 nM). Besides, Shen group's well-established method has been robustly evaluated against the MB method of quantitative measurement of H_2S under different conditions. Also in their studies, it's illustrated that the measurement of hydrogen sulfide using the MB method provides erroneous results making it inappropriate for measuring levels of hydrogen sulfide in biological samples. So, they also put forward that associated results obtained from the current gold standard assay methylene blue are untrustworthy and do not actually quantify H_2S species. Below, some details for Shen's works and results were discussed.

MBB method was applied by Shen et al. in 2011, [182] to measure basal H_2S levels in the plasma of C57Bl/6 J (1.7 ± 0.05μM), CSE heterozygote knockout (0.5 ± 0.03μM), and CSE homozygote knockout mice (0.3 ± 0.03μM). These results indicated the presence of H_2S in plasma down to nanomolar levels. Following, in 2012 [183] free, acid-labile sulfide and bound sulfane sulfur levels were measured in the plasma of wild type C57BL/6J, CSE gene deficient mice and healthy human volunteers by Shen group. It found that the free hydrogen sulfide pool in plasma from healthy human volunteers to be in the low nanomolar level (0.25-0.7 μM/L), but that the acid labile pool was in the low micromolar range (1.5 − 3.5 μM/L). The bound sulfane sulfur pool was found to be significantly smaller like the murine models (0.35 − 0.45 μM/L). In 2013, Shen and coworkers [180] also examined concentration of H_2S in plasma from conventional and germ-free mice. Concentration of free H_2S were 0.025 − 0.03 nmol/mg protein and 0.007 − 0.012 nmol/mg protein in conventional and germ-free mice. Labile sulfide level was 0.06 − 0.08 nmol/mg protein both in conventional and germ-free mice. Bound sulfane

sulfur were 0.024 − 0.036 nmol/mg protein and 0.002 − 0.005 nmol/mg protein in conventional and germ-free mice. But for organ tissue, free H_2S was in the range of 0.15 − 0.9 nmol/mg protein. Labile sulfide and bound sulfane sulfur were 0.5 − 3.2 nmol/mg protein and 0.4 − 3.3 nmol/mg protein, respectively. Note to worthy, by using the similar derivatization/speciation method developed by Shen, Wintner et al. 2010 [185] have published the basal concentration of sulfide in rat blood which was measured by the approach MBB-HPLC/FLD, which was down to approximately 0.7 μM. In this method, a bioequivalence between infused Na_2S and inhaled H_2S gas was established for the first time. But it should be pointed out that both works from Shen and Wintner's contained the steps of extraction of the derivative then achieved the quantification goal. Besides, an MS-based metabolomic assay for the analysis of low-molecular weight persulfides/polysulfides and a proteomic analysis combined with a Tag-Switch assay to detect S-polythiolated protein adducts have been developed by Ida et al. in 2014 [223]. In the experiments, by using cystine as a substrate, the enzymes CSE and CBS can generate persulfide and CysSSH. Herein, regeneration of GSSH and GSSSH from GSSSG catalyzed by glutathione reductase (GSR), GSSSG reacted with GSR and NADPH in Tris·HCl buffer (pH 7.4) at room temperature and followed by incubation with 5 mM MBB at 37 °C for 15 min. Significant levels in the range of 50 – 100 μM of per- and polysulfides are detected in mammalian cells, tissues, and plasma (rodent and human).

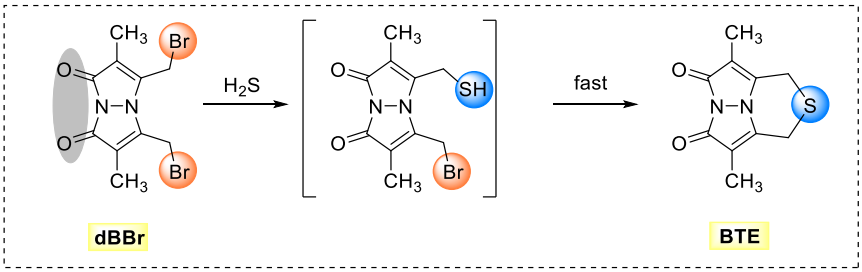

Figure 1.23 Reaction of dBB with H_2S forms the BTE product which can be quantified by fluorescence HPLC.

Additionally, the utilization of another alkylation reagent by Montoya et al. 2014 [224], di-bromobiane (dBBr) was developed for biological sulfide quantification. Reaction of H_2S with dBB can be in formation of bimane thioether (BTE) which is readily detected and quantified by HPLC−FLD. As indicated in **Figure 1.23**. And the mechanistic investigation has been revealed that the dBB derivatization-based method is proven to be highly sensitive for H_2S but it is incompatible for application in studies in which other thio-containing compounds exist.

Based on the prevalence of the MBB method for the quantification of biologically relevant sulfide pools, some investigators like Tan et al. 2017 [184] sought to broaden this method to report the use of other highly sensitive fluorescent alkylating agent. 3-bromomethyl)-2, 6, 7-trimethyl-1H, 5H-pyrazolo [1,2-a] pyrazole-1, 5-dione (MMB) is an isomer of MBB, which can react with hydrosulfide anion (HS^-) to produce sulfide-pardimane (SPB) under suitable conditions. Thereafter, SPB can be purified by RP-HPLC and quantified by a diode array detector (DAD) due to its hydrophobic property and strong ultraviolet-visible (UV-vis) absorptions. The limit of detection for SPB was down to 0.03 nmol/mL. Similarly, product SPB has strong UV-vis absorption (λmax = 390 nm) and fluorescence, and the interference from other substances is minimal when SPB was quantified by UV detector at 390 nm. As shown in **Figure 1.24** shows the nucleophilic reaction between MMB and thiols groups.

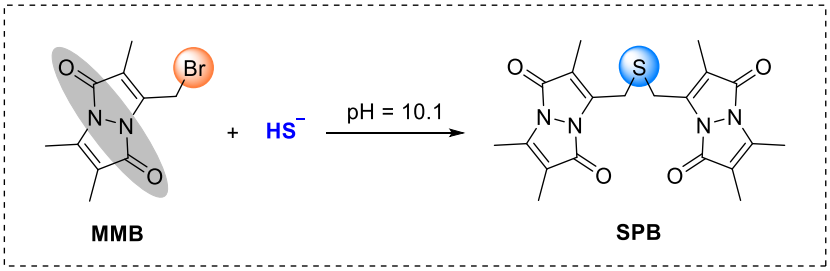

Figure 1.24 The proposed reaction between MMB (isomer of MBB) and HS^-.

Some actual studies also preceded by Tan et al. [184]. In Tan's work, in rat blood taken from the aorta, plasma was centrifuged, and a vascular calcification (VC) model was established by administration of vitamin D3 plus nicotine (VDN). In the VDN group, the mean H_2S content in plasma (22.48 ± 3.37 nmol/mL) was significantly lower than that of the control group (37.56 ± 4.88 nmol/mL) ($p < 0.05$). The H_2S content in the plasma of the VDN + NaHS group (33.48 ± 2.08 nmol/mL) was greater than that of the VDN group (22.48 ± 3.37 nmol/mL) ($p < 0.05$). This result was the same level as reported in 2015 by Shen et al. [181]. In 2018 and 2021, Renieris et al. and Dominic et al. applied MBB method to biological H_2S pools analysis which blood taken from COVID-19 patients. These results could conclude that H_2S is a potential marker for severity and outcome of pneumonia by the SARS-CoV-2 coronavirus. In 2019, Nagy and coworkers [178] systematically investigated a number of experimental parameters to improve the sensitivity of the derivatization protocol also reported the results of sulfide levels in human plasma, the range of free sulfide was 43 ± 2 nM, the acid sulfide and bound sulfane

sulfur were 2 – 4 μM and several nanomolar respectively. The detection limit is also in the low nanomolar range. Apart from normal derivatization step carried out in aqueous conditions, a novel three-layer H_2S chip was designed by Baniya et al. 2019 [225] (**Figure 1.25**). It is designed for separation of all pools of H_2S from plasma samples along with liberation, separation and trapping of H_2S steps the same procedure and reagents used as Shen group [183].

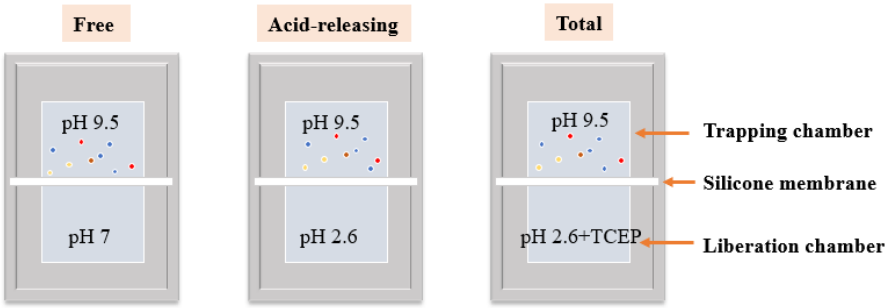

Figure 1.25 Schematic diagram of three-layer H_2S chip.

Ibrahim et al. 2021 [226] reviewed a wide variety of quantification methods employed for the measurement of H_2S in biological samples. It is noted that, in recent years, much attention has been concentrated on measuring sulfide levels by using the MBB method coupled with HPLC-FLD. It was employed to detect various biological sulfide pools with considerable sensitivity and the low nanomolar range of the LOD can be achieved. Interestingly, Malaeb et al. 2022 [227] described the first stable isotope dilution LC-MS/MS assay for hydrogen sulfide in biological matrices.

Though many endeavors have been previously published to measuring the level of H_2S, due to the ease of reacting with other species and H_2S species is easy to be oxidized. It is also rare to have a consensus for determination of the actual amount of bioavailable H_2S. In

Table 1.7, application of MBB method by using HPLC-FLD or LC-MS techniques for RSS measurements in some significant cases was summarized. To address this problem, we optimized the critical parameters of MBB method in the derivatization step and established a protocol for fast and easy detection of sulfide concentration. Then we examined H_2S bioavailability in its various forms including free, acid labile, and bound sulfane sulfur. And based on previous published results, we first time validated the method of quantification of H_2S in biological matrices which MBB method combined with HPLC-FLD were employed in this work.

Table 1.7 Application of MBB derivatization method hyphenated with HPLC-FLD or LC-MS for RSS measurements in previous studies.

Method	Sulfide type measured	Specimen type	Detected levels	Reference
MBB+HPLC-FLD	Free HS^-/H_2S	Human serum	Not detected	Togawa et al. 1992 [221]
		Plasma from mice	15 nM	Shen et al. 2010 [222]
	Protein-bound sulfide	Human serum	1.3 ± 0.6 μM	Togawa et al. 1992 [221]
	Free and reversible bound HS^-/H_2S	Whole blood from rat	0.4 – 0.9 μM	Wintner et al. 2010 [185]
		Various organs from mouse	ca. 0.108 – 0.904 pm/mg protein	Shen et al. 2013 [180] Yuan et al. 2015 [228]
		Plasma from human, rat, and mice	2 nM	Shen et al. 2015 [181]
	Free HS^-/H_2S	Blood from COVID-19 patients	0.3 μM	Dominic et al. 2021 [229]
	Sulfide pool	Human plasma	<7 nM	Shen et al. 2012 [183] Rajpal et al. 2018 [144]
MBB+LC-MS	Free and reversible bound HS^-/H_2S	Mouse brain	ca. 2.5 pm/mg protein	Morikawa et al. 2012 [230]
		Whole blood from mice, beagle dogs, domestic pigs and cynomolgus monkeys	0.3 – 1.2 μM	Wintner et al. 2010 [185]
		In plasma and tissues like aorta, heart, lung and brain	0.25 nM	Shen et al. 2014 [186]
	Persulfide/polysulfide	Mammalian cells , human plasma, mouse plasma, and tissue	micromolar range	Ida et al. 2014 [223]
	Free and reversible bound HS^-/H_2S	A broad range of biological matrices, such as blood, plasma, tissues, cells, and enzymes	sub-nanomolar scale	Tan et al. 2017 [187]
	H_2S and H_2S_n	Mouse brain	0.030±0.004 μmol/g protein and 0.026±0.002 μmol/g protein	Koike et al. 2017 [179]

Mass spectrometry is a powerful technique with higher sensitivity and specificity than other analytical detection methods. It can provide corresponding molecular weights and structural information for analytes, which make it more specific than fluorescence-based method [231]. Using derivatization based-HPLC coupled with ESI/MS methods for detection of standard derivate SDB was demonstrated to be a log-order more sensitive than HPLC-FLD, and with a lower detection limit of 0.25 nM [186]. More importantly, the previously data have confirmed that the application of sulfide dibimane is proven to be a valid indicator of H_2S bioavailability[187]. Recently, some works using different derivatization reagents to determine the concentrations of H_2S *in vitro* assisted liquid chromatography-mass spectrometry (LC-MS) have been published. Lee *et al*. utilized a novel stable isotope-coded thiol-reacting reagent (2-iodoacetanilide) to quantify hydrogen sulfide in HepG2 cells. The measurement of H_2S derivatives was exhibited good linear range 1 - 1000 nM [232]. Moreover, a pair of isotope reagents, *N*-(acridin-9-yl)-2-bromoacetamide (AYBA) and *N*-(1,2,3,4-[$^2H_4$]-acridin-9-yl)-2-bromoacetamide ([$^2H_4$]AYBA) were used to quantify low-molecular-weight thiols in human cervical cancer (HeLa) cells [233]. Both are for cellular metabolites analysis. Taken together, there only exist a very few endeavors with tandem mass spectrometry for the determination of biological H_2S concentrations which are simultaneously able to present advantageous sensitivity and selectivity. Therefore, it remains challenging to measure the levels of hydrogen sulfide accurately and reliably in a broad range of biological matrices, such as blood, plasma, tissues and cells by a validated and robust method with mass spectrometry.

In the present study, we employed reverse phase-HPLC coupled with both a conventional fluorescence detector (HPLC-FLD) and a state-of-art mass spectrometry (HPLC-MS) to examine the presence of H_2S in biological matrices by derivatization using MBB as the fluorescent alkylating regent. Herein, we quantified biologic hydrogen sulfide pools, that is free H_2S, acid-labile sulfide, and bound sulfane sulfur. This validated detection and quantification method allows for highly sensitive, accurate of endogenous hydrogen sulfide in complex biological matrices. It is thought to potentially provide comprehensive and precise information regarding critically evaluating hydrogen sulfide concentrations of biological relevance under normal or pathophysiological conditions.

1.2 Primary aim of this study

During my doctoral research activities, I mainly focused on optimization and validation of the MBB RP-HPLC method for sulfide determination, including its speciation for the determination of free sulfide, acid-labile sulfide and bound sulfane sulfur in human serum samples. This study is part of a collaboration with the Laboratorio RAMSES, IRCCS Istituto Ortopedico Rizzoli and it aims to demonstrate the use of sulfide as biomarker in some orthopedic diseases. This work has been published in 2022 [234]. Overall, the study is described in detail according to the following points:

A detailed experimental condition analysis was carried out, focusing on the parameters applied during the derivatization reaction procedure, which are based on a two-step nucleophilic reaction of fluorescent reagent MBB with sulfide compounds. A comprehensive study was conducted on advantages, disadvantages, and limitations of the key parameters, shedding light on the significance of the employed experimental conditions (temperature, MBB concentration, pH value, incubation time and serum sample handling) to obtain adequate readouts able to reflect the real derivatization.

Meantime, the objective of validation of an analytical procedure is to demonstrate its ability for the intended purposes. Therefore, we aimed to the validation of quantitative analytical method MBB RP HPLC-FLD used in this study. Corresponding validation of the calibration procedure for H_2S species quantification was proposed and established for the first time. Parameters like linearity (both statistical analysis of lower and higher range of Na_2S standard solutions were included). LOD, LOQ, accuracy, precision, and repeatability were determined according to ICH harmonized tripartite guideline Q2(R1) [235].

The optimized detection method has been applied to human sera obtained from treating patients in sulfur spring where cause the production of a naturally occurring H_2S gas to monitor the true state of the sulfur concentration levels, which may associate with the pathogenesis of various diseases.

1.3 Experimental approach

1.3.1 Chemicals and Supplies

Anhydrous sodium sulfide (CAS: 1313-82-2, Na_2S, Sigma-Aldrich, Cat. No. 407410-10G HPLC grade, purity ≥98.0%, product of USA), Monobromobimane (CAS: 71418-44-5, MBB, Sigma-Aldrich, Cat. No. 4380-10MG purity ≥97%, product of USA), Tris(hydroxymethyl)aminomethane (CAS: 77-86-1, Sigma-Aldrich CHEMIE GmbH, Cat.:15,456-3 Lot.:01927DE-417 Tris-base, purity ≥99.9%, ultrapure grade, product of Germany), Trifluoroacetic acid (CAS: 76-05-1, TFA, Sigma-Aldrich, Cat. No. T6508-500MLHPLC grade, purity ≥99.5%, product of USA), 5-sulfosalicylic acid dihydrate (CAS: 5965-83-3, SSA, Sigma-Aldrich CHEMIE GmbH, Cat. No. S2130-100G purity ≥99.0%, product of Germany), Sodium dihydrogen phosphate dihydrate (CAS: 13472-35-0, $NaH_2PO_4 \cdot 2H_2O$, Sigma-Aldrich, Cat. No. 71500-250G, product of Italy), Diethylenetriaminepentaacetic acid (DTPA) (CAS: 67-43-6, purity ≥99.0%, Sigma-Aldrich, Cat. No. D6518-5G, product of USA), Tris(2-carboxyethyl) phosphine (CAS: 51805-45-9, TCEP, Sigma-Aldrich, Cat. No. C4706-2G), purity ≥98.0%, product of India), bovine serum albumin lyophilized powder (CAS: 9048-46-8, BSA, Sigma-Aldrich, Cat. No. A2153), Hydrochloric acid (CAS: 7647-01-0, HCl, 37%, Sigma-Aldrich CHEMIE GmbH, Cat. No. 30721-1L-M, product of Germany), and Phosphoric acid (CAS: 7664-38-2, H_3PO_4 85%, Sigma-Aldrich, Cat. No. 695017-500ML) were used to adjust the pH value of the buffer solution and purchased from Merck (Darmstadt, Germany). Acetonitrile (CAS: 75-05-8, ACN, Sigma-Aldrich, Cat. No. 34851-2.5L, purity ≥99.9%, ultrapure grade, product of France) and LC-grade methanol (CAS: 67-56-1, MeOH, Sigma-Aldrich, Cat. No. 34860-1L-R) were obtained from Merck. The purified deionized water used throughout the study was obtained from a Milli-Q purification system (ELGA LC134, 0.2-micron filter, 18.5 mΩ cm^{-1}, Merck Milli-pore, Darmstadt, Germany). Sterile 2 mL BD Vacutainer tubes with clot/activator (BD Vacutainer®, Plastic Serum Tube 2 mL with Red Hemogard Closure. Cat. no. 368493, additive: Silica (Clot Activator)) were used to collect serum samples from patients. BD empty tubes (Vacumed®, 13 × 75 mm no additive x 3 mL of blood, Cat. no. 42912, white cap) were used during the determination of different H_2S levels in serum. BD Quincke point spinal needles

20G 0.9 × 90 Mm were used during the speciation protocol.

1.3.2 Instrumentation and analytical methods

Derivatized samples were separated and SDB was quantified using an Agilent 1260 Infinity HPLC system, equipped with a G1379B degasser, G1312B binary gradient pump, G1329B autosampler, G4212B diode array detector, G1321A fluorescence detector, and a Chemstation Chromatography Workstation. Separations were carried out at room temperature on an Agilent Eclipse XDB-C18 chromatography column (4.6 × 250 mm), with an average particle size of 5.0 µm.

Analyte separation was performed using a binary mixture comprising a mobile phase A (water) and a mobile phase B (acetonitrile), which were adjusted with 0.1% (v/v) trifluoroacetic acid (TFA), at a flow rate of 0.6 mL/min. The gradient elution started at 85:15 (v/v) and decreased to 68% water in 3 min. Then, it dropped to 55% and remain this gradient for 13 min. Afterwards, the system was kept in isocratic elution mode for 1 min and then brought back to initial conditions 85:15 (v/v) in 3 min, and left in this condition for 3 min to stabilize the pressure of the chromatographic system. The chromatographic separation was thus completed in 23 min. **Table 1.8** shows the HPLC conditions.

Table 1.8 HPLC condition and gradient eluent program.

Column	Eclipse XDB-C18 column, 4.6 × 250 mm, 5.0 µm			
Temperature	Ambient			
Eluent A	H_2O (%) + 0.1%TFA			
Eluent B	ACN (%) + 0.1%TFA			
Detection	Fluorescence detector at Excitation 390 nm, Emission 475 nm			
Injection volume	30 µL			
Gradient timetable	**Time (min)**	**A%**	**B%**	**Flow rate (ml/min)**
	0	85	15	0.6
	3	68	32	0.6
	16	55	45	0.6
	17	85	15	0.6
	20	85	15	0.6

Specifically, the excitation and emission wavelengths of the fluorescence detector were set to Ex390nm and Em475 nm, respectively. Quantitative determinations were carried out using

peak area measurements at the emission wavelength. The absorption wavelengths of the UV detector were set at both 276 nm and 390 nm where SSA and MBB/SDB have maximum absorption. The sample volume injected in the chromatographic system was optimized and set at 30 µL. All solutions were filtered prior to analysis through a 0.2 µm syringe filter and injected in three replicates. The data were processed, and the area signals were integrated using an automated software system. Chromatographic peaks were checked, and identification was achieved by comparing retention times. Additionally, to confirm the peak identity, an UPLC chromatographic system model (ACQUITY H-CLASS) coupled with a model Xevo G2-XS Quadrupole/Time Of Flight Mass Spectrometer (UPLC-QTOF-MS, Waters Corp. Milford, MA, USA) was used. The mobile phase, gradient program, and column were the same as used for the HPLC-FLD system. The injection volume was 10 µL. Procedures applied on sulfide pools determination of biological specimen by coupling with MBB method and analytical techniques including HPLC-FLD and UPLC-ESI/MS were shown in **Figure 1.26**. The instrumentation set-up was described in detail in the following sections.

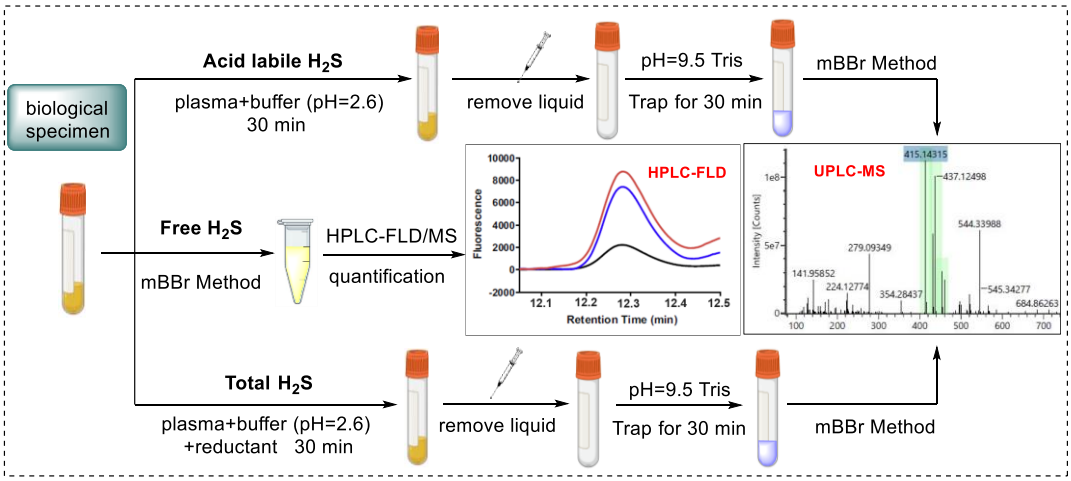

Figure 1.26 Overview of MBB method for measuring free sulfide and sulfide pools in human serum samples.

1.3.2.1 Glove box

According to the literature survey, we learned that the chemical mechanism of sulfide oxygenation process is quite complicated, and thiosulfate production is predicted to predominate when the flux of H_2S is low and oxygen tension is high. Oxidation of sulfide may either produce or consume hydrogen ions, depending on the products and other conditions. As shown in the equation is the course of the oxidation reaction in **Figure 1.27**.

$$2HS^- + O_2 + 2H^+ \longrightarrow 2H_2O + 2S \quad (1)$$

$$2HS^- + 2O_2 \longrightarrow H_2O + S_2O_3^{2-} \quad (2)$$

$$2HS^- + 4O_2 \longrightarrow 2SO_4^{2-} + 2H^+ \quad (3)$$

Figure 1.27 Oxidation of aqueous hydrosulfide ions by oxygen.

To prevent and mitigate the effects possibly caused by the oxygen tension, both derivatization and speciation steps were optimized and carried out in a hypoxia chamber (1% O_2). In **Figure 1.28** it is shown the type of glove box instrumentation applied in this work.

Figure 1.28 Scienceware Portable Glove Box System H50028-0000.

1.3.2.2 Ultra performance liquid chromatography electrospray ionization time-of-flight mass spectrometry (UPLC-ESI/TOF MS)

Instrumentation system consist of two main parts:

1) UPLC Waters ACQUITY H-CLASS: It allows for the separation and purification on analytical scale of chemical compounds from simple or complex mixtures.

2) Waters Xevo G2-XS QTOF MS with ESI source: This system allows for determination of the accurate mass of the analyzed chemical compounds thus managing determination of the molecular formula.

In this study, ESI-TOF MS analyses were performed in negative-ion mode. ESI-TOF conditions were: capillary voltage, 3kV; sample cone voltage, 40 V; ion source temperature, 120 °C; desolvation temperature, 600 °C; cone gas flow, 50L/h; desolvation gas flow, 1000L/h; mass range: 50 – 1200 m/z; sample flow rate, 0.6 ml/min.

1.3.3 MBB-sulfur derivatization step

It's known several experimental analytical conditions of the MBB protocol derivatization, particularly in the first step of alkylation of H_2S/HS^-, can change the endogenous balance of H_2S species, possibly resulting to readouts that do not represent the true speciation and the correct "free sulfide levels" in biological samples. In particular, alkylation has been shown to perturb sulfur speciation and influence sulfide detection in a concentration- and time-dependent manner. For example, at high concentration MBB can cleave longer dialkyl polysulfide chains and extract H_2S from these bound sulfane-sulfur pools, thus leading to the shifting speciation of sulfur species; MBB can liberate sulfide from sulfide pools when increasing reaction times above 7 – 10 min [193]. Moreover, light exposure can influence the measurement as MBB is a light sensitive reagent [183]; fluorescent light and sunlight cause a significant loss in measured sulfide levels [178]. Another critical experimental setting is the reaction temperature: while 4 °C was shown to minimize enzymatic production or degradation of H_2S [183], raising the temperature to 37 °C increased the values by 4 – 5 times compared to room temperature (RT) [178]. Finally, other critical parameters include pH (increased pH results in increased releasing [178]), and the influence of O_2 (1% represents the ideal condition for derivatization yield) [182].

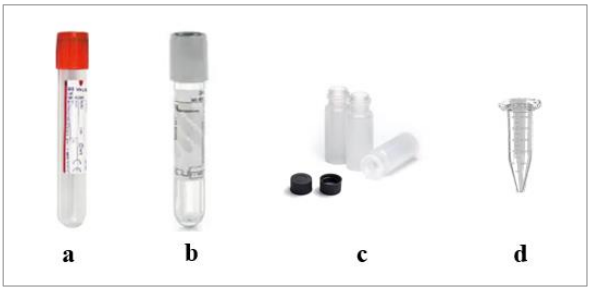

Figure 1.29 Various types of tubes used during optimization step.

Moreover, as the anion HS^- and H_2S have a high propensity to oxidize, especially in the presence of trace metal ions in water solutions [236], the presence of chelators (such as DTPA and EDTA) are needed; this can increase derivatization yield. The tubes used for blood sampling with or without additive can also affect the reaction yield [178]. Different tubes containing (a) BD vacutainer tube with clot-activator/gel additive, (b) BD vacutainer tube without additive, (c) Polypropylene tube and (d) Eppendorf tube was used during optimization of the speciation step (see **Figure 1.29**).

In addition, a validated calibration procedure has not yet been described in previous literature. Most papers described protocols for free H_2S quantification in human serum; however, only a very few papers reported the application of the HPLC-FLD method for determination of the H_2S species (free, acid-labile, and bound sulfane sulfur) [181, 183]. Based on the MBB methods proposed, here we optimized and validated a highly sensitive, robust, and high throughput HPLC-FLD method for the selective determination and quantification of free, acid labile, and bound sulfane sulfur in human serum samples. Among the derivatization parameters, applied MBB concentration, temperature and sample handling conditions were more thoroughly studied in this work to develop a robust protocol able to limit potential alterations of H_2S pools. Furthermore, corresponding validation of the calibration procedure was proposed for the first time; linearity, LOD, LOQ, and repeatability were determined.

1.3.4 Preparation of Buffer Solutions and Reagents

The 100 mM phosphate buffer solution (PB-A) was prepared by mixing 80 mM $NaH_2PO_4 \cdot 2H_2O$ with DTPA at a final concentration of 0.1 mM. The pH value was adjusted to 2.6 by adding 0.1M phosphoric acid (H_3PO_4). The 100 mM phosphate buffer solution (PB-B) was obtained by addition to PB-A solution with TCEP at a final concentration of 1.0 mM. Due to the rapid oxidation of sulfide, high pH buffers containing reducing agents must be used for an accurate determination of this form of sulfur. The 100 mM Tris-HCl buffer solution was prepared by mixing Tris-base with DTPA at a final concentration of 0.1 mM. Then the pH value was adjusted to 9.5 by adding 0.2 M hydrochloric acid (HCl).

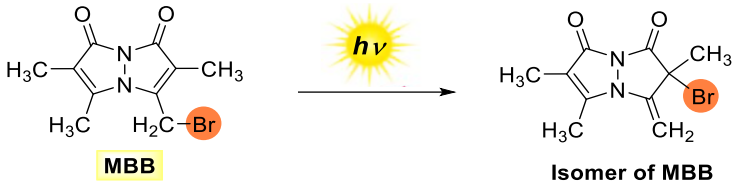

Figure 1.30 Photolytic isomerization of MBB derivative give exomethylene derivative.

Notably, the MBB reagent is moderately soluble in medium polarity organic solvents such as acetonitrile and dichloromethane, and it is slightly soluble in water. Therefore, we choose to prepare a 1.5 mM solution of MBB dissolved in acetonitrile. This solution was kept in an amber container and protected from light to avoid photolysis. Otherwise, the MBB is susceptible to convert into the isomer , as shown in **Figure 1.30** is the structure of exomethylene derivative

[237]. Unless otherwise specified, all stock solutions were prepared daily and used within an hour of preparation to reduce oxidation caused by exposure to oxygen [200].

1.3.5 Standard and Solutions

Exogenous administration: In experimental settings, levels of H_2S can be manipulated by the administration of exogenous H_2S or H_2S releasing compounds. Exposure to gaseous H_2S, sulfide-sodium salts, slow-releasing H_2S donors, hybrids of H_2S-donors and other known substances, such as thiosulfate, cysteine analogs and modulation of the expression or activity of H_2S producing enzymes are several options for adjusting H_2S levels commonly used in experimental settings. In this present study, we designed sulfide-sodium salts to simulate the H_2S levels, and exposure to gaseous H_2S thermal spring as a novel treatment for patients by altering their H_2S levels. Therefore, sodium sulfide (Na_2S) was employed as a source of H_2S for standard solutions in the following biological investigations. The use of Na_2S in such studies is reasonable since both H_2S and Na_2S form HS^- rapidly in aqueous solutions resulting in comparable physiologic and toxicologic responses. Firstly, a 5 mM stock solution of Na_2S in water was freshly prepared and stored in an opaque centrifuge tube at RT. Seven calibration standards (0.8, 1.6, 3, 6, 12.5, 25, and 50 μM Na_2S) were then prepared by diluting the original stock solution with MilliQ water. Water and solvents were deoxygenated by sonication before usage, and every day all working standard solutions were freshly prepared for derivatization. The use of a micropipette allows for the same specification in the process of dilution (1000 μL micropipette), then minimize the system error among every calibration series.

1.3.6 Patients and serum samples

The presented method shows high sensitivity and allows for the quantification of H_2S species with a limit of detection of 0.5 μM introduced in the section of paragraph 1.4 Results. It can be then successfully applied for measurements of H_2S levels in the serum of patients subjected to inhalation with vapors rich in H_2S. The validated procedure was applied to serum samples obtained from 4 post-menopausal women (age: 55 ± 2.9) recruited at the Rizzoli Orthopedic Institute. Under informed consent (AVEC 442/2018/OSS/IOR), patients were subjected to inhalation treatment of sulfureous waters at the thermal spring of Castel San Pietro Terme (Bologna, Italy), where the concentration of H_2S is 14.6 mg/L.

Each patient underwent a cycle of 30-min inhalation treatment for 12 consecutive days. Blood samples were taken before the treatment (T0), immediately after the 12-day treatment (T1), and three days after completion of the treatment (T2) (see **Figure 1.31**.) Blood samples were collected in "serum collection tubes" that were carefully sealed to avoid leaking of the gaseous phase. Serum was collected by centrifugation of blood at 3500 rpm for 15 min at 4 °C. Serum samples were transferred in polypropylene tubes and immediately frozen at −20 °C, for up to 1 month until analysis, with no further cycles of freezing and thawing.

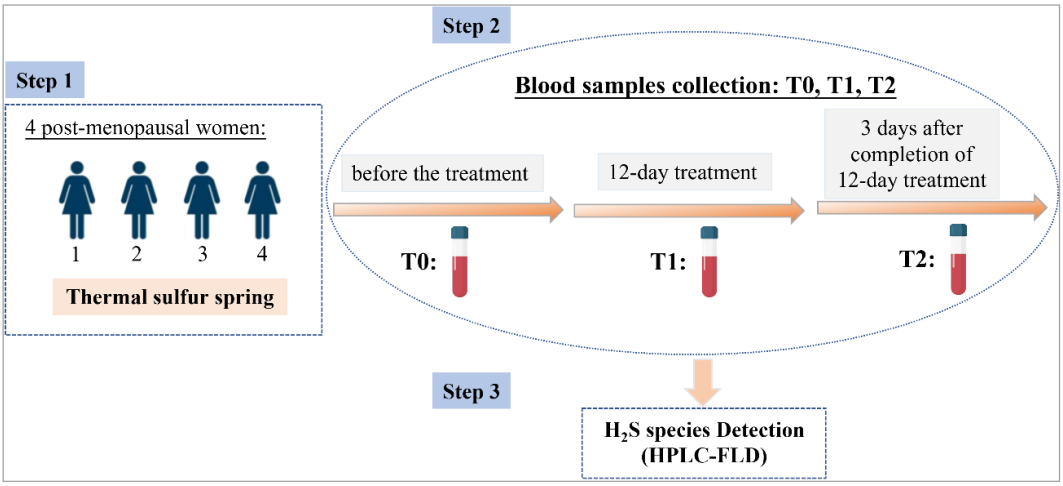

Figure 1.31 Schematic illustration for serum samples collection from patients.

1.3.7 Derivatization procedure

Before the derivatization procedure, all the materials were placed in a hypoxic chamber, which was then purged with nitrogen gas to 1% O_2. All working solutions were freshly prepared, and the entire derivatization procedure was carried out as quickly as possible and under dim light environment.

The protocol chosen for the derivatization of H_2S species with MBB was as following. Firstly, 30 µL of standard solution or blank or serum sample was mixed with 70 µL Tris-HCl buffer solution and 50 µL of 1.5 mM MBB. Eppendorf PCR tubes containing these reagents were immediately capped tightly, vigorously vortexed for 5 s, and incubated in dark condition for 30 min at RT. Then, the reaction was stopped by adding 50 µL of 200 mM 5-sulfosalicylic acid (SSA) to the tubes, which were further vortexed for 5 s. SSA quenches the reaction by two ways: 1) it causes precipitation of the dissolved proteins inside the serum samples; 2) it causes fluorescence quenching of bovine serum albumin (BSA) through a static quenching mechanism

[238]. Finally, 200 µL of the resulting solution was transferred from PCR tubes to autosampler vials equipped with a 200 µL plastic insert vial for HPLC quantification of the SDB derivatization product. It must be mentioned that H_2S readily binds to glass materials. Therefore, polypropylene plastic insert vials were used for preparation of samples in this investigation.

1.3.8 Detection of H_2S species in serum samples

'H_2S' will be used as a generic term to encompass the mixture of H_2S, HS^-, and S^{2-} that exist in equilibrium in aqueous solutions at the actual pH value. To obtain free H_2S values (free H_2S, HS^- S^{2-}), the derivatization procedure was applied to serum sample by centrifuging the final reaction samples at 13,000 g for 10 min before transferring supernatants into the HPLC vials, and then analyzing them by HPLC-FLD. In **Figure 1.32** and **Figure 1.33**, the H_2S speciation and derivatization step are respectively shown.

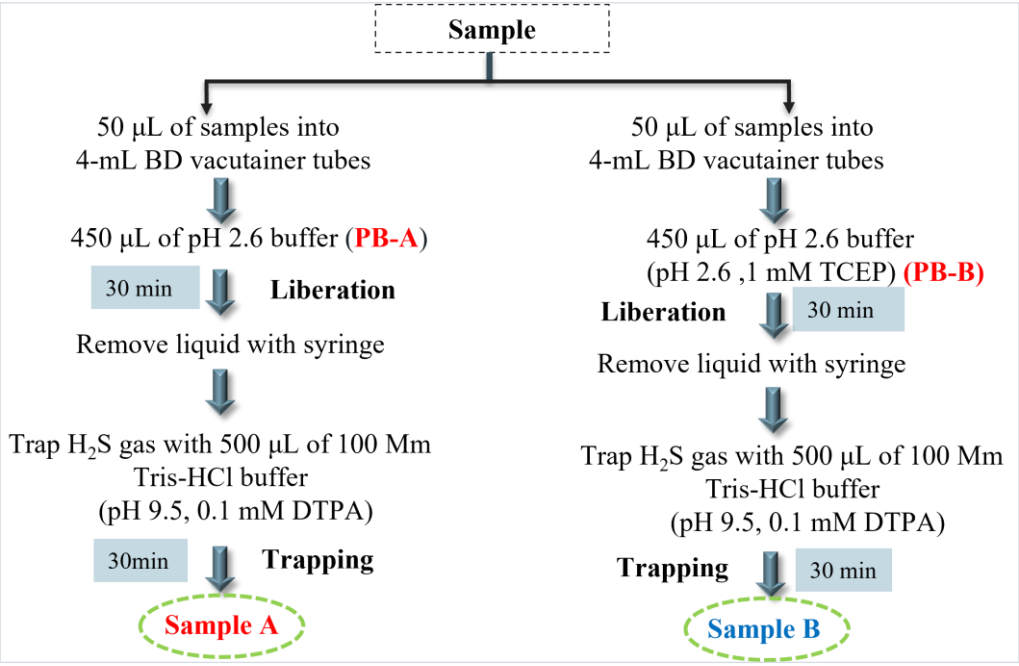

Figure 1.32 Schematic illustration of the workflow for H_2S species speciation step.

The acid-labile sulfide and bound sulfane sulfur were detected following the speciation protocol based on the selective liberation of H_2S, as already described by Shen et al. [183]. Briefly, a volume of 50 µL of serum samples was added into two sterile empty BD vacutainer collection tubes without additive. Subsequently, 450 µL of PB-A or PB-B was added to the two tubes, respectively. Notably, PB-A solution was maintained at a pH 2.6and keep sample in an acidic environment. Thus, H_2S can be released from acid labile pools; PB-B contains TCEP, which

cleaves the disulfide bonds of sulfane sulfur and releases sulfane sulfur atom. After 30 min incubation on a rocker, all tubes were placed in a hypoxic chamber and the solution was removed using a syringe with a spinal needle (1.0 mL) without inverting the tubes. Hereafter, 500 µL of Tris-HCl buffer solution was added, to trap the volatilized H_2S for 30 min incubation on the rocker. All procedures of volatilization and trapping of H_2S were conducted in a hypoxic chamber at RT.

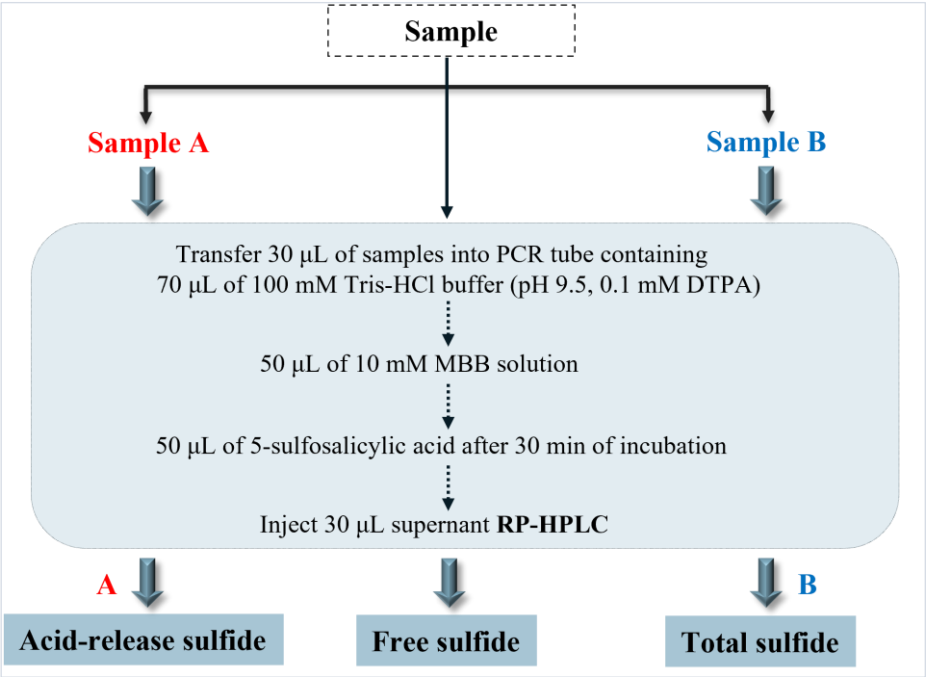

Figure 1.33 Schematic illustration of the derivatization workflow for H_2S species.

Finally, an aliquot of solution was derivatized from each tube following the procedure described above, and analyzed using HPLC-FLD technique. The sample treated with the acid liberation protocol (PB-A) gave the acid sulfide value (acid-released H_2S), while the sample treated in acid condition, with the addition of the reducing agent TCEP (PB-B) for disulfide bonds, gave the total sulfide value (total H_2S). Finally, the acid-labile sulfide level and the bound sulfane sulfur levels were calculated as follows:

$$\textit{acid-labile sulfide level} = \textit{acid-released } H_2S - \textit{'free } H_2S\textit{'}$$

$$\textit{bound sulfane sulfur level} = \textit{total } H_2S - \textit{acid-released } H_2S$$

The acid-labile sulfide level is calculated by using the acid-released value minus the free sulfide value. The bound sulfane sulfur level is calculated by using the total H_2S value minus the value of acid-released H_2S.

1.4 Results

1.4.1 Method validation and statistical analysis

The calibration procedure was defined and validation parameters, such as linearity, LOD, limit of quantification (LOQ), intra- and inter-day precision, and matrix effect, were determined.

Calibration curves were performed using seven Na_2S standards (0.8 – 50 μmol/mL) as described in paragraph 2.3. The absolute peak area was plotted against the different derivatization products concentrations, and the curves were fitted both by polynomial and linear regression analysis. LOD and LOQ were calculated for the linear model as, respectively, 3.3 and 6 times the ratio between the root mean squared error (RMSE) and the slope of the model. RMSE is defined as the mean of the squared differences between the experimental responses and the response values recalculated by the model.

Five replicates of each point were analyzed to determine the intra- and inter day precision. This process was repeated three times over three days to determine the inter-day precision using freshly prepared calibration curves. Significant differences between inter- and intra-day replicates were checked by Student's t-test.

All values are reported as Mean ± Standard Deviation. Statistics were performed by using R statistical software (R Core Team, Vienna, Austria).

Data obtained from human samples were analyzed with an ANOVA test for repeated measures, followed by a Dunnett multiple comparison test.

Method validation is a process of proving that an analytical method is acceptable for the intended purpose [239-241]. It is a documented evidence, which provides a high degree of assurance that it will consistently meet its pre-determined specifications and quality attributes [242]. In pharmaceutical industry, chromatography is most commonly used technique for quantitative and qualitative analysis of drug substances including those of biological origin [243-245]. Specifically, in this work HPLC-FLD was applied for quantitative determination of biomarker H_2S species in human serum. To validate the analytical method, experiments must be performed to fully characterize some critical parameters, such as sensitivity, linearity, precision, repeatability, limit of detection (LOD), and limit of quantification (LOQ). All these

parameters were routinely determined within the framework for method validations established by regulatory bodies such as the International Conference for Harmonisation (ICH), the US Food and Drug Administration (FDA), the United States Pharmacopeia (USP), and the International Union of Pure and Applied Chemistry (IUPAC) .

Sensitivity and linear range

A key characteristic of any sensing platform is its sensitivity towards a target analyte. As such, we investigated the response of MBB fluorescent probe (1.5 mM) when exposed to a range of Na_2S concentrations. Fluorescence response of the product SDB examined in inter-day and intra-day were shown in the **Figure 1.34**. When exposed to different range of Na_2S concentrations. The results demonstrated increasing fluorescence intensities in different concentration ranges 0.8 – 6 μM and 0.8 – 50 μM, respectively, indicating a different sensitivity range towards H_2S species.

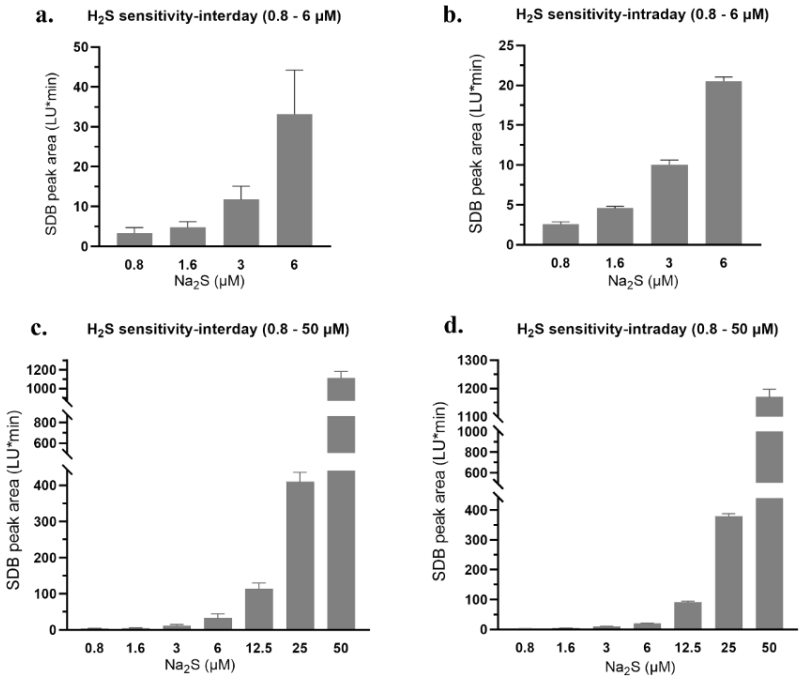

Figure 1.34 Fluorescence response of SDB examined during inter-day and intra-day when exposed to increasing concentrations of Na_2S which in the range 0.8 – 6 μM and 0.8 – 50 μM, respectively. (Data represent the average values of n = 3 measurements)

As shown in **Figure 1.35**, linear correlation and non-linear regression (3 datasets) were employed in a concentration range 0.8 – 6 μM and 0.8 – 50 μM, respectively. A higher correlation coefficient was demonstrated with intra-day datasets than inter-day datasets for the range of 0.8 – 6 μM and 0.8 – 50 μM indicating a good fitness of intra-day experimental data.

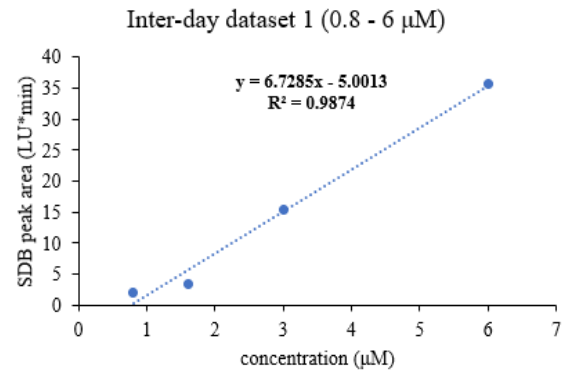
Inter-day dataset 1 (0.8 - 6 µM)
y = 6.7285x - 5.0013
R² = 0.9874
SDB peak area (LU*min)
concentration (µM)

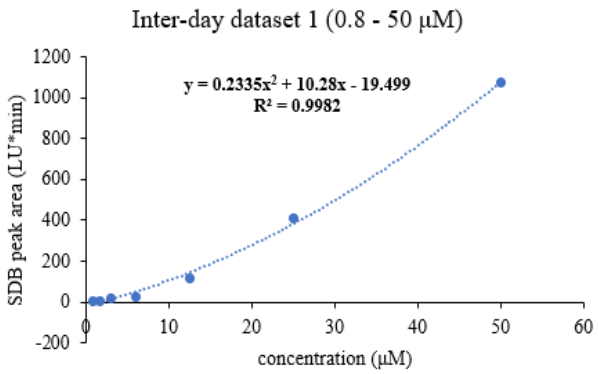
Inter-day dataset 1 (0.8 - 50 µM)
y = 0.2335x² + 10.28x - 19.499
R² = 0.9982
SDB peak area (LU*min)
concentration (µM)

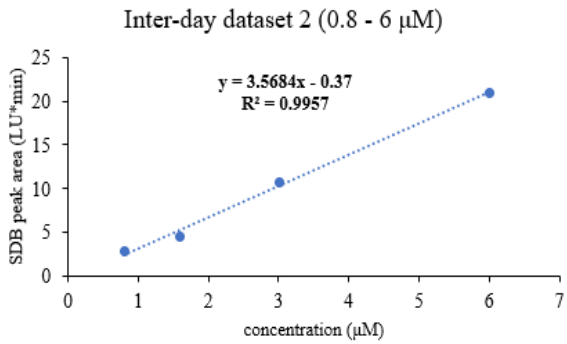
Inter-day dataset 2 (0.8 - 6 µM)
y = 3.5684x - 0.37
R² = 0.9957
SDB peak area (LU*min)
concentration (µM)

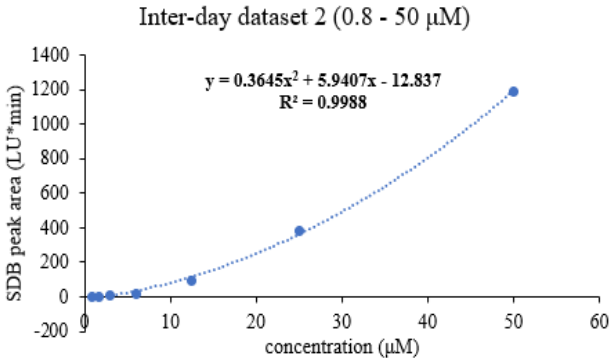
Inter-day dataset 2 (0.8 - 50 µM)
y = 0.3645x² + 5.9407x - 12.837
R² = 0.9988
SDB peak area (LU*min)
concentration (µM)

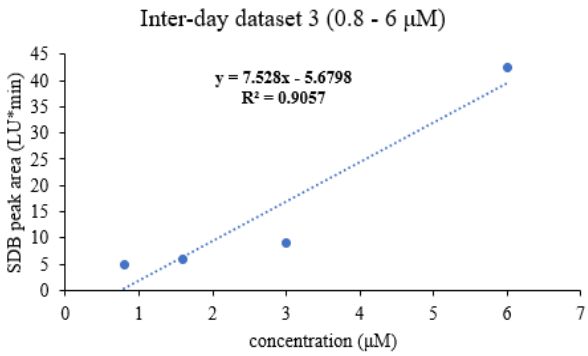
Inter-day dataset 3 (0.8 - 6 µM)
y = 7.528x - 5.6798
R² = 0.9057
SDB peak area (LU*min)
concentration (µM)

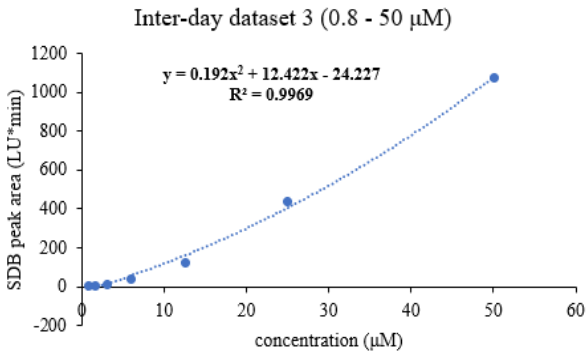
Inter-day dataset 3 (0.8 - 50 µM)
y = 0.192x² + 12.422x - 24.227
R² = 0.9969
SDB peak area (LU*min)
concentration (µM)

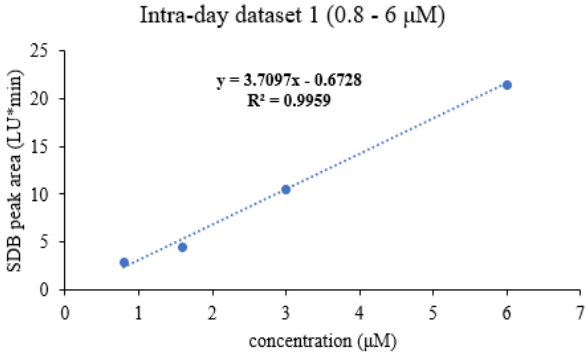
Intra-day dataset 1 (0.8 - 6 µM)
y = 3.7097x - 0.6728
R² = 0.9959
SDB peak area (LU*min)
concentration (µM)

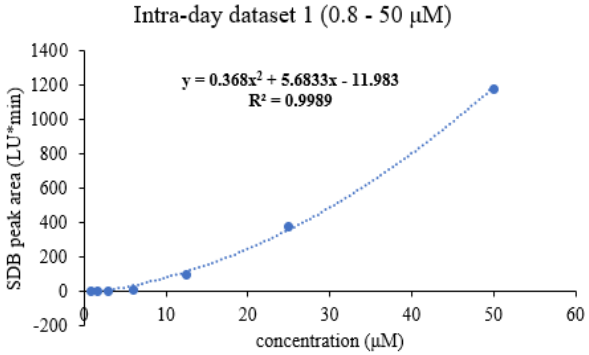
Intra-day dataset 1 (0.8 - 50 µM)
y = 0.368x² + 5.6833x - 11.983
R² = 0.9989
SDB peak area (LU*min)
concentration (µM)

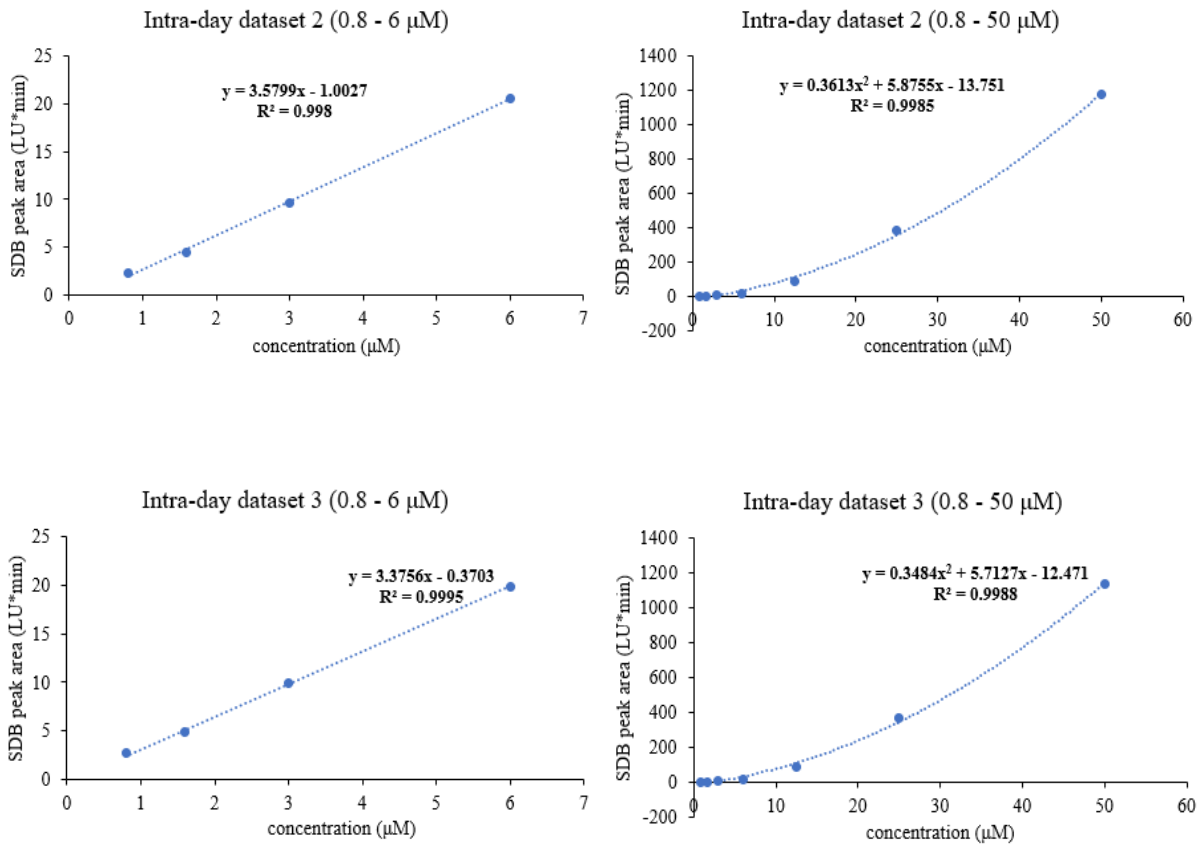

Figure 1.35 Linear (0.8 – 6 µM) and polynomial (0.8 – 50 µM) regression analysis showing correlation between concentration of Na_2S and fluorescent intensity of SDB.

Intra-day and inter-day precision (repeatability)

Calibration curves were performed using seven Na_2S standards (0.8-50 µmol/mL), as described in paragraph 1.5.5. The data points of calibration curves were repeated in triplicates on the same day for intra-day precision and on three different days for inter-day precision (

Table 1.9). Relative standard deviation (RSD) was less than 15% which is acceptable according to ICH guidelines. To evaluate robustness of the method, repeatability of experimental responses of the calibration standards was investigated. Three measurements were prepared for each concentration on three different days and the average of the relative experimental responses was calculated. Similarly, average of the three repeated intra-day measures was calculated. To verify whether the averages corresponding to the same concentrations obtained in intra-day and inter-day are significantly different or not, a comparison *t-test* was performed with confidence level set at 95%.

Table 1.9 Precision study for the determination of H_2S species derived from Na_2S standard solution.

(*% Relative Standard Deviation* = % *RSD* = $\frac{SD\ (standard\ deviation)}{mean}$x100).

Inter-day precision study (0.8 – 50 μM)						
Na_2S (μM)	**SDB peak area (LU*min)**			**Mean**	**SD**	**RSD (%)**
	Set 1	Set 2	Set 3			
0.8	2.2	2.9	4.9	3	1	0.3
1.6	3.4	4.6	6.3	5	1	0.4
3	15.5	10.7	9.1	12	3	0.8
6	35.6	21	42.8	33	9	2.7
12.5	119.7	95.4	126.3	114	13	4.0
25	407.1	384.9	437.3	410	21	6.5
50	1074.2	1191.6	1071.5	1112	56	17.0
Intra-day precision study (0.8 – 50 μM)						
Na_2S (μM)	**SDB peak area (LU*min)**			**Mean**	**SD**	**RSD (%)**
	Set 1	Set 2	Set 3			
0.8	2.9	2.3	2.5	3	0.2	0.1
1.6	4.6	4.3	4.8	5	0.2	0.1
3	10.7	9.6	9.8	10	0.5	0.1
6	21	20.6	19.9	21	0.5	0.1
12.5	95.4	88.6	91.4	92	3	0.8
25	384.9	383.3	368.7	379	7	2.2
50	1191.6	1179.2	1140.6	1170	22	6.6

Table 1.10 Media responses of the calibration concentrations prepared in intra and inter-day, and the p-value obtained from the comparison *t-test.* (Results are represented as mean ± SD, n = 3)

Na_2S **(μM)**	Intra-day (**LU*min**)	Inter-day (**LU*min**)	**p-value**
0.8	2.6 ± 0.2	3.3 ± 1.1	0.5
1.6	4.6 ± 0.2	4.8 ± 1.2	0.8
3	10.0 ± 0.5	11.8 ± 2.7	0.4
6	20.5 ± 0.5	33.1 ± 9.1	0.2
12.5	91.8 ± 2.8	113.8 ± 13.3	0.1
25	379.0 ± 7.3	409.8 ± 21.5	0.3
50	1170.5 ± 21.7	1112.4 ± 56.0	0.3

LOD and LOQ determination by the optimized method

LOD and LOQ were calculated for the linear model as, respectively, 3.3 and 6 times the ratio between the root mean squared error (RMSE) and the slope of the model (b):

$$LOD = \frac{3.3 * RMSE}{b}$$

$$LOQ = \frac{6 * RMSE}{b}$$

RMSE is the mean of the squared differences between the experimental responses and the response values recalculated by the model.

Regression model

The calibration method was validated by studying its significance and descriptive and predictive capabilities. The calculated results will be introduced in paragraph: 1.4.3.2 Calibration curve: optimization and validation.

The calibration standards are analyzed with HPLC-FLD. Signals area (LU*min) are plotted as a function of relative concentrations of calibration standards series. A fitting is performed to obtain the best regression model, whose fundamental parameters are shown in **Table 1.11** with the relevant formulas, where y_i are the experimental responses, $\bar{y}$ is the mean value of responses (i.e. the ordinate of the model centroid), $\hat{y}_i$ the recalculated responses, n is the number of measurements performed, and p' is the number of regression coefficients.

Emphasis is mainly placed on an examination of the residuals to check the model adequacy in regression analysis [246]. A good regression model is characterized by high values of TSS, MSS, and by a low value of RSS, which represent respectively a wide exploration space and a high correlation between experimental responses (or signals) and recalculated ones. (see significances of TSS/MSS/RSS in **Table 1.11**). Consequently, a good model will be characterized by a small standard deviation and a correlation coefficient close to 1.

The study of the parameters described in **Table 1.11** only allows for an evaluation of the descriptive capability. To evaluate also predictive capabilities of the model it is necessary to introduce two other parameters, the PRESS (Predictive Residual Sum of Squares) [247] and the prediction coefficient Q^2:

$$\text{PRESS} = \sum_i \left(y_i - \hat{y}_{i/i}\right)^2$$

In PRESS computation, predicted responses are considered instead of the calculated ones: $\hat{y}_{i/i}$ is the predicted value for the i-th object using a model that does not include such object in the training set.

$$Q^2 = 1 - \frac{PRESS}{TSS}$$

In PRESS computation, predicted instead of calculated responses are considered: $\hat{y}_{i/i}$ is the predicted value for the *i*-th object using a model that does not include such an object in the training set.

As in the case of R^2, a good predictive model will be described by a Q^2 close to 1.

Table 1.11 Parameters of the regression model.

Parameters	Formula	Significance
$\bar{y}$	-	Mean value of responses
$\hat{y}_i$	-	Recalculated responses
n	-	Number of measurements performed
p'	-	Number of regression coefficients
TSS (total sum of squares)	$\sum_i (y_i - \bar{y})^2$	TSS is an estimation of the distance between experimental responses and the centroid of the model
RSS (residual sum of squares)	$\sum_i (y_i - \hat{y}_i)^2$	RSS is an estimation of the distance between the experimental responses and the recalculated ones
MSS (model sum of squares)	$\sum_i (\hat{y}_i - \bar{y})^2$	The MSS value indicates the difference between TSS and RSS, it is an estimate of the distance between the calculated responses and the centroid of the model
RMSE (Standard deviation of regression: root mean squared error)	$\sqrt{\frac{RSS}{n - p'}}$	RMSE provides reliable information about the accuracy of the results of numerical models
R^2 (correlation coefficient)	$1 - \frac{RSS}{TSS}$	R^2 quantifies the correlation between experimental signals and corresponding standards concentrations

ANOVA test

To verify the significance of the model, an Analysis Of the Variant (ANOVA) test is performed [248].The test involves the calculation of the F_{OSS} parameter, which represents the comparison

between the variability attributed to the regression errors (quantified by RSS) and to the model (quantified by MSS).

$$F_{oss} = \frac{MSS/p}{RSS/(n-p')}$$

The model is significant if RSS is not bigger than MSS, i.e., if F_{OSS} is much greater than the F_{TAB} parameter (depending on the chosen significance α, generally set at 0.05 or 5%, and on the degrees of freedom). In this case, the corresponding p-value becomes lower than the chosen significance.

***t-Test* on regression coefficients**

Once verified that the model has a good correlation between the experimental responses and the relative concentrations, and once its significance has been ascertained with the ANOVA test, it is necessary to evaluate the significance of the regression coefficients by a comparison with the value 0.

To do this, a t-test is performed [249], which involves calculation of the t_{OSS} parameter, i.e. the ratio between the absolute value of the coefficient and its standard deviation.

$$t_{OSS} = \frac{|b_j - 0|}{S_{b_j}} = \frac{|b_j|}{S_{b_j}}$$

The regression coefficient is significantly different from 0 if t_{OSS} is greater than the corresponding t_{TAB} parameter (depending on the degrees of freedom and the significance). If the corresponding p-value is smaller than the significance; the smaller the p-Value, the greater the influence of the coefficient on the model.

For the validation of a calibration curve or a higher order polynomial function, it is necessary to consider that a good model is obtained if the known term is not significantly different from 0, i.e. if t_{OSS} is lower than t_{TAB} and if the relative p-value is higher than significance. This indicates that at zero concentration corresponds a signal that is not significantly different from zero.

Response Plots

Last step of the validation consists in the evaluation of descriptive and predictive capabilities of the model by analyzing the response plots. These are obtained by graphing the calculated and predicted responses as a function of the experimental responses.

If the model is good, the fitting functions will be linear functions characterized by described by

small standard deviation, correlation coefficient R^2 close to 1, and intercept and slope values not significantly different from 0 and 1, respectively. This would indicate that the recalculated responses are very close to the experimental ones.

All values are reported as mean ± standard deviation. Statistics were calculated using R statistical software (R Core Team, Vienna, Austria). Calculations, fitting, plotting, and statistical analyses were performed using Microsoft Excel 16.0 (Microsoft Corporation) and GraphPad Prism 8.0 (Graphpad Software Inc.). Data obtained from human samples were analyzed with an ANOVA test for repeated measures, followed by a Dunnett multiple comparison test [250].

1.4.2 RP-HPLC-FLD separation of derivatization product

Separation performance for the SDB product was verified, implementing an already reported HPLC-FLD method [181] and increasing the injected volume to 30 µL. Representative chromatograms of the derivatization protocol applied to a blank sample (water), a standard solution (6 µM Na_2S), and a serum sample are reported in **Figure 1.36** (a). A stoichiometric excess of MBB, 1.5 mM was used to ensure a rapid and complete reaction. The chromatogram of a MBB solution diluted by acetonitrile is also shown, to indicate retention time of the MBB excess. A standard sample and blank sample were used to attribute the SDB peak in serum samples. SDB (highlighted in red), was eluted at tR = 11.8 min, while the excess of MBB was eluted later (tR = 12.8 min).

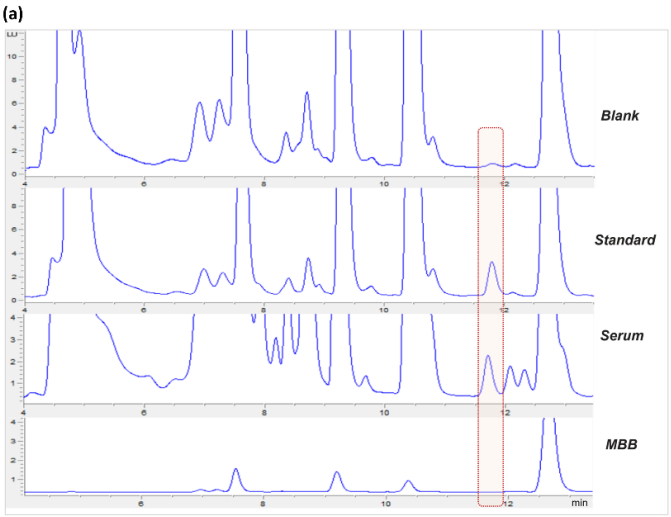

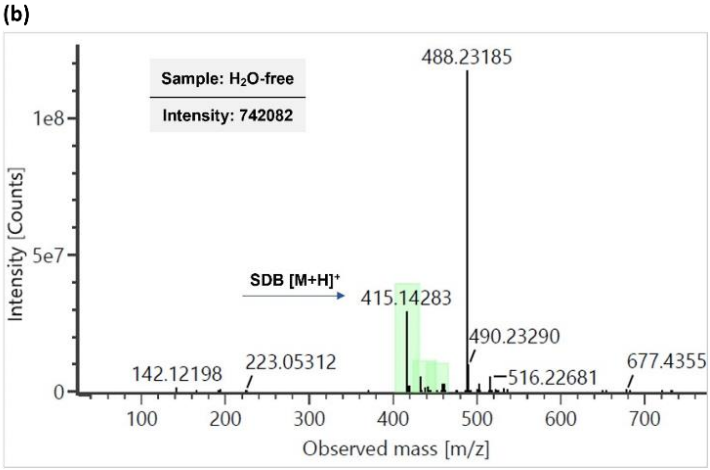

Figure 1.36 (a) Representative HPLC-FLD chromatograms of blank (H_2O), standard solution (6 μM Na_2S), serum, and MBB. (b) MS spectrum of H_2S derivatives. The molecular ion of SDB $[M + H]^+$ is shown at 415.14 m/z.

UPLC-QTOF-MS analysis allowed the SDB peak identity to be confirmed. **Figure 1.36** (b) shows the MS-spectrum of the SDB peak. The m/z of 415.14 corresponds to the molecular ion of SDB [186].

1.4.3 Sulfide levels quantification, method development

1.4.3.1 Derivatization method optimization

The first step of the derivatization procedure is a bimolecular reaction between H_2S and MBB, to give the intermediate sulfide monobimane species; then, a nucleophilic attack with a second MBB molecule yields the SDB product. However, the conditions used to optimize the reaction yield may strongly influence biological equilibria of the H_2S levels, affecting the ratio between the different forms of sulfide. A compromise between high yield and preservation of equilibrium, together with analytical performance of the method, must be established. Particularly, based on a few studies in serum samples with the HPLC-FLD-MBB method for H_2S species quantification [182, 183]. We have highlighted all the issues comprehensively discussed in previous publications such as oxygen concentration and exposure to light, pH condition for derivatization reaction, and trapping time on the speciation protocol. Moreover, we considered some crucial parameters such as pH value, reaction time, MBB concentration, temperature, and sample handling conditions for further optimization. Taken together, we used pH 9.5 Tris HCl as buffer, 1% O_2, a 30 min reaction time, and a dark environment as reaction conditions.

pH and reaction time

According to previous investigations in literature, firstly an optimization of parameters such as pH value and incubation time during MBB derivatization reaction was carried on. We performed the derivatization step using Tris HCl buffer in different pH value (pH 9.5 and 10), and we also tested the reaction at different incubation times (30 min and 120 min, respectively). The measured SDB peak signals decreased at pH > 9.5. As indicated in **Figure 1.37** . An increasing SDB yield obtained when the incubation time from 30 up to 120 minutes, but together with a rise in the worktime that doesn't allow high throughputs during the working day. For this reason, the reaction time has been reset to 30 minutes. Thus, pH 9.5 and 30-min incubation in dark were employed as the reaction conditions for the activities following discussed.

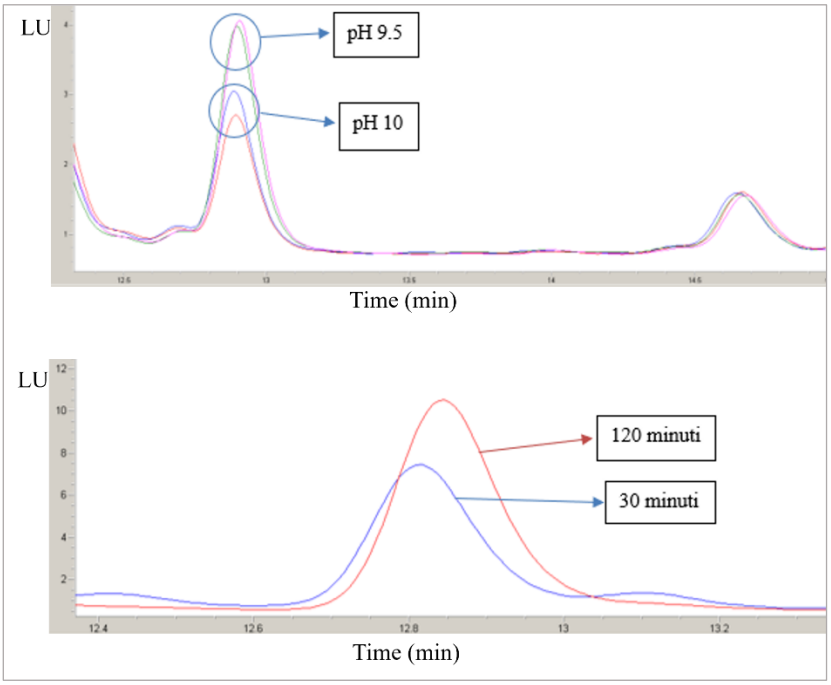

Figure 1.37 Screening of pH value (30 min) and reaction time (pH9.5): HPLC-FLD chromatograms of 50 µM Na_2S solution derivatized with 10 mM MBB.

MBB Concentration

For the derivatization of a 12.5 µM Na_2S solution, we tested the effect of lowering the concentration of MBB from 10 mM (as mostly used in the literature [181-183]) to 1.5 or 0.15 mM. The resulting chromatograms are shown in **Figure 1.38**. The use of 10 mM MBB provided the highest peak area for SDB, but also two high peaks corresponding to by-products. The use

of the lowest MBB concentration (0.15 mM) reduced the formation of by-products but also the SDB peak intensity, due to the incomplete derivatization of free H_2S. Notably, it has been observed that the use of 1.5 mM MBB allowed for preservation of the SDB peak intensity, and it reduced by-product formation together with a reduced MBB solution consumption which still retains a good derivatization yield.

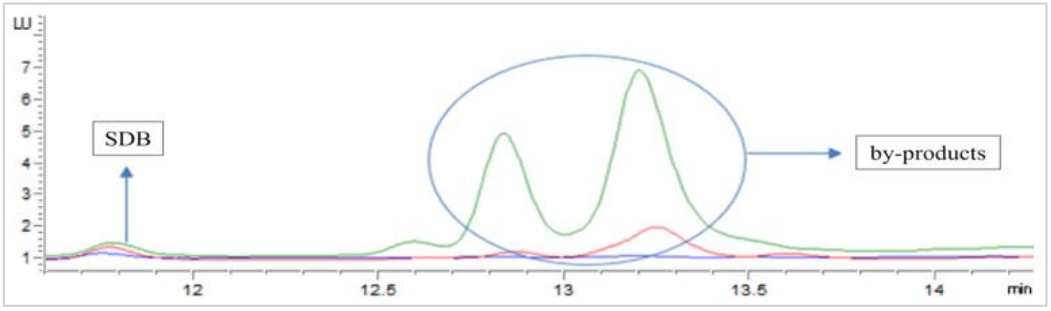

Figure 1.38 HPLC-FLD chromatograms of 12.5 µM Na_2S solution derivatized with 10 mM (green), 1.5 mM (red) and 0.15 mM (blue) MBB.

Temperature

For the derivatization of a 12.5 µM Na_2S solution, we then tested the effect of increasing temperature from RT to 50 °C. To clarify the effect of these conditions on the biological samples, a serum sample, and a simulated body fluid solution (SBF) were also analyzed. To mimic the composition of human serum, in terms of ion and protein concentrations, the SBF solution was prepared by dissolving 4 mg/mL serum albumin in phosphate buffer saline at pH = 7.4. The peak area values obtained for SDB are reported in **Table 1.12**.

Table 1.12 SDB peak area of different samples at RT and 50 °C.

SDB peak area (LU*min)	RT	50 °C
Na_2S 12.5 µM	270	800
Serum	63	207
SBF	2	230

Increasing the temperature caused an increasing trend in SDB formation for all the analyzed solutions, as shown in **Table 1.12**. Both in standard solutions and serum sample, a nearly 3-fold increase in the reaction yield was observed with increasing temperature (from RT to 50 °C). Notably, SDB was detected in SBF only at 50 °C, thus suggesting the extraction of H_2S from protein (BSA) contained in SBF. As a consequence, it is not recommended to set reaction

temperature at 50 ºC during the serum sample derivatization step because of its desulfuration effect on S-proteins and S-amino acids present in blood. Release of HS^- within the sample would cause an increase in the signal associated with SDB, thus altering levels of the various types of endogenous sulfide detected by this method. Accordingly, RT was chosen as the optimal temperature for the derivatization procedure.

Serum Handling (Storage Conditions, Aging, Dilution)

The effect of serum handling (storage conditions, aging, and dilution) during the pre-analytical phases was considered. In the protocol we maintained some of the experimental conditions previously published once confirmed the absence of any significant difference for SDB yield (pH 9.5 Tris HCl as buffer, 30 min, 1% O_2, dark environment) [182, 183]. Finally, for the derivatization reaction we used our optimized parameter values for MBB concentration and temperature, at different sample handling conditions.

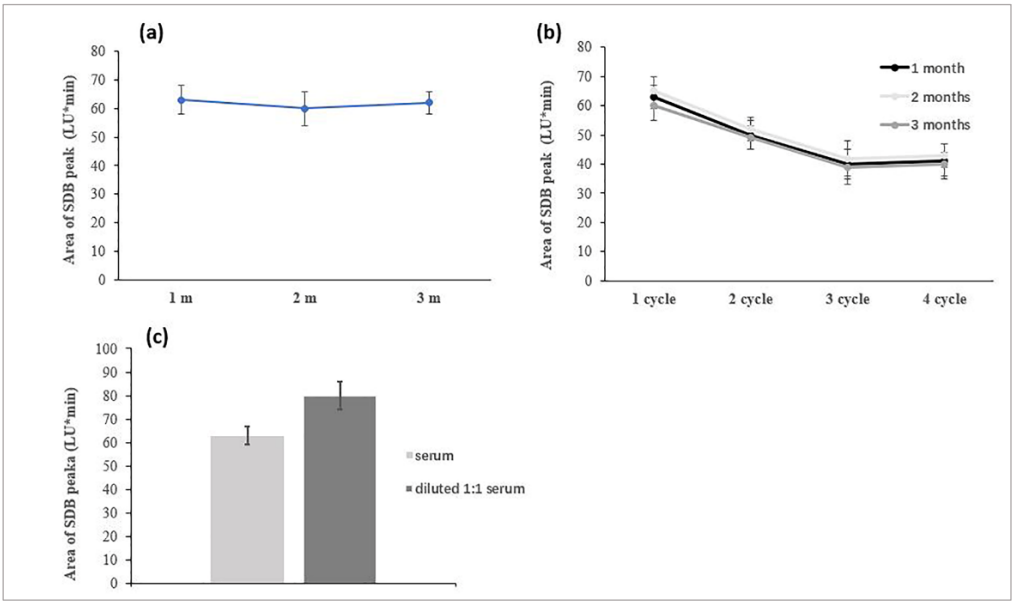

Figure 1.39 SDB peak areas for a serum sample (a) stored at −20 °C for 1, 2 or 3 months; and (b) after repeated freeze–thawing cycles at 1, 2, or 3 months. (c) Effect on SDB peak area of 1:1 dilution in physiological solution of serum samples.

As for the sample storage procedure, no significant differences were found between area values of the SDB peaks obtained from the three aliquots of serum sample stored at −20 °C for up to 3 months (**Figure 1.39** (a)). Conversely, repeated freeze–thawing cycles lead to a significant reduction of the SDB signal obtained from the same serum sample (**Figure 1.39** (b)). Because of complexity of the serum matrix, and to reduce potential chemical and instrumental

interferences, a 1:1 sample dilution with physiological solution was considered. The derivatization yield for free H_2S was compared for diluted and undiluted samples (**Figure 1.39** (c)). The diluted sample showed a higher yield for the SDB formation, indicating that potential equilibrium shifts had occurred after the dilution. Therefore, in the optimized protocol aliquots of serum samples (at −20 °C, different storage times, and thawed once) were directly analyzed following the described derivatization procedure; no dilution was performed.

Speciation Protocol Tubes

For the acid-labile sulfide and bound sulfane sulfur quantification, the protocol described in part 2.6 was applied. A 2-mL BD vacutainer tube with clot-activator/gel was initially used during sample treatment for H_2S pool release. However, when the derivatized Tris-Cl (blank) and serum samples were analyzed, even the blank sample showed a peak at the SDB retention time (tR = 11.8 min) with an area equivalent to that of a 15 μM Na_2S standard solution (data not shown). The identity of this peak was confirmed through UPLC-MS analysis, and the MS intensity of SDB peaks from the analyzed samples (acid H_2S from serum, total H_2S from serum, acid H_2S from Tris-Cl and total H_2S from Tris-Cl) are reported in **Figure 1.40**.

To further investigate the origin of this peak in the blank samples, and potential interferences due to the reagents and sample treatment, several blank samples were derivatized for the free sulfide determination using the 2-mL BD vacutainer tube with clot-activator/gel instead of the PCR tube. The resulting products were analyzed by UPLC-QTOF-MS. All the analyzed samples showed the peak at tR = 11.8 min, and the identity of SDB was confirmed by MS. Despite the serum sample showing higher intensities of SDB for H_2S species, significant signals were also obtained when Tris/PB/H_2O was used as blank samples for the free determination. These results would indicate potential interferences due to the silicone adsorbed on the 2-mL BD vacutainer tubes used for all the derivatizations. Nevertheless, when empty BD vacutainer tubes without additive were used for the speciation protocol, no FLD signal was detected at the derivatization time with blank samples (tR = 11.8 min) (data not shown). Accordingly, BD tubes without additive were used in the optimized protocol.

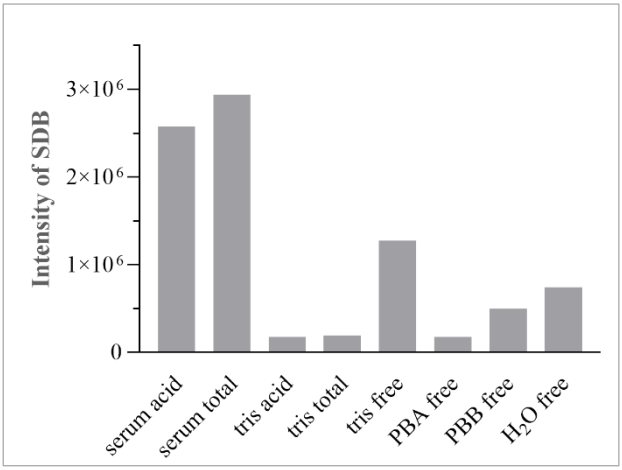

Figure 1.40 MS intensity of SDB peak for: serum acid (acid H_2S from serum), serum total (total H_2S from serum), tris acid (acid H_2S from Tris-HCl), and tris total (acid H_2S from Tris-HCl). Tris free (free H_2S from Tris-HCl), PBA free (free H_2S from PB-A), PBB free (free H_2S from PB-B), and H_2O free (free H_2S from H_2O).

1.4.3.2 Calibration curve: optimization and validation

In this work, Na_2S solutions in the concentration range 0.8 – 50 µM were prepared, derivatized, and used for the calibration curve. We decided to explore a wide range of H_2S concentrations, because we could not predict where the real samples would have fallen and based on the levels of H_2S in serum samples reported in literature [178, 183]. In **Figure 1.41**, some representative, overlapped chromatograms are shown.

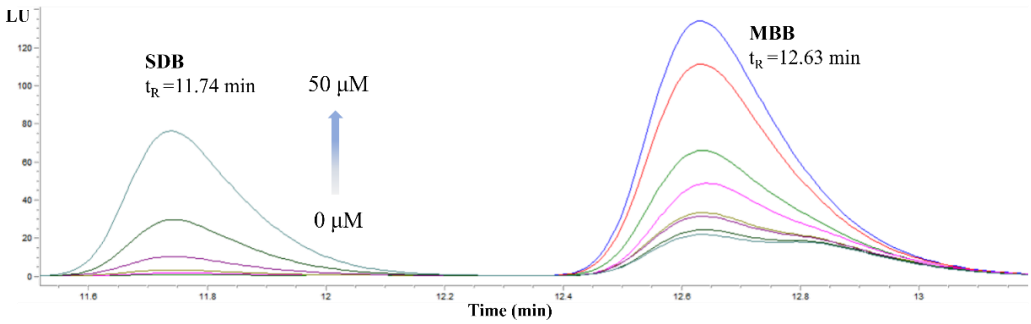

Figure 1.41 Representative chromatograms of overlaid calibration series: blank, 0.8, 1.6, 3, 6, 12.5, 25, and 50 µM. (Peaks of SDB and MBB approximately at 11.74 min and 12.63 min, respectively.)

Moreover, as some authors used spiked serum samples with the addition of Na_2S as calibration solutions [184], to limit the matrix effect we explored a standard addition procedure (A standard addition procedure: Two sets of parallel experiments were carried out: One is the Na_2S standard solutions prepared with MilliQ water. Another one was followed the same procedure to prepare Na_2S standard solutions, but the final spiked sample was obtained by the dilution of Na_2S standard solutions with a spiked serum sample. For example, "serum+ Na_2S 5 µM" was

prepared by diluting standard sample Na_2S 10 μM with the same volume of serum sample, therefore, half concentration of Na_2S standard solutions with a spiked serum sample can be obtained.). We then compared the SDB peak area values obtained from Na_2S standard solutions with the peak from a spiked serum sample at the same standard concentrations. The results showed that the addition of a standard solution of Na_2S to the serum sample gave a lower value of SDB peak area, with a concentration dependent trend (**Table 1.13**). These data indicate that after the addition of Na_2S to serum sample, a portion of sulfide can be trapped by the matrix, making unreliable the correlation between SDB product yield and sulfide concentration. Therefore, this supports the choice of determining the calibration curve for the HPLC-FLD MBB method using Na_2S standard solutions.

Table 1.13 SDB peak area of standard Na_2S sample and spiked serum samples.

	Na_2S 5 μM/ serum+ Na_2S 5 μM	**Na_2S 12.5 μM/ serum+ Na_2S 12.5 μM**	**Na_2S 25 μM/ serum+ Na_2S 25 μM**
SDB peak area (LU*min)	25/22	180/100	400/200

The wide calibration range here selected required the use of polynomial regression, as reported in **Figure 1.42** (a). The calibration curves were calculated using a second-degree polynomial regression (parabolic), where the independent variable (x) is the standard concentration, and the dependent variable (y) is the area value of the FLD peaks. The resulting model equation is y=a+bx+cx^2. The curve parameters are summarized in **Table 1.14**. The R^2 value of 0.998 and the model p-value close to 0 demonstrate that the parabolic model is a good fit for the data.

To assess measurements repeatability, three replicates of each standard were prepared in different days. Inter-day repeatability was successfully verified by performing, for each concentration, a Student's t-test between the inter-day replicates and the standards used for the calibration. The relative p-values were never below the chosen significance level ($\alpha = 0.05$): this showed no significant differences between the standards and the inter-day replicates.

To further validate the parabolic model, a leave-one-out cross-validation (CV) was performed [251]. This method consists in removing an experimental point from the dataset, computing the model with all the remaining points, and then projecting the removed point onto the model. This procedure was repeated for all the points, and the recalculated responses (in this case the FLD peak areas) were compared to the experimental values. The comparison could be

performed by computing a linear regression between recalculated and experimental responses ($y_{recalculated}=a+by_{experimental}$): the intercept (a) and the slope (b) of such a model should be not significantly different from 0 and 1, respectively. This would indicate a good match between

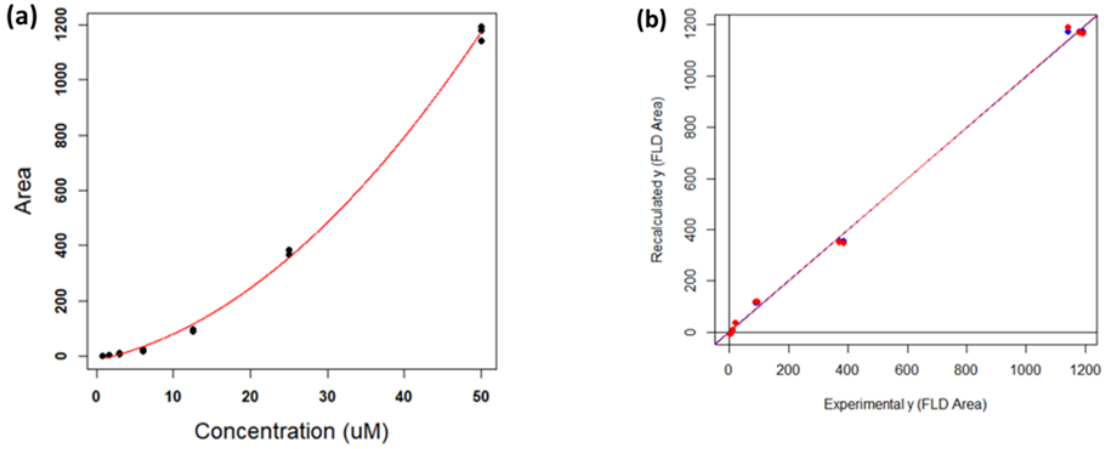

Figure 1.42 (a) Parabolic regression in the concentration range 0.8–50 µM. (b) Regression lines of the validation methods using cross-validation (CV) (in red) and calibration (in blue).

Parameter	Value
a (AU)	− 13.2
s_a (AU)	6.61
b (AU µM^{-1})	5.87
s_b (AU µM^{-1})	0.930
c (AU µM^{-2})	0.358
s_c (AU µM^{-2})	0.0181
R^2	0.998
RMSE (AU)	18.16
model p-value	< 2.20 10^{-16}

Table 1.14 Parabolic regression parameters. All values are reported with the corresponding measure unit, AU stands for (FLD) area unit. RMSE stands for root mean squared error.

recalculated and experimental values. Moreover, the responses can be recalculated by projecting them directly onto the original model without removing any point, and calculating the same linear regression (Calibration method). The results of such a procedure are reported in **Figure 1.42** and **Table 1.15**. **Figure 1.42** (b) shows that the two lines (blue and red) coincide with the first quadrant bisector. The line parameters reported in **Table 1.15** show, besides the

goodness of the models due R^2 close to 1 and low p-values, that the two intercepts and slopes, also considering the corresponding standard deviations, are not significantly different from the ideal values of 0 and 1.

	CV	**Calibration**
Intercept	− 0.108	0.429
$s_{Intercept}$	0.685	0.520
Slope	0.999	0.998
s_{Slope}	0.0122	0.00969
R^2	0.997	0.998
RMSE	22.3	17.8
model p-value	< 2.20 E-16	< 2.20 E-16

Table 1.15 CV and calibration regression line parameters.

Indeed, high standard deviations were obtained for the calculated concentrations (data not shown) when the twelve unknown samples (four samples collected at three different times of H_2S inhalation) were interpolated. This made all the calculated concentrations not significantly different from zero. These results revealed the poor prediction ability of the parabolic model. The inaccuracy of the method indicated poor prediction of the concentration value. However, we noticed that the interpolated areas of the unknown samples were always in the range 5–15 AU. This means that the unknown samples were interpolated in the lowest concentration range of the curve and far from the centroid, which is around 600 AU. In general, for all the regression models, the standard deviation calculated for a projected sample is lowest if the sample is close to the model centroid, while it increases, also dramatically, in the external portions. Therefore, the high standard deviation values could be due to the non-optimal performance of the model in that response region.

Consequently, we decided to reduce the standard concentration range to 0.8 – 6 µM. This corresponds to a range whose centroid is close to the unknown signals. In this way, it was also possible to simplify the regression model to a linear, rather than parabolic, model. The calibration line is reported in **Figure 1.43**, and the corresponding parameters are reported in **Table 1.16**. Both **Figure 1.43** and **Table 1.16** indicate, in this restricted concentration range, a

good fit of the standards to the linear model. R^2 is close to the ideal value of 1 (0.995) and the p-value of the model is highly significant (4.77 10−13). Moreover, the intercept is not significantly different from 0.

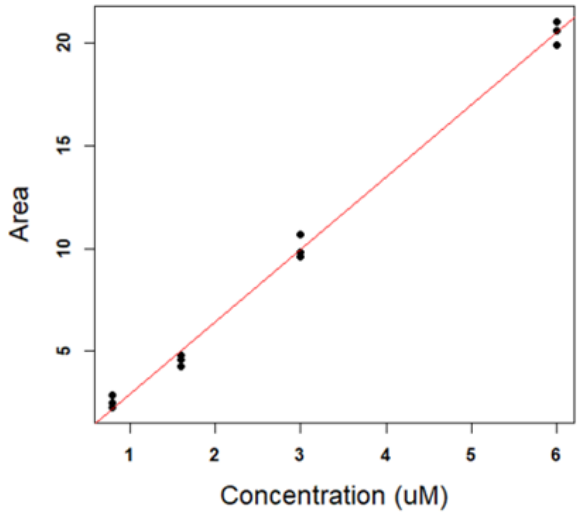

Figure 1.43 Linear regression in the concentration range 0.8–6 µM.

Parameter	Value
Intercept (AU)	− 0.581
$s_{Intercept}$ (AU)	0.260
Slope (AU μM^{-1})	3.51
s_{Slope} (AU μM^{-1})	0.0749
R^2	0.995
RMSE (AU)	0.514
model p-value	$4.77\ 10^{-13}$

Table 1.16 Linear regression parameters. All the values are reported with the corresponding measure unit, AU stands for (FLD) area unit.

LOD and LOQ for the method were calculated from the linear model as 3.3×RMSE⁄Slope and 6×RMSE⁄Slope, respectively. LOD resulted to be 0.5 µM, and LOQ was 0.9 µM.

1.4.4 Efficacy of the method on human serum samples

To evaluate performance of this method in a clinical setting, we quantified the different sulfide species in the serum of four patients enrolled into an interventional clinical trial at Rizzoli Orthopedic Hospital, based on a cycle of 12 inhalation treatments with sulfurous water with

high H_2S content. The linear model was used to calculate the concentration values. **Figure 1.44** shows that the sulfurous thermal treatment (STW) had a strong effect on the total concentration of H_2S, which increased significantly from T0 (before the treatment) to T2 (three days after the completion of the 12-day inhalation treatment) by over 40% ($p < 0.0001$). Nonetheless, concentration of free H_2S remained steady treatment throughout the experiment. Consequently, the acid-labile and the bound sulfane sulfur fractions also increased three days after the end of treatments. These results highlighted the specificity of the method, which could detect differences in specific H_2S levels. While the biological implications of these findings remain to be elucidated, these data show that an exogenous source of gaseous H_2S affected the serum levels of the different H_2S pools.

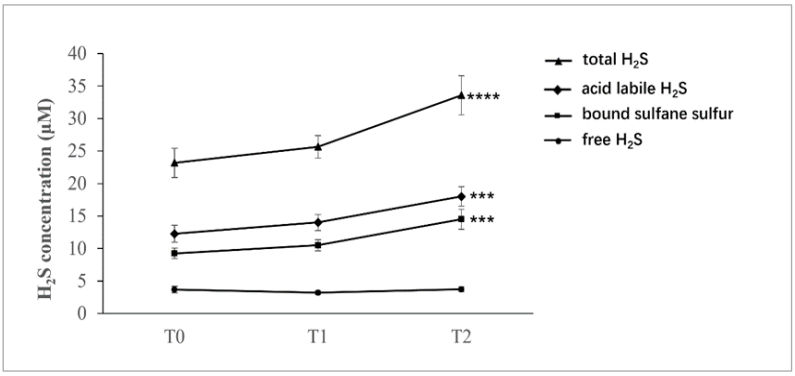

Figure 1.44 H_2S levels in serum samples collected before the treatment (T0), immediately after the 12-day treatment (T1), and three days after completion of the treatment (T2). **** = $p < 0.0001$ vs. values at baseline (T0); *** = $p < 0.005$ vs. values at baseline (T0).

1.5 Discussion

A panel of preclinical studies has established that free H_2S and relative H_2S species act as important signaling molecules in cells and tissues. Moreover, they have emerged as important determinants of susceptibility or prognosis in certain pathologies and may work as key biomarkers [144, 252-254].

In the context of musculoskeletal diseases, animal studies have ascertained that H_2S triggers an antioxidant response sufficient to inhibit osteoclast differentiation [255], and supports osteoblast differentiation and bone formation [54, 256, 257], thereby mitigating the osteoporosis induced by hormone depletion or chronic glucocorticoid treatment [258]. Importantly, circulating levels of H_2S were associated with a lower bone mass in a murine model of post-menopausal osteoporosis [259], and H_2S biosynthesis was shown to be impaired

in the osteoarthritic joint [260]. No information is yet available for regulation of bone tissue by sulfide pools in both physiology and pathology.

The reproducible quantification of H_2S species (free, acid labile, and bound sulfane sulfur) would help to identify their divergent regulatory roles in several biological processes and help to define the range of concentration of H_2S released from pharmacological donors and to obtain a targeted delivery of H_2S at the desired dose. Thus, finding a reliable and sensitive method for H_2S detection and analysis is still a challenge. Physiological and pharmacological features of H_2S has been demonstrated by Mancardi and co-workers [261].

The use of colorimetric detection based on methylene blue has been declining in the literature, due to several limitations: it lacks sensitivity at low (<1 μM) H_2S concentrations, which makes it inappropriate for measuring lower biological levels of H_2S; formation of dimers and trimers of methylene blue; interference with other colored substances; and strong acid chemical pretreatment [168]. Electrochemical techniques, such as sulfide ion-selective and polarography, have been developed to detect H_2S in whole blood and tissues [173]. However, sulfide ion-selective electrodes are prone to fouling and, similarly to the methylene blue method, cannot provide information in real-time or on living tissue and are not sensitive enough for most biological samples [198]. In addition, values obtained from this indirect method tend to be somewhat lower than those using direct methods. Polarography sensors, tend to drift, must be frequently calibrated, and consume sulfide slowly, thus hampering measurements with very small volumes [177]. The most sensitive technique for measuring physiological sulfide levels in pure biological samples, gas chromatography, potentially liberates bound sulfane sulfur because of irreversible sulfide binding or shifts in phase transition equilibria and is not capable of determining the level of H_2S in real time [149]. Despite the impressive effort being put into the development and validation of accurate and reliable methods for the determination of sulfide levels in the past few years, most of these methods still show several limitations [226].

HPLC-FLD based on MBB derivatization represents the most interesting approach for H_2S species analysis in plasma or tissue samples, with advantages related to its high sensitivity and specificity. During sample preparation, biological equilibria can be modified, releasing free H_2S, which may alter the actual levels; consequently, a robust and reproducible analytical protocol

must be designed. Complicating the matter is the fact that sulfide exists in multiple forms: free sulfides such as S^{2-}, HS^-, H_2S, acid-labile and bound sulfane sulfur. These different forms of sulfide make quantitative measurement of bioavailable H_2S difficult and have led to variable reported levels in the literature.

Here, we applied some reaction conditions (pH 9.5, Tris HCl as buffer, 1% O_2, 30 min, dark environment) already discussed in previous papers [178]. The results were in line with these studies and showed no significant differences. Next, we analyzed crucial parameters (MBB concentration, sample handling, tubes for the speciation protocol) that would significantly affect the HPLC-FLD method results.

First, we aimed to reduce the MBB used in the protocol, since high concentration MBB can cleave longer dialkyl polysulfide and this would increase the throughput of the method by consuming less key reagent. The best results were obtained with 1.5 mM MBB, a concentration able to quantify sulfide in a wide interval range, giving greater sensitivity to the technique and reducing the production of by-products. However, previous evidence has shown that a 1.1–10 MBB concentration can extract H_2S from bound sulfane sulfur pools [193]; therefore, we cannot exclude the possibility that "free sulfide levels" at least partially measured a release from long polysulfides, instead of direct alkylation of free sulfide.

Then, we aimed at optimizing the protocol temperature. The increase in temperature from RT leads to greater yield of the derivatization reaction on Na_2S standard solutions and serum, with a consequent increase of the sensitivity of the method. However, the SBF used to mimic a biological sample showed a value for SDB formation only at higher temperature; thus, suggesting the extraction of H_2S from proteins contained in SBF and the alteration of the levels of the various types of endogenous sulfide detected using this method. Albumin contains cysteine residues that are sensitive to thermal degradation, with the consequent release of sulfide in the monoprotonated form (HS^-). While the Na_2S standard solution has a reserve of sulfide proportional and limited to the quantity of Na_2S present, the biological matrix (serum sample) contains various species of sulfide that can be enclosed in metal clusters or linked to proteins, and whose release in solution can be stimulated by external agents; in a selective way, using specific reagent and chemical conditions, as for the speciation protocol; or in a non-

specific manner, as by increasing the reaction temperature. Consequently, RT was chosen, to avoid contamination of the endogenous sulfide levels.

Additionally, we tested a dilution of serum samples, but we showed that no dilution should be applied to the serum sample prior to derivatization. In the optimized protocol, 30 µL of serum was directly derivatized without dilution. Since one of the aims of the presented work was to develop a robust protocol able to give reproducible values for H_2S levels (free, acid-labile, and bound sulfane) in blood, we highlighted that an empty BD-vacutainer must be used during the speciation protocol, to avoid interference in the SDB quantification, due to the presence of clot activator in the tube.

Finally, we studied the standard calibration procedure: we first prepared a stock solution of Na_2S, then we diluted it to obtain 0.8, 1.6, 3, 6, 12.5, 25, and 50 µM concentrations, which were then derivatized; these standards were used for the calibration curve and a validation was performed with a leave-one-out cross-validation (CV). To our knowledge, this is the first report to employ this validation. Current HPLC-FLD MBB-based protocols for H_2S levels quantification mostly derivatize the standard solution of Na_2S and then dilute the relative SDB purified to obtain different calibration standards, to calculate the calibration curve; consequently, issues related to the derivatization procedure, which can strongly affect the reaction yield and quantitative results [182, 183, 193], are not well considered. Some authors instead reported the use of serum samples spiked with Na_2S as calibration solutions [184]. In this study, we compared the SDB peak area obtained for Na_2S standard solutions, and a spiked serum sample added at the same standard concentrations. The results indicate that after the addition of Na_2S to the serum sample, a portion of sulfide can become trapped by the matrix. Therefore, standard addition to the serum matrix does not represent a robust quantitative analytical approach. Thus, the calibration curve was determined by using calibration standards diluted using a stock solution of Na_2S before derivatization. A LOD of 0.5 µM was determined, indicating a high sensitivity with respect to similar reported methods [181, 184].

Then, we tested the present analytical approach in a group of patients undergoing a cycle of inhalation treatment with H_2S: rich water; this route of administration was chosen because the concentration of free H_2S in the waters (14.6 mg/L) is biologically relevant, as it falls within

the low micromolar concentrations shown to be bioactive in a broad series of preclinical studies. Moreover, whether the exposure to an exogenous source of H_2S can influence the circulating levels of RSS in humans is an unanswered question, with potential clinical relevance, as the replacement of sulfur was shown to be an effective strategy in certain pathological conditions characterized by lower-than-average RSS in blood. Particularly, we demonstrated that, in a preclinical mouse model of post-menopausal osteoporosis, replacement of decreased H_2S levels in serum with intraperitoneal administration of sodium hydrosulfide prevented the bone loss occurring due to estrogen deficiency [144]. Notably, the findings of the present study show that this method could detect a change in the different pools of H_2S in the serum of patients. After the end of treatment (timepoint T2), the total H_2S increased by over 40% relative to baseline levels, resulting from a similar increase in the acid-labile and bound sulfane sulfur pools; on the other hand, the treatment had no effect on the free H_2S pool, suggesting that the exogenous free H_2S quickly reacted with the proteins of the biological matrices in blood. In the context of studies on osteopenia-osteoporosis, this finding could be of relevance, since we could analyze and eventually correlate the H_2S species modulation in serum, due to sulfurous water inhalation, to biomarkers of bone remodeling.

1.6 Conclusions

We optimized and validated a MBB derivatization method coupled with a HPLC-FLD protocol for H_2S species quantification in human serum samples and validated for the first time the procedure of calibration. Crucial factors influencing the actual H_2S species level were excluded from the protocol. Furthermore, we provided evidence of the importance of the procedure of preparation of standard solution and the relative calibration. Overall, the optimized method results in a more efficient derivatization of H_2S with MBB, with a low perturbation of sample equilibria, giving a robust value for endogenous H_2S species. Although this method cannot achieve absolute quantification of H_2S species, it is a good method for relative quantification. Significant progress had been put forward in indirectly determining the action of vapor sulfide on the primary target organs. By revealing a modulation in H_2S species in patients that underwent sulfurous water inhalation, we demonstrated that the method proposed is a reliable tool to measure H_2S species in biological matrices. This validated detection and quantification

method can improve H_2S species relative quantification in physiology, pathology, and for helping to track H_2S levels in the context of pharmacological exogenous H_2S treatments. As shown in **Figure 1.45**, it's shown a graphical overview for sulfur species measurements.

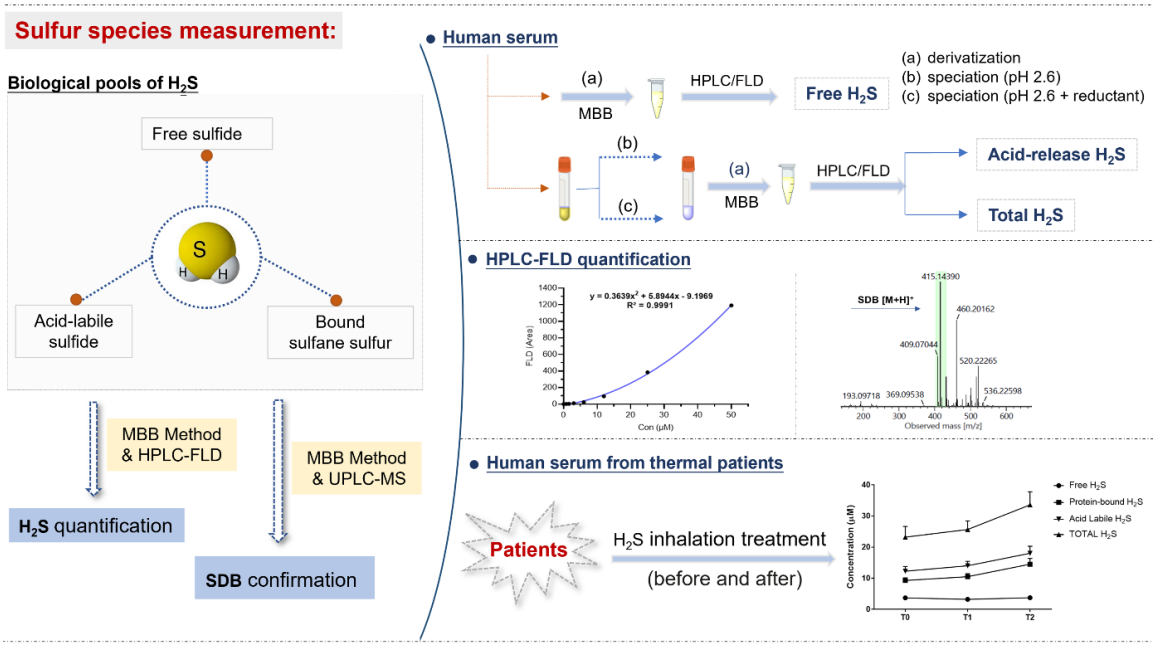

Figure 1.45 Graphical overview of the present study for sulfur species measurements.

Chapter 2. Application of MBB/HPLC-FLD method to a biomimetic Silk Fibroin-PLGA multilayer electrospun scaffold

2.1 Introduction

The sulfur species research field is growing rapidly in the last decades. Considerable evidence is accumulating on the role of endogenous gasotransmitter H_2S as a mediator of several biological functions and its deficiency has been associated with different disorders. Many H_2S-releasing agents have been developed as potential therapeutic tools for diseases related with impaired H_2S production and/or activity. Some of these compounds are in advanced clinical trials. Thus, translational medicine involving the sustained and controlled release of H_2S is of great value for both scientific and clinical uses. However, the use of existing H_2S donors is usually limited because of the instant release and short half-time of H_2S.

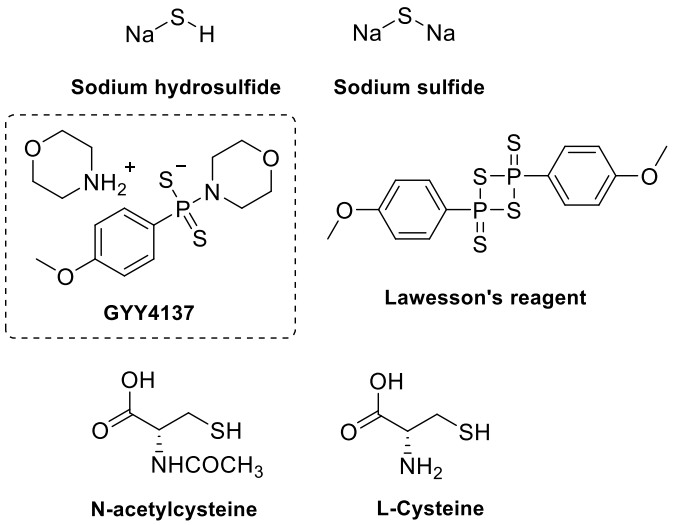

Figure 2.1 Structures of various H_2S salts and donors used for basic research.

With a view to those unsolved problems on H_2S donation, some investigators have overviewed the recent progress and contributions to chemistry and biological applications of H_2S releasing agents used as pharmaceuticals [262-265]. The data generated can be generally divided into two groups: (1) obtained using exogenous sources of H_2S and (2) obtained by modifying endogenous H_2S synthesis. For the first group, the administration of gaseous H_2S is heavily limited due to a difficult control and risk of overdose. In contrast, the use of H_2S-releasing agents can ensure a convenient and safer strategy for slow H_2S release controlling. Nowadays, there are agents that either directly release H_2S when in solution (NaHS, Na_2S, Lawesson's

reagent, GYY4137) or function as a precursor for endogenous H_2S synthesis (N-acetylcysteine, L-cysteine) [266]. The structures of these compounds were shown in **Figure 2.1**.

In this work, we placed more emphasis on study the exogenous sources of H_2S, especially for GYY4137 [266], a novel slow-releasing H_2S donor, which behaves as source of exogenous H_2S. It is a promising drug for the prevention and treatment of several diseases through controlling of the H_2S release. In the context of scaffolds for tissue engineering, the use of silk fibroin (SF) has been widely proposed for several applications. SF shows superior biocompatibility, controllable biodegradation, and attractive mechanical properties thanks to a balance of modulus, breaking strength, and elongation, which contributes to its toughness and ductility. Furthermore, SF scaffolds have been demonstrated to stimulate human osteoblast-like cell attachment, growth, and proliferation; to be suitable for tissue regeneration. Furthermore, due to the instability of GYY4137 in the solvent needed to prepare silk fibroin solutions (formic acid), the electrospinning of the donor together with the silk fibroin turned out to be impossible. Therefore, a multilayer structure was realized, consisting of a PLGA mat containing GYY4137 sandwiched between two silk fibroin nanofibrous layers. With further optimized derivatization steps of the MBB-RP HPLC method developed in hand, a novel silk fibroin scaffold loaded with different concentrations of GYY4137, i.e., 0, 2 and 5% w/w with respect to the weight of PLGA was analyzed to study their H_2S release. This novel designed scaffold was proposed by the Polymer Science and Biomaterials research group headed by Prof Maria Letizia Focarete at the Department of chemistry "Giacomo Ciamician" and INSTM UdR of Bologna, University of Bologna.

As described in chapter 1, specifically, the 'H_2S' mentioned and detected in this chapter also represents the 'H_2S species'. Because at physiological pH and temperature, gaseous H_2S is a weak acid in aqueous solution, about 20% of the total sulfide is undissociated, 80% undergoes the first dissociation, while the second dissociation is negligible. Thus, significant amounts of H_2S and hydrosulfide coexist and both species contribute directly to the measured levels of sulfide.

2.2 Experimental approach

Equipment required:

HPLC-FLD instrumentation, Ultrasonic instrument, Hypoxic chamber and Vortex mixer, described in paragraph 1.3.2 were applied to all samples analysis proposed in H_2S-releasing tests. Heating oven and thermostatic tilting bath were also used in this project.

Sample preparation:

Degradation of GYY: About 0.38 mg of GYY4137 without embedding in any mat were placed in a 2 mL Eppendorf PCR tube with a tight cap, 1mL of Phosphate Buffer (**PB**: 0.1 M, pH= 7.4) were added to the tube in a glove box after its sonication for 30 min. **PB**: only 1 mL of PB; **GYY4137**: GYY4137 + 1 mL of PB. Each sample was incubated in the tilting bath at 37°C for 168 h and each withdrawal carried out in hypoxic chamber glove box. After each withdrawal, the solution was refilled with the same amount of PB in the glove box.

H_2S release of Multilayer: About 5 mg of each multilayer mat (a square of 1.3 x1.3 cm) were assembled on the cell-crown (24 well) and placed in a 20 mL plastic tube with a tight cap. **MB**: Multilayer blank: sandwich consisting in an inner layer of PLGA and the two outside layers of silk fibroin sample without GYY4137; **M2%:** Multilayer Silk-PLGA+2%GYY4137-Silk: sandwich consisting in an inner layer of PLGA loaded with 2% w/w of GYY4137 and two outside layers of silk; **M5%:** Multilayer Silk- PLGA+5%GYY4137-Silk: sandwich consisting in an inner layer of PLGA loaded with 5% w/w of GYY4137 and two outside layers of silk.

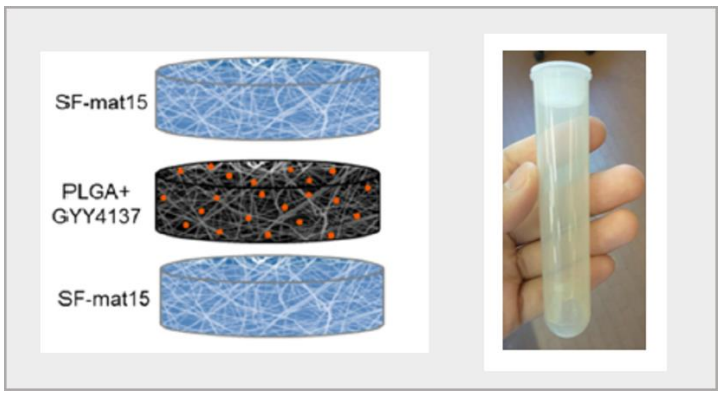

Figure 2.2 Biomimetic Silk Fibroin-PLGA multilayer electrospinning scaffold and tight tubes used in the controlled release of H_2S tests.

Figure 2.2 shows how the samples prepared and tube used for releasing tests. 5 mL of PB incubated in the tilting bath at 37°C for 168h. But sample MB, M2%, M5% were incubated in the tilting bath by addition of 4 mL of PB at 37°C for 168h. Each withdrawal carried out in hypoxic chamber glove box. After each withdrawal, the solution was refilled with the same

amount of PB in the glove box.

Solutions to be prepared:

Phosphate buffer saline (0.1 M, 0.5 L, pH= 7.4) HK_2PO_4 8.7g, adjust pH value to 7.4 with 37% HCl at room temperature;

Tris-HCl buffer (pH 9.5, 0.1 mM DTPA): 1.21 g Tris-HCl and 4.0 mg DTPA, then put them into the 100 mL volumetric flask with 2/3 Milli-Q water inside. Dissolve the compounds completely then adjust the pH value to 9.5 by adding 0.2 M hydrochloric acid drop by drop;

MBB solution: 1.5 mM, 2 mg monobromobimane in 5 mL Acetonitrile, the solution should be kept in an amber container and protected from light to avoid photolysis;

SSA: 200 mM (218 mg 5-sulfosalicylic acid in 5 mL water).

It should be noted that all working solutions mentioned above are employed fresh in the following protocol.

Preparation of stock solution and calibration series:

A modified MBB/HPLC-FLD method was applied in a slow H_2S-releasing donor agent (GYY4137). Temperature was set at 50 ^oC to improve the sensitivity of reaction during sample incubation in the derivatization step. Sodium sulfide (Na_2S) was used as a source of hydrogen sulfide for standard solutions. A 12.8 mM stock solution of Na_2S in phosphate buffer (0.1 M, pH= 7.4) was freshly prepared and stored in a 10 mL opaque centrifuge tube at RT. First, 30 μL of calibration standard was mixed with 70 μL Tris-HCl buffer solution (100 mM, pH = 9.5) followed by 50 μL MBB solution (1.5 mM). Eppendorf PCR tubes containing these reagents were immediately capped, vortexed vigorously for 5 seconds and incubated for 30 min in the dark at 50 ℃. Then, the reaction was stopped with the addition of 50 μL of 200 mM 5-sulfosalicylic acid, and further vortexed for 5 s. Finally, 200 μL of the mixed solution was transferred from PCR tubes to HPLC autosampler vials equipped with a 200 μL plastic insert vial for quantification of SDB derivatization product. During the derivatization procedure, all materials were purged in a hypoxic chamber with nitrogen gas to 1% O_2. The entire derivatization procedure was carried out under dim light. The flowchart of the calibration series preparation followed by derivatization step is shown in **Figure 2.3**:

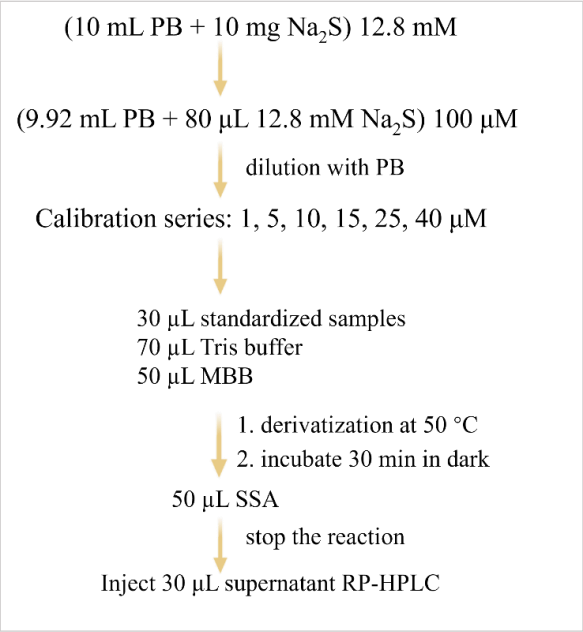

Figure 2.3 Schematic illustration of the standard solution derivatization procedure and reaction conditions for sulfide measurement.

Respective six final concentrations of calibration standards (1, 5, 10, 15, 25, and 40 µM Na_2S) were then prepared by diluting the stock solution with phosphate buffer. Deoxygenate the water and solvents by bubbling with argon for 30 min before usage, and all working standard solutions were freshly prepared for derivatization every day. Calibration curve for sulfide-dibimane (SDB) quantitation was obtained in **Figure 2.4**, Dashed line represents the fitted polynomial regression to the measured data points with the intercept going through, but not set to zero. Polynomial regression analysis showing correlation between concentration of hydrogen sulfide and fluorescence areas of SDB. Equation:

$y = 0.0133x^2 + 10.87x - 5.2437$, $R^2 = 0.999$.

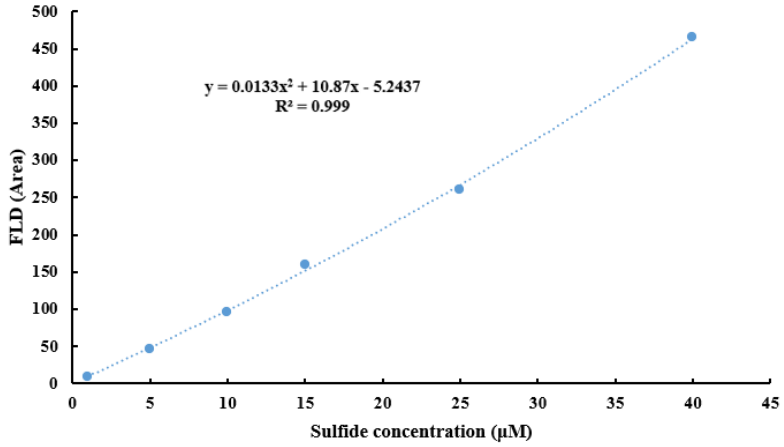

Figure 2.4 Calibration curve for sulfide-dibimane (SDB) quantitation.

Representative standardized procedure for H_2S release with MBB RP HPLC-FLD method for sulfide measurement:

The electrospun silk fibroin and GYY4137/PLGA mats were assembled and sterilized before being subjected to H_2S release studies. In this work, the MBB method with HPLC-FLD, which is suitable for sensitive quantitative measurement of sulfide was employed.

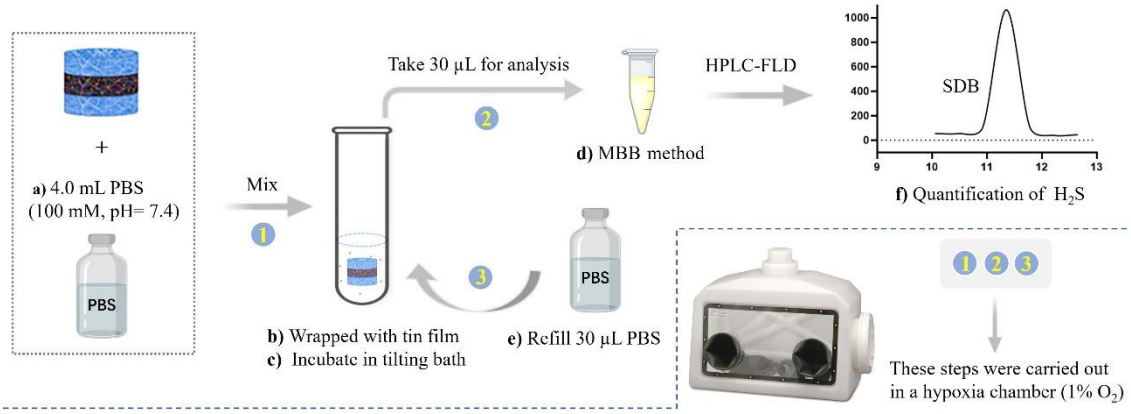

Figure 2.5 Schematic representation of the quantification procedure of H_2S donor GYY4137.

The schematic procedure for H_2S release study from the assembled scaffolds is indicated in **Figure 2.5**, (a) PB was sonicated for 30 min before use to remove dissolved gasses and/or entrained gas bubbles. (b) The combination sample consisted of scaffold and GYY4137 was first put into a 20 mL plastic tube, then added with 4.0 mL PB in a hypoxic chamber. The tube was then wrapped with aluminum film and incubated in a thermostatic shaking bath at 37 °C. (c) Released H_2S dissolved in aqueous solution was derivatized with the fluorescent alkylating agent MBB. (d) Each sampling was carried out in hypoxic chamber (1% O_2). After each withdrawal, the PB solution was refilled with the same amount of PB (30 µL). (e) Quantification of hydrogen sulfide: derivatization of H_2S with MBB, forming SDB product via S-alkylation. The resultant fluorescent SDB is analyzed by HPLC-FLD. (f) All these operation steps 1,2,3 was carried out in a hypoxic chamber (1% O_2) at room temperature.

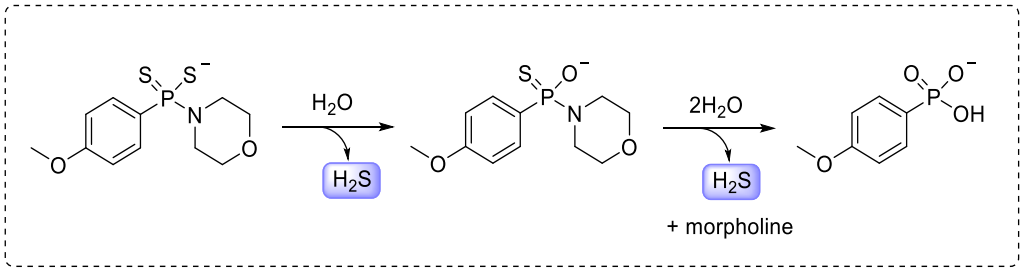

Figure 2.6 GYY4137 releases H_2S upon hydrolysis.

As shown in **Figure 2.6**, two molecules of H_2S are released per molecule of GYY4137 upon the process of hydrolysis [267].

2.3 Results

2.3.1 Degradation of GYY4137

Firstly, the above-described standardized procedure was applied to GYY4137 in PB solutions in order to check and verify the releasing efficacy of GYY4137 molecule as H_2S donor when incubated in phosphate buffer solution. During incubation, we took samples for derivatization with MBB at seven different timepoints (0, 2, 5, 20, 44, 52, and 168 h) and obtained the normalized levels of sulfide level (μg mol^{-1}/mg GYY4137) calculated by using the calibration equation. No signal was detected after derivatization step and HPLC-FLD analysis for all sampling timepoints (data not shown).

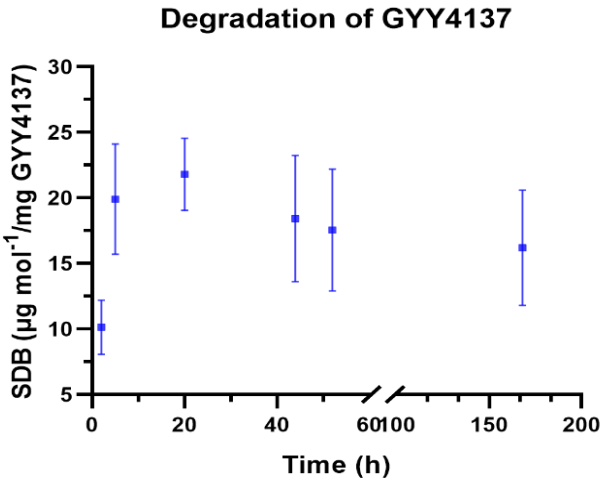

Figure 2.7 H_2S-releasing of GYY4137 from 0 h to 168 h. (Data points represent the average value of n=4 with error bars showing their standard deviation.)

In contrast, as indicated in **Figure 2.7**, from 2 to 5 hours incubation in the tilting bath a remarkably increasing trend in sulfide concentration was observed. Then, a slight rise in concentration occurred from 5 h to 20 h incubation. Afterwards, the concentration shows an insignificantly downward trend from 20 h to 52 h, and the concentration of sulfide remains in a relatively stable range even after 168 h of incubation.

2.3.2 H_2S release of sterilized multilayer samples

The investigation of the H_2S release kinetics from the multilayer scaffolds, performed in phosphate buffer according to a properly designed procedure, documented a controlled delivery

over 168 h and the possibility of modulating it by acting on GYY concentration inside the PLGA layer. The highest release registered for M5% with respect to M2% lies in the more evident "swelling" effect observed for the scaffolds with the increase of GYY concentration. In addition, to eliminate the artifacts induced by single/multi-layer scaffolds, incubation of GYY4137 without combining any layers was conducted to do a comparison with multilayer samples in which the material of GYY4137 was contained in the scaffolds. H_2S-releasing tests were carried out from 0 h to 168 h. During incubation, we took samples for derivatization with MBB at ten different timepoints (0, 2, 5, 19, 23, 28, 48, 72, 96, and 168 h) and obtained the normalized levels of sulfide level (μg mol^{-1}/mg mat) calculated by using the calibration equation.

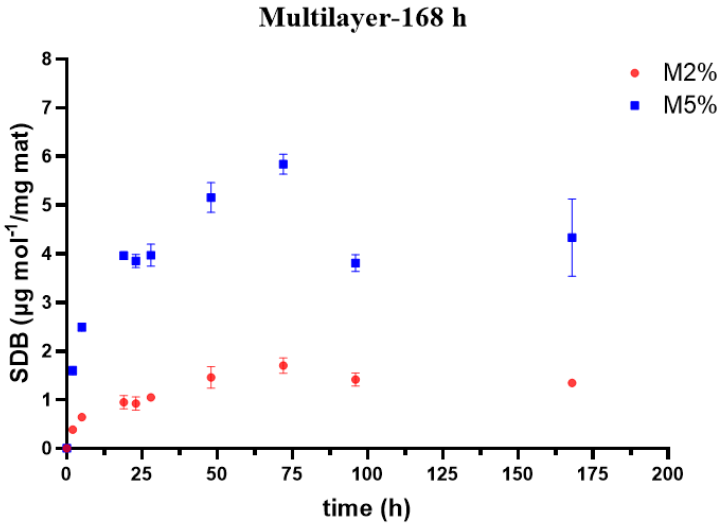

Figure 2.8 H_2S-releasing of multilayer samples from 0 h to 168 h. (Data points represent the average value of n=6 with error bars showing their standard deviation.)

Conversely, in **Figure 2.8**, area signals of SDB were observed for multilayer samples assembled with different mass concentrations of GYY4137 (2% and 5% w/w) highlighting a controlled kinetic for H_2S release. The results indicated that the concentration of sulfide presents an increasing trend and reaches the highest value in 72 hours, while a significant and a slight decrease of sulfide levels is observed for M5% and M2% from 72 h to 96 h' incubation, respectively. Then the concentration of sulfide remains relatively stable up to 168 h.

2.4 Conclusions

In this section, the designed scaffold has a multilayer architecture consisting of two external layers of electrospun silk to endow the scaffold with superior biomimetic properties and an

internal layer of PLGA nanofibers incorporating a H_2S donor, GYY4137, to achieve slow-release kinetics of H_2S. The release of H_2S in the incubation medium was determined by applying an optimized analytical method based on the derivatization of MBB and high-performance liquid chromatography with fluorescence detection (HPLC-FLD) with high sensitivity and a limit of detection of 0.5 μM for the quantification of H_2S species in our previous work [234]. The proposed analytical approach demonstrated its tunability by acting on the donor's different concentration inside the PLGA nanofibers. Our application of MBB RP HPLC-HLD method for the kinetic study of H_2S release also demonstrated that embedding an H_2S donor in multilayer silk fibroin scaffolds is a suitable strategy to achieve H_2S release in a controlled manner. Importantly, it is found that this H_2S-releasing devices were able to mitigate the cytotoxic effect induced by prolonged serum starvation as compared to control mats [268]. The study was conducted by group headed by Prof. Maria and Letizia Focarete in university of Bologna. The obtained results demonstrated this scaffold in vitro has the potential role in maintaining cell integrity and promoting tissue regeneration. It paves the way for the use of H_2S-releasing mats in bone regeneration and in different biological tissues in the near future.

Chapter 3. H_2S species measurement based on monobromobimane derivatization coupled with size exclusion chromatography fluorescence/ultraviolet detection and inductively coupled plasma-mass spectrometry (SEC-FLD/UV-ICP/MS)

3.1 Introduction

ICP-MS is proved to be one of the most powerful detection techniques for trace elements due to its high sensitivity, low mass interference, wide linear dynamic range, and isotopic analysis ability etc. [269]. Notably, coupling of efficient separation techniques (such as HPLC, GC) with ICP-MS has opened possibilities for elemental speciation with high sensitivity and selectivity. Sulfur-containing compounds are ubiquitous both in the environment and in biological matrices. Through literature investigation, the number of applications of sulfur (S) analysis using ICP-MS as detector has increased significantly. The expansion in this topic over the last 20 years is reported in **Figure 3.1**.

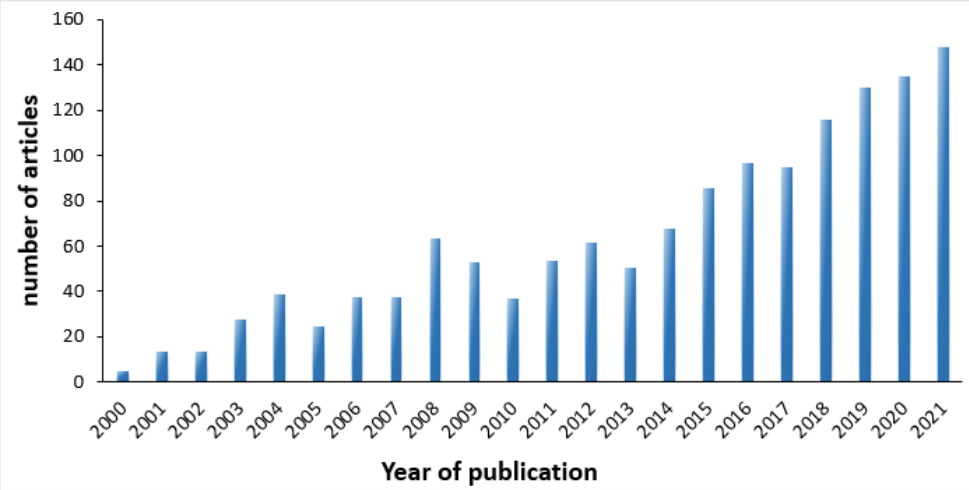

Figure 3.1 Number of peer-reviewed papers listed in the Web of Science® database over the last 20 years on sulfur analysis by ICP-MS (search terms in topic: sulfur and ICP-MS).

As we know, the elemental species in biological samples are complex and cover a wide range of chemical bonds. Previously, ion chromatography (IC) has been employed to separate multiple anions of sulfur. However, IC eluent chemistry have the potential to alter sulfur speciation and some sulfur species, e.g., polysulfides, are too reactive for accurate quantification [270, 271]. Besides, determination of low abundance species may be significantly affected by matrix interference. In order to meet the need of detection, changes in

elemental speciation include matrix removal as well as enrichment of target species should be achieved. For this proposed aim a research project, developed in collaboration with Prof José Manuel Costa Fernández and Prof. Jorge Ruiz Encinar at University of Oviedo through the Marco Polo program, was carried out.

The main point was to use the derivatization step based on MBB derivatization for H_2S species to meet the requirements and solve the problem caused by sulfur speciation alteration and matrix complexity prior to detection in ICP-MS. During this project, I put the basis for the development of a sensitive and reliable analytical method for sulfur elemental speciation sourced from H_2S biological pool in biological samples by means of ICP-MS detection.

3.2 Experimental approach

Prior to conducting experiments for H_2S species detection in biological samples, several challenges should be taken into consideration when ICP-MS hyphenated techniques are applied to study the level of H_2S species; (1) Residual proteins existing in the samples (matrix effects), such as Bovine serum albumin (BSA). (2) High concentration of sulfur-containing element from 5-sulfosalicylic acid dihydrate (SSA) in the reaction system will interfere the H_2S species detection of SDB mix. (3) Extremely low concentrations of target species also need to be detected. To solve these problems, proposed solutions were provided by hyphenating SEC-UV/FLD with ICP-MS, as shown in **Figure 3.2**.

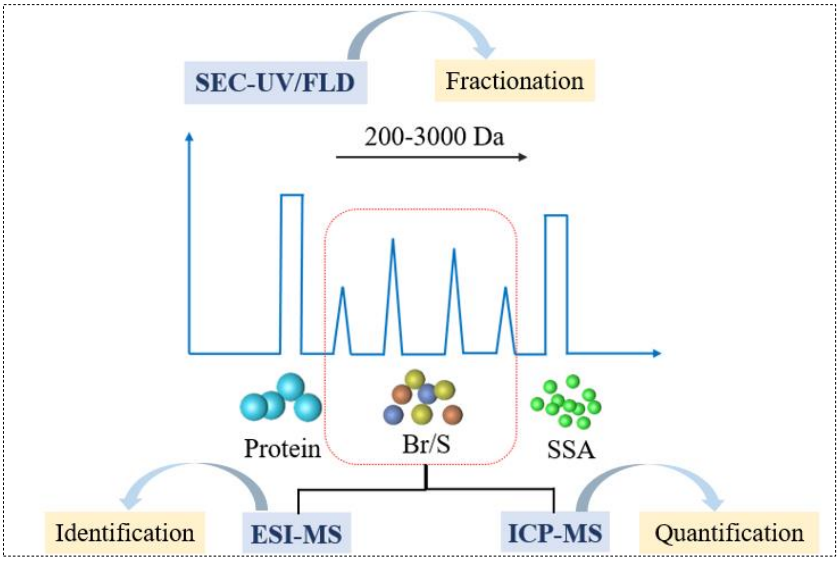

Figure 3.2 Proposed solution by hyphenated SEC-UV/FLD with ESI-MS and ICP-MS for H_2S species identification and quantification.

Thus, by using SEC-UV and Fluorescence, it's possible to discard the proteins which would cause blockage of the ICP-MS micro-nebulizer. Also, it's possible to discard the high concentration of SSA by using SEC column separation according to molecular size. Besides, collection of the fractions which containing bromine (Br) and sulfur (S) elements can achieve subsequent identification with ESI-MS and quantification with ICP-MS instruments.

Instrumentation set-up

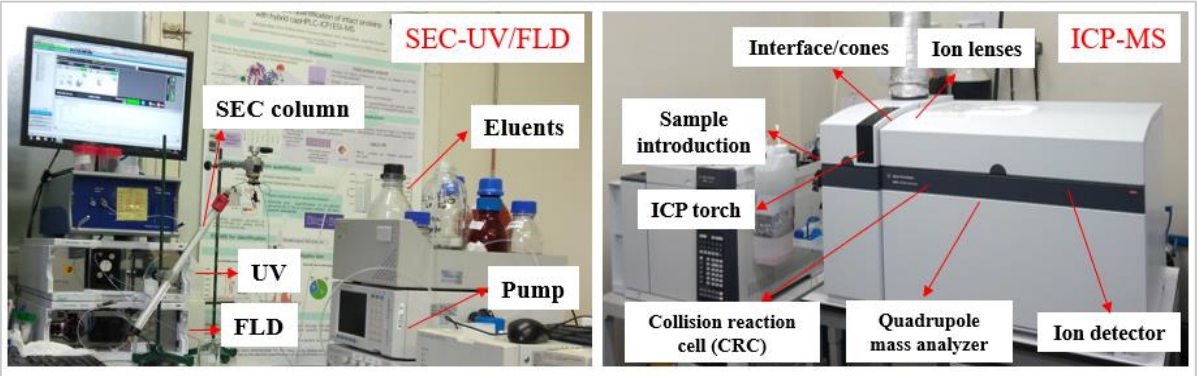

Figure 3.3 Mainframe of SEC-UV/FLD-ICP/MS instrumentation.

As shown in **Figure 3.3**, size exclusion chromatograph-Ultraviolet/visible/Fluorescence detector (SEC-UV/FLD) coupled with inductively coupled plasma-mass spectrometry (ICP-MS) were assembled for H_2S species characterization and quantification purposes.

Materials and methods

Chemicals and methods were described in paragraph 1.3.1. Sodium sulfide (Na_2S) was served as a source of H_2S species.

3.3 Preliminary studies

This work was intended as a preliminary study in order to define the feasibility of a separation-detection-quantification platform to analyze biological samples and quantify sulfur species by means of SEC-UV/FLD-ICP-MS. The results regard the use of standard samples obtained with calibration solutions, the evaluation of interferences and the ability to achieve protein-free fractions for selective detection in ICP-MS. For this last aim, the separative outcome of standard solutions of BSA was evaluated and compared to derivatized samples.

In this preliminary study, through optimization of separation conditions, 0.35 mL/min was selected as the SEC flow rate.

The calibration range was optimized as follows: a series of Na_2S calibration standards (0, 5, 10,

25, 50, 100, 200, 500 μM) were prepared by appropriate mixture and dilution of the original stock solution (5 mM Na_2S) with Milli-Q water in an opaque centrifuge tube at room temperature. Subsequently, Na_2S standards were derivatized to perform a calibration curve with the concentration of Na_2S standards as abscissa, and area of sulfur elemental from SDB peak as ordinate.

Firstly, experiments were carried out to develop a suitable chromatographic method for separation of SDB mix (Na_2S+MBB+SSA) after derivatization. The conditions employed in the following studies are in standard samples of 20 mM SSA and 175 μM MBB were prepared and injected for characterization with FLD (Ex 390/Em 475nm) and UV (267/365/390nm), respectively. Therein, SSA has the max UV absorption at 267nm. In addition, there are two main peaks generated by MBB solution at tR= 61 min (minor) and 87 min (major).

Standard samples of 20 mM SSA and 175 μM MBB were prepared and injected for characterization at FLD (Ex 390/Em 475nm) and UV (267/365/390nm), respectively.

SSA has the max absorption at UV 267nm. In addition, there are two main peaks generated by MBB solution at tR= 61 min (minor) and 87 min (major) at UV 390 nm, but three peaks obtained at tR= 54 min, 61 min (major) and 87 min at FLD 390/475 nm. The overlapped chromatograms were shown in **Figure 3.4**. It is worth noting that these generated peaks of MBB observed may be caused by the photolysis of MBB reagent mentioned in paragraph 1.5.5.

Table 3. 1 Chromatographic conditions.

SEC Column	Superdex Peptide 10/300 GL column (10 mm LD * 300 mm) (100 and 7000 Da)
Pump	The Shimadzu LC-10ADvp Solvent Delivery Pump
Temperature	Ambient
Buffer saline	50 mM phosphate buffer, 150 mM NaCl (pH 7.4)
Flow rate	0.35 (mL/min)
Detection	FLD at Ex 390 nm/Em 475 nm, UV at 276 nm and 390 nm
Injection volume	50 μL (loop 20 μL)

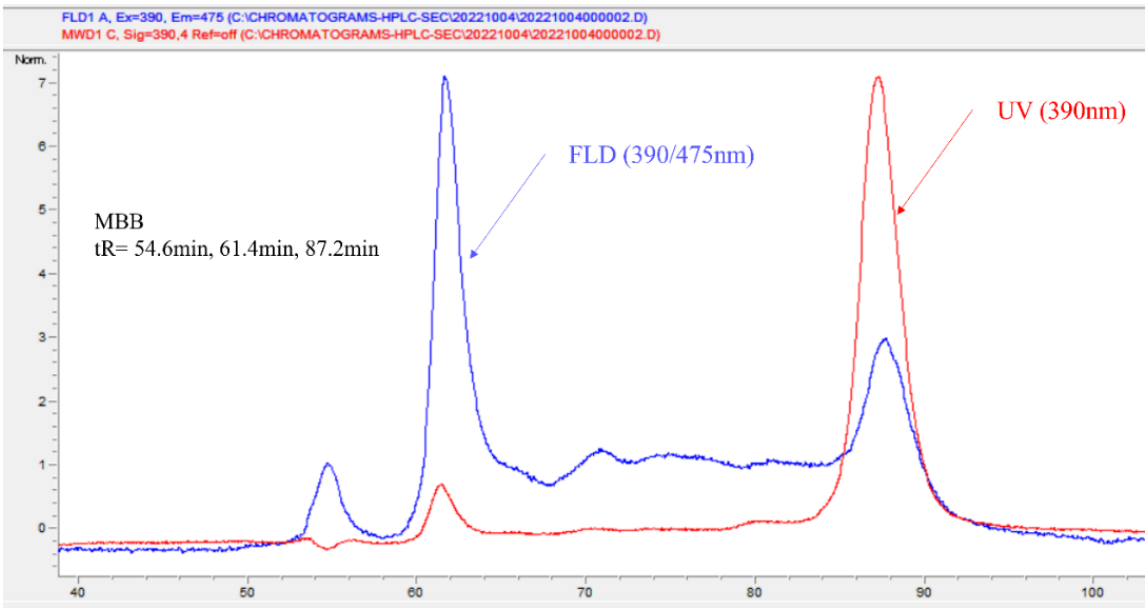

Figure 3.4 Overlaid chromatograms of MBB at FLD 390/475 nm (blue), UV 390 nm (red).

The overlaid chromatograms of SSA, MBB, 0 µM SDB mix blank at FLD 390/475 nm were indicated in **Figure 3.5**.

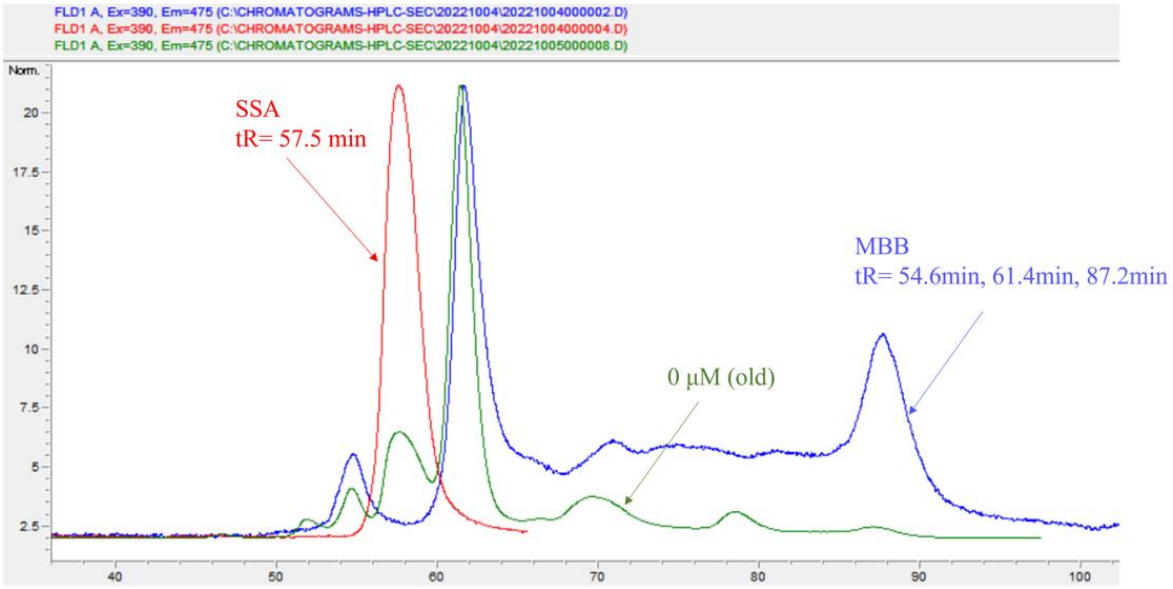

Figure 3.5 Overlaid chromatograms of SSA (red), MBB (blue), 0 µM SDB mix (green) at FLD 390/475 nm.

Following, as shown in **Figure 3.6**, a fractionation plan was devised and fractions 1-7 were collected and stored at 4-degree C for further identification by employing ESI-MS techniques. This is needed to understand what species are formed and understand which can be the best peak (or combination of peaks) to study through ICP-MS.

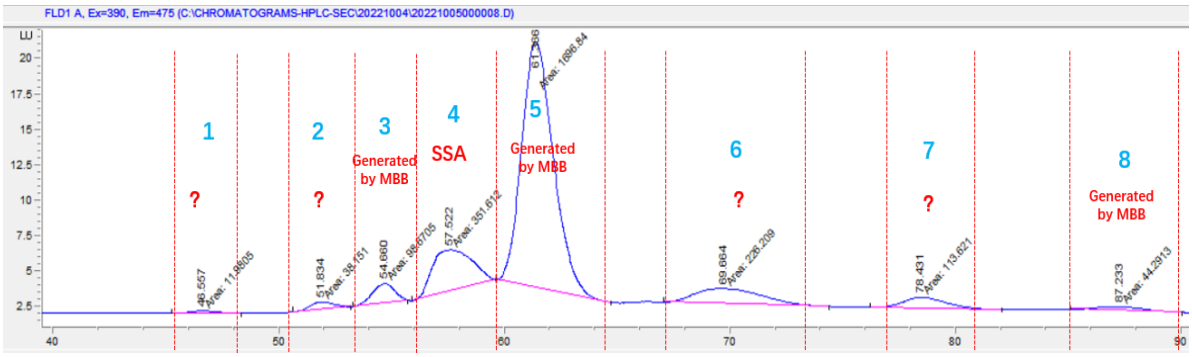

Figure 3.6 Fractionations 1-8 were collected of 100 µM SDB mixture at FLD 390/475 nm.

Unfortunately, ESI-MS was unavailable at the time of my stay in University of Oviedo, and the analyses are currently ongoing. When this point will be clarified, the method will be carried out to the final steps including peak identification and species quantification in the biological fluid.

In the meantime, preliminary work through ICP-MS was performed to ensure that the interfering species (protein and SSA) would not be an obstacle for ICP-MS detection and the SEC mobile phase would be compatible with the downstream analyses.

Bovine serum albumin (BSA) and SSA standard samples were injected into SEC-ICP-MS. The results in **Figure 3.7** indicated that sulfur element was detected at tR= 22min and 57.5min, respectively.

This outcome proved that no proteins exist in SDB mix samples since the retention times are very distant, and injecting Na_2S derivatives fractions would not result in blocking of the micro-nebulizer of ICP-MS instrument. The following experiments on SDB mix will be carried out with ICP-MS analysis after identification of SDB and MBB are achieved.

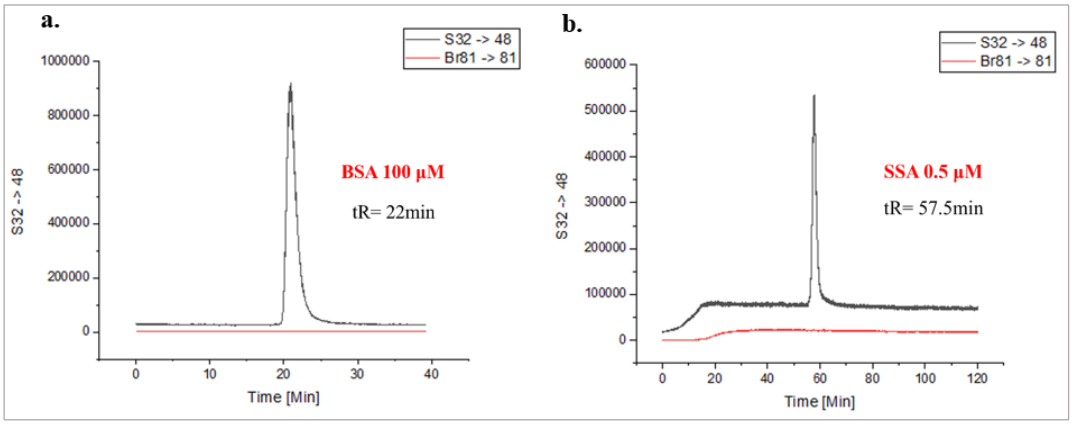

Figure 3.7 Chromatogram of samples (a)100 µM BSA (tR = 22min) and (b) 0.5 µM SSA (tR = 57.5min) observed through SEC-ICP/MS.

3.4 Future research activities

The purpose of this protocol was to establish a multi-platform for the analysis and quantification of derivatized H_2S species in biological samples by using hyphenated SEC-UV/FLD with ICP-MS techniques. Future research activities will be focused on the determination of a SDB derivative sourced from reaction system between H_2S species in presence of MBB. Specifically, SDB and MBB can be employed to detect species belonging to the bromine and sulfur-containing compounds, respectively. The abundance of sulfur or bromine elements derived from SDB product and the excessive MBB is expected to be determined by employing the measured counts of selected isotope ($^{32}S/^{48}SO_2$ and $^{79}Br/^{81}Br$). Thus, an external calibration curve can be generated from the two proposed elements. However, the initial results failed to provide significant information associated with SDB product by now. The further research activities will put more effort into the method optimization to improve the sensitivity of SEC-ICP-MS techniques. Then, it's expected for the first time to establish a multi-platform for the quantification of H_2S species in biological samples. Afterwards, method validation also will be considered routinely in future research activities, such as parameters linearity, LOD, LOQ etc.

General conclusions and outlook

Sulfur is known as a biologically active element, and the determination and biological relevance of the sulfur compounds, particularly that of H_2S species, has received critical attention in scientific community. Detection of these sulfur levels might give valuable information in some systemic diseases and metabolic disorders. In spite of toxic properties, volatile H_2S has been lately regarded as a new gasotransmitter, based on high concentration found in healthy biological tissues. However, there is much doubt about the reliability of the common assay methods used. Sulfur quantification is often hindered by numerous artifacts, such as the instability of sulfide, high volatility, the susceptibility to oxidation, the erroneous release of sulfide from some tube additives, and adsorbed on glass material. All these reasons may result in artificially raised or reduced levels and explain the large discrepancy among the reported extensive works. Moreover, most reports do not differentiate the most important three forms of H_2S levels, i.e., free, acid-labile and bound sulfane sulfur. These different forms may have distinctive functions and it is necessary to establish reliable and validated methods to discriminate among these significant forms. Thus, we can gain more insight in the physiological role of the various forms through the elucidation of the chemical properties of these labile sulfides.

In this thesis work, I optimized and validated a MBB derivatization method coupled with a HPLC-FLD protocol for H_2S species quantification in human serum sample and validated for the first time the procedure of calibration. Crucial factors influencing the actual H_2S species level were considered and excluded from the protocol. Furthermore, we provided evidence of the importance of the procedure of preparation of standard solution and the relative calibration. Overall, the optimized method results in a more efficient derivatization of H_2S with MBB, with a low perturbation of sample equilibria, giving a robust value for endogenous H_2S species. Although this method cannot achieve absolute quantification of H_2S species, it is a good method for relative quantification. Importantly, initial progress had been put forward in indirectly determining the action of vapor sulfide on the primary target organs. This work was part of a research collaboration between our group and the RAMSES IRCCS of Istituto Ortopedico Rizzoli. By revealing a modulation in H_2S species in patients that underwent sulfurous water

inhalation, we demonstrated that the method proposed is a reliable tool to measure H_2S species in biological matrices. This validated detection and quantification method can improve H_2S species relative quantification in physiology, pathology, and for helping to track H_2S levels in the context of pharmacological exogenous H_2S treatments.

Additionally, H_2S-releasing tests were performed with the further optimized MBB RP HPLC-HLD method on a biomimetic silk fibroin scaffold with a H_2S donor, GYY4137. This study was conducted in collaboration with Prof Maria Letizia Focarete and the research group in University of Bologna. A slow release of H_2S was achieved and monitored. It's suggested that silk fibroin scaffolds loaded with GYY4137 could be released in a suitable controlled way. The findings may demonstrate that high steady state of H_2S preserved in the silk fibroin scaffold and has potential for local delivery at sites of tissue injury. This may be also helpful for further proposed application in the future in clinical settings.

A preliminary study regarding the characterization and quantification of sulfur species in biological samples by means of SEC-ICP-MS was also carried on thanks to an international collaboration with the group of Prof. Prof José Manuel Costa Fernández and Prof Jorge Ruiz Encinar, in University of Oviedo, and a Marco Polo grant. The preliminary study confirmed the feasibility of this approach and most of all confirmed that it is possible to isolate derivatized sulfur species from protein interferences, allowing a safe detection through ICP-MS, otherwise impossible.

In the future, research activities will still emphasize on the method development to establish a multi-platform for the quantification of H_2S species in biological specimen. In particular, we will focus on the method optimization to improve the sensitivity of SEC-ICP-MS techniques. Thus, it's possible to gain more insight into the sulfur pool levels of biological relevance. This may be helpful to obtain insight on the mechanism and the efficacy of therapies based on sulfur-treatment.

Appendices a-d

a. List of abbreviations and acronyms

Abbreviations	Name
AMI	Myocardial infarction
AD	Alzheimer disease
AECOPD	Acute exacerbation of COPD
ALS	Acid-labile sulfide
AAS	Atomic absorption spectroscopy
ANOVA	Analysis of variance
BMT	Bisulfide methyltransferase
BSS	Bound sulfane sulfur/Bound sulfur species
BSA	Bovine serum albumin
CV	Cross-validation
CBS	Cystathionine β-synthase
CSE	Cystathionine γ-lyase
CAT	Cysteine aminotransferase
CNS	Central nervous system
CVD	Cardiovascular disease
COPD	Chronic obstructive pulmonary disease
CL	Chemiluminescence
DAO	D-Amino acid oxidase
DTT	Dithiothreitol
dBBr	4,6-dibromomethyl-3,7-dimethyl-l,5 -diazabicyclo [3.3.0]octa-3,6-diene-2,8-dione
DTPA	Diethylenetriaminepentaacetic acid
ETHE1	Ethylmalonic encephalopathy 1 protein
EDTA	Ethylenediaminetetraacetic acid
GYY4137	Morpholin-4-ium-4 methoxyphenyl(morpholino)

	phosphinodithioate
GSH	Glutathione
GSSG	Glutathione disulfide
GC-FPD	Gas chromatography with flame photometric detector
GC/ECD	Gas chromatography with an electron capture detector
GC/MS	Gas chromatography with mass spectrometry
HAS	human serum albumin
HEPES	(4-(2-hydroxyethyl)-1-piperazineethanesulfonic acid)
IOP	Intraocular pressure
IAM	Iodoacetamide
IC	Ion chromatography
LOD	Limit of Detection
LOQ	Limit of Quantification
LSS	Labile sulfur species
MBB	Monobromobimane (4-bromomethyl-3,6,7-trimethyl-l,5-diazabicyclo[3.3.0]octa-3,6-diene-2,8-dione)
MB	Methylene blue
NF-kB	Nuclear factor-kappa B
Nrf2	Nuclear factor erythroid 2-related factor 2
NMR	Nuclear magnetic resonance
NEM	N-ethylmaleimide
PLGA	Poly(lactic-co-glycolic acid)
PLP	Pyridoxal phosphate
PD	Parkinson’s Disease
PAD	Peripheral arterial disease
qBBr	4-bromomethyl-3,7-dimethyl-6-trimethylammoniomethyl-l,5-diazabicyclo [3.3.0]octa-3,6-diene-2,8-dione (as bromide salt)
RSS	Reactive sulfur species

RP-HPLC	Reversed phase high-performance liquid chromatography
ROS	Reactive oxygen species
RNS	Reactive nitrogen species
RDS	Rate-determining step
RMSE	Root mean squared error
SSA	5-sulfosalicylic acid dihydrate
SAAs	Sulfur-containing amino acids
SQR	Sulfide quinone oxidoreductase
SOD	Superoxide dismutase
STEMI	ST-elevation myocardial infarction
SAM	S-adenosyl-L-methionine
SIM	Selected ion monitoring
SCD	Sulfur chemiluminescence detector
SBBr	4-p-sulfobenzoyloxymethyl-6-bromomethyl-3,7-dimethyl-l,5-diazabicyclo[3.3.0]octa-3,6-diene-2,8-dione (as tetramethylammonium salt)
SMB	Sulfide-monobimane
SDB	Sulfide dibimane
SBF	Simulated body fluid solution
3-MST	3-mercaptopyruvate sulfurtransferase
3-MP	3-mercaptopyruvate
TSR	Thiosulfate reductase
TSST	Thiosulfate sulfurtransferase
TSMT	Thiol-S-methyltransferase
TCEP	Tris(2-carboxyethyl) phosphine
UC	Ulcerative colitis

b. List of tables

c. List of figures

Acknowledgements

In this part, I will take this precious opportunity to express my appreciation to those specifically mentioned here who have involved and guided my path during my dissertation completing.

First and foremost, I would like to show my deepest gratitude to my supervisor, Prof. Pierluigi Reschiglian, a respectable and responsible academic. In the past three years, as a leader, you motivated me with a positive and capacious attitude. You were always there when I need you and allowed me to try what I wanted during the course of my project work. Besides, I would like to express my thanks to my co-supervisor Prof. Daniele Fabbri and Prof. Barbara Roda, I felt so lucky that having the chance to work with you and under your supervision. Without your enlightening instruction, support and resourceful, it would not be possible to complete my PhD dissertation smoothly for every step of the way. You gave me so much support and advice and provided me the best discussion also guidance academically. I am grateful for your help on sharpening the professional skills of analytical science. Your intellectual contributions and scientific suggestions to the project pushed me and made me a better researcher. Thank you Prof. Andrea Zattoni, who introduced to me a lot when I initially entered into the analytical lab. Thanks Prof. Valentina Marassi for always being enthusiastic and taking good care of everything in our lab. You are an industrious person and always attends to the solution of important business even on remote way. It truly impressed everyone and created a wonderful and harmonious lab environment. Furthermore, many thanks to the help and patience of my colleagues Stefano Giordani and Junjie Wang in my past PhD studies. Your excellent autonomy in the management of the experiments and hardworking attitude inspiring me a lot. It was great to work with you in the same lab. All in all, you are really one of the best tutors and colleagues I have ever met. Meantime, thanks Dr. Paolo Neviani, Dr. Alessandro Zappi and Chiara Di Tonto for the theoretical support and kind discussion for the problems during my project research. I would like to thank Dr. Elisabetta Petri for assistance with the collaborative project and sharing the expertise in Electrospinning. Without your efforts, much of the application work presented in this thesis would not be possible. A special thanks to my lovely colleagues JunWei Zhao, Ningjing Jiang, Wentao Song, Renren Sun and Tingting He who have being working in the same department of chemistry. Thank you for always being my side and always being kind

to me. That really made my learning easier and life happier as well as made me never felt lonely in a foreign country. The great companionship and friendship during the three years spent in the Bologna will surely be a memorable part to me in my future life.

Besides, heartfelt thanks to give leaders Prof. José Manuel Costa Fernandez and Prof. Jorge Ruiz Encinar who are responsible for the optical and mass spectrometry research in the Analytical and Bioanalytical Spectrometry Group (GEAB), respectively. You are both respectable and resourceful scholars in my heart. Thanks for allowing my mobility research in your group at University of Oviedo in Spain for three months. Your hospitality made me relax when discussed the project with you. Constantly, you are approachable for discussion and have been always giving me feedbacks and constructive suggestions. And your vigorous academic activities and insightful scientific discussions enlightened me in the supplementary part of the thesis finally made it more integrated. I would also like to thank Dr. Francisco Calderon Celis for useful instructions and intellectual contributions when applying coupled instruments for quantification experiments. And I am grateful to my colleague Dr. Julia Ruiz Allica, especially for the help at the beginning of my studying at the group. During the co-working of three months mobility research. I really have received endless help from all collaborators. Above all, my scientific journey was perfect with the help of all group members in a supportive and collaborative research environment.

Also, this research was funded by Italian Ministry of Health, grant number RF-2016-671 02362238, which paid the APC. I’m grateful for the scholarship from China Scholarships Council (CSC), which provided the generous scholarship covering all my financial expenditure during PhD period and made this dissertation defense possible. Absolutely it played a significant role both in assuring my study and life issues solving. What’s more, I would like to acknowledge all the staff at University of Bologna, "Giacomo Ciamician", Department of Chemistry. I shall extend my thanks to the Laboratorio RAMSES, IRCCS Istituto Ortopedico Rizzoli (Bologna), for serum samples providing, and thanks to Prof Maria Letizia Focarete and Dr. Elisabetta Petri, for silk fibroin scaffold and H_2S donor GYY4137 providing. Attribute to their technical supporting, I can successfully complete these twoproposed research projects.

Last but not least, I truly feel blessed to have supportive and beloved family members. I would

like to express a special thanks to my parents (Wang Jing and Zhang yin) and brothers (Zhang Tong and Zhang Qingsong) for many years encouragement during my journey through three-year duration of PhD study. You were being there for me and never failed to motivate me all the time when my work or life was tough. Your selfless love helped me persevere and helped me get out of hardship. It's an inspiration for me to keep improving both in the past and future studies. Additionally, I have to thank my boyfriend Ding Zhanghao. You are really a considerate boy and give every care to me in life throughout my thesis writing process. Thanks for all feeling of beloved and happiness you brought to me.

References

[1] P. Nagy, Z. Palinkas, A. Nagy, B. Budai, I. Toth, A. Vasas, Chemical aspects of hydrogen sulfide measurements in physiological samples, *Biochim Biophys Acta* **1840**(2) (**2014**) 876-891.
[2] C.K. Y., M.J. Carrel, Kinetics of Oxidation of Aqueous Sulfide by O2, *Environmental Science & Technology* **6**(6) (**1972**) 529-537.
[3] E. Cuevasanta, A. Denicola, B. Alvarez, M.N. Moller, Solubility and permeation of hydrogen sulfide in lipid membranes, *PLoS One* **7**(4) (**2012**) e34562.
[4] Q. Li, J.R. Lancaster, Jr., Chemical foundations of hydrogen sulfide biology, *Nitric Oxide* **35** (**2013**) 21-34.
[5] B. Ramazzini, De morbis artificum diatriba [diseases of workers], *Am J Public Health* **91** (**1713**) 1380–1382.
[6] R.J. Reiffenstein, W.C. Hulbert, S.H. Roth, Toxicology of Hydrogen Sulfide, *Annual Review of Pharmacology and Toxicology* **32** (**1992**) 109-134.
[7] D.H. Truong, M.A. Eghbal, W. Hindmarsh, S.H. Roth, P.J. O'Brien, Molecular mechanisms of hydrogen sulfide toxicity, *Drug Metab Rev* **38**(4) (**2006**) 733-744.
[8] T.L. Guidotti, Hydrogen Sulfide: Advances in Understanding Human Toxicity, *International Journal of Toxicology* **29**(6) (**2010**) 569-581.
[9] T.H. Milby, R.C. Baselt, Hydrogen sulfide poisoning: Clarification of some controversial issues, *American journal of industrial medicine* **35**(2) (**1999**) 192-195.
[10] D.C. Dorman, F.J.-M. Moulin, B.E. McManus, K.C. Mahle, R.A. James, M.F. Struve, Cytochrome Oxidase Inhibition Induced by Acute Hydrogen Sulfide Inhalation: Correlation with Tissue Sulfide Concentrations in the Rat Brain, Liver, Lung, and Nasal Epithelium, *Toxicological Sciences* **65**(1) (**2002**) 18–25.
[11] A.A. Khan, M.M. Schuler, M.G. Prior, S. Yong, R.W. Coppock, L.Z. Florence, L.E. Lillie, Effects of hydrogen sulfide exposure on lung mitochondrial respiratory chain enzymes in rats, *Toxicology and applied pharmacology* **103**(3) (**1990**) 482-490.
[12] V. Vitvitsky, O. Kabil, R. Banerjee, High turnover rates for hydrogen sulfide allow for rapid regulation of its tissue concentrations, *Antioxid Redox Signal* **17**(1) (**2012**) 22-31.
[13] K.R. Olson, A practical look at the chemistry and biology of hydrogen sulfide, *Antioxid Redox Signal* **17**(1) (**2012**) 32-44.
[14] X. Cao, L. Ding, Z.Z. Xie, Y. Yang, M. Whiteman, P.K. Moore, J.S. Bian, A Review of Hydrogen

Sulfide Synthesis, Metabolism, and Measurement: Is Modulation of Hydrogen Sulfide a Novel Therapeutic for Cancer?, *Antioxid Redox Signal* **31**(1) (**2019**) 1-38.
[15] J. Yang, P. Minkler, D. Grove, R. Wang, B. Willard, R. Dweik, C. Hine, Non-enzymatic hydrogen sulfide production from cysteine in blood is catalyzed by iron and vitamin B6, *Commun Biol* **2** (**2019**) 194.
[16] O. Kabil, R. Banerjee, Enzymology of H2S biogenesis, decay and signaling, *Antioxid Redox Signal* **20**(5) (**2014**) 770-782.
[17] N. Shibuya, M. Tanaka, M. Yoshida, Y. Ogasawara, T. Togawa, K. Ishii, H. Kimura, 3-Mercaptopyruvate Sulfurtransferase Produces Hydrogen Sulfide and Bound Sulfane Sulfur in the Brain, *Antioxidants & Redox Signaling* **11**(4) (**2009**) 703-714.
[18] N. Shibuya, S. Koike, M. Tanaka, M. Ishigami-Yuasa, Y. Kimura, Y. Ogasawara, K. Fukui, N. Nagahara, H. Kimura, A novel pathway for the production of hydrogen sulfide from D-cysteine in mammalian cells, *Nat Commun* **4** (**2013**) 1366.
[19] P.K. Moore, M. Whiteman, (2015) Chemistry, Biochemistry and Pharmacology of Hydrogen Sulfide, Springer.
[20] K.R. Olson, Y. Gao, F. Arif, K. Arora, S. Patel, E.R. DeLeon, T.R. Sutton, M. Feelisch, M.M. Cortese-Krott, K.D. Straub, Metabolism of hydrogen sulfide (H2S) and Production of Reactive Sulfur Species (RSS) by superoxide dismutase, *Redox Biol* **15** (**2018**) 74-85.
[21] R. Hosoki, N. Matsuki, H. Kimura, The Possible Role of Hydrogen Sulfide as an Endogenous Smooth Muscle Relaxant in Synergy with Nitric Oxide, *Biochemical and Biophysical Research Communications* **237**(3) (**1997**) 527-531.
[22] R. Wang, Two's company, three's a crowd: can H2S be the third endogenous gaseous transmitter?, *The FASEB journal* **16**(13) (**2002**) 1792-1798.
[23] R. Wang, The Gasotransmitter Role of Hydrogen Sulfide, *Antioxidants and Redox Signaling* **5**(4) (**2003**) 493-501.
[24] M.M. Gadalla, S.H. Snyder, Hydrogen sulfide as a gasotransmitter, *J Neurochem* **113**(1) (**2010**) 14-26.
[25] M. Vandiver, S.H. Snyder, Hydrogen sulfide: a gasotransmitter of clinical relevance, *J Mol Med (Berl)* **90**(3) (**2012**) 255-263.
[26] K.R. Olson, K.D. Straub, The Role of Hydrogen Sulfide in Evolution and the Evolution of Hydrogen Sulfide in Metabolism and Signaling, *Physiology (Bethesda)* **31**(1) (**2016**) 60-72.
[27] M. Kumar, R. Sandhir, Hydrogen Sulfide in Physiological and Pathological Mechanisms in Brain, *CNS Neurol Disord Drug Targets* **17**(9) (**2018**) 654-670.
[28] H. Kimura, The physiological role of hydrogen sulfide and beyond, *Nitric Oxide* **41** (**2014**) 4-10.
[29] H. Kimura, Hydrogen sulfide and polysulfides as signaling molecules, *Proc Jpn Acad Ser B Phys Biol Sci* **91**(4) (**2015**) 131-159.
[30] H. Kimura, Hydrogen sulfide signalling in the CNS - Comparison with NO, *Br J Pharmacol* **177**(22) (**2020**) 5031-5045.
[31] N. Yang, Y. Liu, T. Li, Q. Tuo, Role of Hydrogen Sulfide in Chronic Diseases, *DNA Cell Biol* **39**(2) (**2020**) 187-196.
[32] A. Aroca, C. Gotor, D.C. Bassham, L.C. Romero, Hydrogen Sulfide: From a Toxic Molecule to a Key Molecule of Cell Life, *Antioxidants (Basel)* **9**(7) (**2020**) 621.
[33] C. Szabo, A timeline of hydrogen sulfide (H2S) research: From environmental toxin to biological mediator, *Biochem Pharmacol* **149** (**2018**) 5-19.

[34] H. Kimura, Hydrogen sulfide as a neuromodulator, *Molecular Neurobiology* **26**(1) (**2002**) 13-19.
[35] K. Kida, M. Yamada, K. Tokuda, E. Marutani, M. Kakinohana, M. Kaneki, F. Ichinose, Inhaled Hydrogen Sulfide Prevents Neurodegeneration and Movement Disorder in a Mouse Model of Parkinson's Disease, *Antioxidants & Redox Signaling* **15**(2) (**2011**) 343-352.
[36] H. Kimura, Physiological role of hydrogen sulfide and polysulfide in the central nervous system, *Neurochem Int* **63**(5) (**2013**) 492-497.
[37] K. Abe, H. Kimura, The possible role of hydrogen sulfide as an endogenous neuromodulator, *Journal of Neuroscience* **16**(3) (**1996**) 1066-1071.
[38] Y. Kimura, H. Kimura, Hydrogen sulfide protects neurons from oxidative stress, *The FASEB journal* **18**(10) (**2004**) 1165-1167.
[39] X. Zhang, J.S. Bian, Hydrogen sulfide: a neuromodulator and neuroprotectant in the central nervous system, *ACS Chem Neurosci* **5**(10) (**2014**) 876-883.
[40] Y. Kaneko, Y. Kimura, H. Kimura, I. Niki, L-cysteine inhibits insulin release from the pancreatic beta-cell: possible involvement of metabolic production of hydrogen sulfide, a novel gasotransmitter, *Diabetes* **55**(5) (**2006**) 1391-1397.
[41] H.J. Chen, E.E. Ngowi, L. Qian, T. Li, Y.Z. Qin, J.J. Zhou, K. Li, X.Y. Ji, D.D. Wu, Role of Hydrogen Sulfide in the Endocrine System, *Front Endocrinol (Lausanne)* **12** (**2021**) 704620.
[42] C. Hine, Y. Zhu, A.N. Hollenberg, J.R. Mitchell, Dietary and Endocrine Regulation of Endogenous Hydrogen Sulfide Production: Implications for Longevity, *Antioxid Redox Signal* **28**(16) (**2018**) 1483-1502.
[43] I. Lobb, E. Sonke, G. Aboalsamh, A. Sener, Hydrogen sulphide and the kidney: important roles in renal physiology and pathogenesis and treatment of kidney injury and disease, *Nitric Oxide* **46** (**2015**) 55-65.
[44] D. Feliers, H.J. Lee, B.S. Kasinath, Hydrogen Sulfide in Renal Physiology and Disease, *Antioxid Redox Signal* **25**(13) (**2016**) 720-731.
[45] M. Jimenez, V. Gil, M. Martinez-Cutillas, N. Mane, D. Gallego, Hydrogen sulphide as a signalling molecule regulating physiopathological processes in gastrointestinal motility, *Br J Pharmacol* **174**(17) (**2017**) 2805-2817.
[46] K.R. Olson, A Case for Hydrogen Sulfide Metabolism as an Oxygen Sensing Mechanism, *Antioxidants (Basel)* **10**(11) (**2021**) 1650.
[47] S. Fiorucci, E. Distrutti, G. Cirino, J.L. Wallace, The emerging roles of hydrogen sulfide in the gastrointestinal tract and liver, *Gastroenterology* **131**(1) (**2006**) 259-271.
[48] S.B. Singh, H.C. Lin, Hydrogen Sulfide in Physiology and Diseases of the Digestive Tract, *Microorganisms* **3**(4) (**2015**) 866-889.
[49] Y. Han, Q. Shang, J. Yao, Y. Ji, Hydrogen sulfide: a gaseous signaling molecule modulates tissue homeostasis: implications in ophthalmic diseases, *Cell Death Dis* **10**(4) (**2019**) 293.
[50] Q. Dong, B. Yang, J.G. Han, M.M. Zhang, W. Liu, X. Zhang, H.L. Yu, Z.G. Liu, S.H. Zhang, T. Li, D.D. Wu, X.Y. Ji, S.F. Duan, A novel hydrogen sulfide-releasing donor, HA-ADT, suppresses the growth of human breast cancer cells through inhibiting the PI3K/AKT/mTOR and Ras/Raf/MEK/ERK signaling pathways, *Cancer Lett* **455** (**2019**) 60-72.
[51] D. Wu, W. Si, M. Wang, S. Lv, A. Ji, Y. Li, Hydrogen sulfide in cancer: Friend or foe?, *Nitric Oxide* **50** (**2015**) 38-45.
[52] R.H. Wang, Y.H. Chu, K.T. Lin, The Hidden Role of Hydrogen Sulfide Metabolism in Cancer, *Int J Mol Sci* **22**(12) (**2021**) 6562.

[53] C. Szabo, Gasotransmitters in cancer: from pathophysiology to experimental therapy, *Nat Rev Drug Discov* **15**(3) (**2016**) 185-203.
[54] Y. Liu, R. Yang, X. Liu, Y. Zhou, C. Qu, T. Kikuiri, S. Wang, E. Zandi, J. Du, I.S. Ambudkar, S. Shi, Hydrogen sulfide maintains mesenchymal stem cell function and bone homeostasis via regulation of Ca(2+) channel sulfhydration, *Cell Stem Cell* **15**(1) (**2014**) 66-78.
[55] S. Awata, K. Nakayama, I. Suzuki, K. Sugahara, H. Kodama, Changes in cystathionine gamma-lyase in various regions of rat brain during development, *Biochemistry and molecular biology international* **35**(6) (**1995**) 1331-1338.
[56] J.W. Calvert, W.A. Coetzee, D.J. Lefer, Novel Insights Into Hydrogen Sulfide–Mediated Cytoprotection, *Antioxidants & Redox Signaling* **12**(10) (**2010**) 1203-1217.
[57] H. Kimura, N. Shibuya, Y. Kimura, Hydrogen sulfide is a signaling molecule and a cytoprotectant, *Antioxid Redox Signal* **17**(1) (**2012**) 45-57.
[58] J.W. Elrod, J.W. Calvert, J. Morrison, J.E. Doeller, D.W. Kraus, L. Tao, X. Jiao, R. Scalia, L. Kiss, C. Szabo, H. Kimura, C.-W. Chow, D.J. Lefer, Hydrogen sulfide attenuates myocardial ischemia-reperfusion injury by preservation of mitochondrial function, *Proceedings of the National Academy of Sciences* **104**(39) (**2007**) 15560-15565.
[59] V. Citi, A. Martelli, V. Brancaleone, S. Brogi, G. Gojon, R. Montanaro, G. Morales, L. Testai, V. Calderone, Anti-inflammatory and antiviral roles of hydrogen sulfide: Rationale for considering H2S donors in COVID-19 therapy, *British journal of pharmacology* **177**(21) (**2020**) 4931-4941.
[60] J.L. Wallace, J.G. Ferraz, M.N. Muscara, Hydrogen sulfide: an endogenous mediator of resolution of inflammation and injury, *Antioxid Redox Signal* **17**(1) (**2012**) 58-67.
[61] M. Whiteman, P.G. Winyard, Hydrogen sulfide and inflammation: the good, the bad, the ugly and the promising, *Expert Review of Clinical Pharmacology* **4**(1) (**2011**) 13-32.
[62] A. Ianaro, G. Cirino, J.L. Wallace, Hydrogen sulfide-releasing anti-inflammatory drugs for chemoprevention and treatment of cancer, *Pharmacol Res* **111** (**2016**) 652-658.
[63] J.L. Wallace, R.W. Blackler, M.V. Chan, G.J. Da Silva, W. Elsheikh, K.L. Flannigan, I. Gamaniek, A. Manko, L. Wang, J.P. Motta, A.G. Buret, Anti-inflammatory and cytoprotective actions of hydrogen sulfide: translation to therapeutics, *Antioxid Redox Signal* **22**(5) (**2015**) 398-410.
[64] A. Katsouda, S.I. Bibli, A. Pyriochou, C. Szabo, A. Papapetropoulos, Regulation and role of endogenously produced hydrogen sulfide in angiogenesis, *Pharmacol Res* **113**(Pt A) (**2016**) 175-185.
[65] G. Yang, L. Wu, B. Jiang, W. Yang, J. Qi, K. Cao, Q. Meng, A.K. Mustafa, W. Mu, S. Zhang, S.H. Snyder, R. Wang, H2S as a physiologic vasorelaxant: hypertension in mice with deletion of cystathionine gamma-lyase, *Science* **322**(5901) (**2008**) 587-590.
[66] Y.H. Liu, M. Lu, L.F. Hu, P.T. Wong, G.D. Webb, J.S. Bian, Hydrogen sulfide in the mammalian cardiovascular system, *Antioxid Redox Signal* **17**(1) (**2012**) 141-185.
[67] S.H. Cheung, W.K. Kwok, K.F. To, J.Y. Lau, Anti-atherogenic effect of hydrogen sulfide by over-expression of cystathionine gamma-lyase (CSE) gene, *PLoS One* **9**(11) (**2014**) e113038.
[68] A. Stein, S.M. Bailey, Redox Biology of Hydrogen Sulfide: Implications for Physiology, Pathophysiology, and Pharmacology, *Redox Biol* **1**(1) (**2013**) 32-39.
[69] C. Tang, X. Li, J. Du, Hydrogen Sulfide as a New Endogenous Gaseous Transmitter in the Cardiovascular System, *Current Vascular Pharmacology* **4**(1) (**2006**) 17-22.
[70] S. Yuan, X. Shen, C.G. Kevil, Beyond a Gasotransmitter: Hydrogen Sulfide and Polysulfide in Cardiovascular Health and Immune Response, *Antioxid Redox Signal* **27**(10) (**2017**) 634-653.
[71] D.J. Polhemus, D.J. Lefer, Emergence of hydrogen sulfide as an endogenous gaseous signaling

molecule in cardiovascular disease, *Circ Res* **114**(4) (**2014**) 730-737.
[72] R.A. Dombkowski, M.J. Russell, K.R. Olson, Hydrogen sulfide as an endogenous regulator of vascular smooth muscle tone in trout, *American Journal of Physiology-Regulatory, Integrative and Comparative Physiology* **286**(4) (**2004**) 678-685.
[73] H. Kimura, Hydrogen Sulfide: From Brain to Gut, *Antioxidants & Redox Signaling* **12**(9) (**2010**) 1111-1123.
[74] T. Chang, A. Untereiner, J. Liu, L. Wu, Interaction of Methylglyoxal and Hydrogen Sulfide in Rat Vascular Smooth Muscle Cells, *Antioxidants & Redox Signaling* **12**(9) (**2010**) 1093-1100.
[75] H.J. Sun, Z.Y. Wu, X.W. Nie, J.S. Bian, Role of Endothelial Dysfunction in Cardiovascular Diseases: The Link Between Inflammation and Hydrogen Sulfide, *Front Pharmacol* **10** (**2019**) 1568.
[76] B. Olas, Hydrogen sulfide in signaling pathways, *Clin Chim Acta* **439** (**2015**) 212-218.
[77] J.W. Calvert, S. Jha, S. Gundewar, J.W. Elrod, A. Ramachandran, C.B. Pattillo, C.G. Kevil, D.J. Lefer, Hydrogen sulfide mediates cardioprotection through Nrf2 signaling, *Circ Res* **105**(4) (**2009**) 365-374.
[78] Y. Ji, Y. Li, Z. Zhao, P. Li, Y. Xie, Hydrogen Sulfide Overproduction Is Involved in Acute Ischemic Cerebral Injury Under Hyperhomocysteinemia, *Front Neurosci* **14** (**2020**) 582851.
[79] S.E. Ali, M.A. Farag, P. Holvoet, R.S. Hanafi, M.Z. Gad, A Comparative Metabolomics Approach Reveals Early Biomarkers for Metabolic Response to Acute Myocardial Infarction, *Sci Rep* **6** (**2016**) 36359.
[80] G. Aldini, A. Altomare, G. Baron, G. Vistoli, M. Carini, L. Borsani, F. Sergio, N-Acetylcysteine as an antioxidant and disulphide breaking agent: the reasons why, *Free Radic Res* **52**(7) (**2018**) 751-762.
[81] B. Pedre, U. Barayeu, D. Ezerina, T.P. Dick, The mechanism of action of N-acetylcysteine (NAC): The emerging role of H2S and sulfane sulfur species, *Pharmacol Ther* **228** (**2021**) 107916.
[82] A.R. Bourgonje, A.K. Offringa, L.E. van Eijk, A.E. Abdulle, J.L. Hillebrands, P.H.J. van der Voort, H. van Goor, E.J. van Hezik, N-Acetylcysteine and Hydrogen Sulfide in Coronavirus Disease 2019, *Antioxid Redox Signal* **35**(14) (**2021**) 1207-1225.
[83] E. Streeter, H.H. Ng, J.L. Hart, Hydrogen sulfide as a vasculoprotective factor, *Medical Gas Research* **3**(9) (**2013**).
[84] C.N. Hsu, Y.L. Tain, Preventing Developmental Origins of Cardiovascular Disease: Hydrogen Sulfide as a Potential Target?, *Antioxidants (Basel)* **10**(2) (**2021**) 247.
[85] J. Dai, X. Teng, S. Jin, Y. Wu, The Antiviral Roles of Hydrogen Sulfide by Blocking the Interaction between SARS-CoV-2 and Its Potential Cell Surface Receptors, *Oxid Med Cell Longev* **2021** (**2021**) 7866992.
[86] F. Gorini, S. Del Turco, L. Sabatino, M. Gaggini, C. Vassalle, H2S as a Bridge Linking Inflammation, Oxidative Stress and Endothelial Biology: A Possible Defense in the Fight against SARS-CoV-2 Infection?, *Biomedicines* **9**(9) (**2021**) 1107.
[87] G. Pozzi, E. Masselli, G. Gobbi, P. Mirandola, L. Taborda-Barata, L. Ampollini, P. Carbognani, C. Micheloni, F. Corazza, D. Galli, C. Carubbi, M. Vitale, Hydrogen Sulfide Inhibits TMPRSS2 in Human Airway Epithelial Cells: Implications for SARS-CoV-2 Infection, *Biomedicines* **9**(9) (**2021**) 1273.
[88] S.K. Jain, R. Bull, J.L. Rains, P.F. Bass, S.N. Levine, S. Reddy, R. McVie, J.A. BocchiniJr, Low Levels of Hydrogen Sulfide in the Blood of Diabetes Patients and Streptozotocin-Treated Rats Causes Vascular Inflammation?, *Antioxidants & Redox Signaling* **12**(11) (**2010**) 1333-1337.
[89] C. Szabo, Roles of hydrogen sulfide in the pathogenesis of diabetes mellitus and its complications, *Antioxid Redox Signal* **17**(1) (**2012**) 68-80.

[90] Y.M. Hao, D.W. He, Y. Gao, L.N. Fang, P.P. Zhang, K. Lu, R.Z. Lu, C. Li, Association of Hydrogen Sulfide with Femoral Bone Mineral Density in Osteoporosis Patients: A Preliminary Study, *Med Sci Monit* **27** (**2021**) e929389.
[91] M.M. Perry, B. Tildy, A. Papi, P. Casolari, G. Caramori, K.L. Rempel, A.J. Halayko, I. Adcock, K.F. Chung, The anti-proliferative and anti-inflammatory response of COPD airway smooth muscle cells to hydrogen sulfide, *Respir Res* **19**(1) (**2018**) 85.
[92] Y. Suzuki, J. Saito, M. Munakata, Y. Shibata, Hydrogen sulfide as a novel biomarker of asthma and chronic obstructive pulmonary disease, *Allergol Int* **70**(2) (**2021**) 181-189.
[93] S. Fiorucci, E. Distrutti, Targeting the transsulfuration-H2S pathway by FXR and GPBAR1 ligands in the treatment of portal hypertension, *Pharmacol Res* **111** (**2016**) 749-756.
[94] K.M. Holwerda, S.D. Burke, M.M. Faas, Z. Zsengeller, I.E. Stillman, P.M. Kang, H. van Goor, A. McCurley, I.Z. Jaffe, S.A. Karumanchi, A.T. Lely, Hydrogen sulfide attenuates sFlt1-induced hypertension and renal damage by upregulating vascular endothelial growth factor, *J Am Soc Nephrol* **25**(4) (**2014**) 717-725.
[95] H. van Goor, J.C. van den Born, J.L. Hillebrands, J.A. Joles, Hydrogen sulfide in hypertension, *Curr Opin Nephrol Hypertens* **25**(2) (**2016**) 107-113.
[96] L. Roubenne, R. Marthan, B. Le Grand, C. Guibert, Hydrogen Sulfide Metabolism and Pulmonary Hypertension, *Cells* **10**(6) (**2021**) 1477.
[97] K. Suzuki, G. Olah, K. Modis, C. Coletta, G. Kulp, D. Gero, P. Szoleczky, T. Chang, Z. Zhou, L. Wu, R. Wang, A. Papapetropoulos, C. Szabo, Hydrogen sulfide replacement therapy protects the vascular endothelium in hyperglycemia by preserving mitochondrial function, *Proc Natl Acad Sci U S A* **108**(33) (**2011**) 13829-13834.
[98] M. Medani, D. Collins, N.G. Docherty, A.W. Baird, P.R. O'Connell, D.C. Winter, Emerging role of hydrogen sulfide in colonic physiology and pathophysiology, *Inflamm Bowel Dis* **17**(7) (**2011**) 1620-1625.
[99] S.U.C. MD, H.-D. Eisner, G. Dusel, H.K. MD, W.S. MD, Antagonistic Effects of Sulfide and Butyrate on Proliferation of Colonic Mucosa, *Digestive diseases and sciences* **41**(12) (**1996**) 2477-2481.
[100] B.W. Perridon, H.G.D. Leuvenink, J.-L. Hillebrands, H.v. Goor, E.M. Bos, The role of hydrogen sulfide in aging and age-related pathologies, *Aging (Albany NY)* **8**(10) (**2016**) 2264–2289.
[101] A.S. Sokolov, P.V. Nekrasov, M.V. Shaposhnikov, A.A. Moskalev, Hydrogen sulfide in longevity and pathologies: Inconsistency is malodorous, *Ageing Res Rev* **67** (**2021**) 101262.
[102] M.S. Vandiver, B.D. Paul, R. Xu, S. Karuppagounder, F. Rao, A.M. Snowman, H.S. Ko, Y.I. Lee, V.L. Dawson, T.M. Dawson, N. Sen, S.H. Snyder, Sulfhydration mediates neuroprotective actions of parkin, *Nat Commun* **4** (**2013**) 1626.
[103] D. Giovinazzo, B. Bursac, J.I. Sbodio, S. Nalluru, T. Vignane, A.M. Snowman, L.M. Albacarys, T.W. Sedlak, R. Torregrossa, M. Whiteman, M.R. Filipovic, S.H. Snyder, B.D. Paul, Hydrogen sulfide is neuroprotective in Alzheimer's disease by sulfhydrating GSK3beta and inhibiting Tau hyperphosphorylation, *Proc Natl Acad Sci U S A* **118**(4) (**2021**) e2017225118.
[104] B.D. Paul, S.H. Snyder, Gasotransmitter hydrogen sulfide signaling in neuronal health and disease, *Biochem Pharmacol* **149** (**2018**) 101-109.
[105] X. Cao, L. Cao, L. Ding, J.S. Bian, A New Hope for a Devastating Disease: Hydrogen Sulfide in Parkinson's Disease, *Mol Neurobiol* **55**(5) (**2018**) 3789-3799.
[106] L. Liu, J. Wang, H. Wang, Hydrogen sulfide alleviates oxidative stress injury and reduces apoptosis induced by MPP(+) in Parkinson's disease cell model, *Mol Cell Biochem* **472**(1-2) (**2020**) 231-

240.
[107] X.Y. Hou, Z.L. Hu, D.Z. Zhang, W. Lu, J. Zhou, P.F. Wu, X.L. Guan, Q.Q. Han, S.L. Deng, H. Zhang, J.G. Chen, F. Wang, Rapid Antidepressant Effect of Hydrogen Sulfide: Evidence for Activation of mTORC1-TrkB-AMPA Receptor Pathways, *Antioxid Redox Signal* **27**(8) (**2017**) 472-488.
[108] Y.H. Chen, W.Z. Yao, B. Geng, Y.L. Ding, M. Lu, M.W. Zhao, C.S. Tang, Endogenous hydrogen sulfide in patients with COPD, *Chest* **128**(5) (**2005**) 3205-3211.
[109] J.L. M.D., C.J. Ellis, J.K.F. B.S., J.S. M.A., M.D.L. M.D., Fecal Hydrogen Sulfide Production in Ulcerative Colitis, *The American Journal of Gastroenterology* **93**(1) (**1998**) 83-87.
[110] F. L.Suarez, J. K.Furne, J. Springfield, M. D.Levitt, Bismuth Subsalicylate Markedly Decreases Hydrogen Sulfide Release in the Human Colon, *Gastroenterology* **114**(5) (**1998**) 923-929.
[111] K. Eto, T. Asada, K. Arima, T. Makifuchi, H. Kimura, Brain hydrogen sulfide is severely decreased in Alzheimer's disease, *Biochemical and Biophysical Research Communications* **293**(5) (**2002**) 1485-1488.
[112] R. Wang, Physiological implications of hydrogen sulfide: a whiff exploration that blossomed, *Physiol Rev* **92**(2) (**2012**) 791-896.
[113] M.C. Gruhlke, A.J. Slusarenko, The biology of reactive sulfur species (RSS), *Plant Physiol Biochem* **59** (**2012**) 98-107.
[114] A. Bilska-Wilkosz, M. Iciek, Reactive Sulfur Species (RSS) in Physiological and Pathological Conditions and in Therapy, *Antioxidants (Basel)* **11**(8) (**2022**) 1576.
[115] C. Szabo, Hydrogen sulphide and its therapeutic potential, *Nat Rev Drug Discov* **6**(11) (**2007**) 917-35.
[116] C.E. Paulsen, K.S. Carroll, Cysteine-mediated redox signaling: chemistry, biology, and tools for discovery, *Chem Rev* **113**(7) (**2013**) 4633-4679.
[117] A.M. Westley, J. Westley, Biological sulfane sulfur, *Analytical Biochemistry* **195**(1) (**1991**) 63-67.
[118] T.V. Mishanina, M. Libiad, R. Banerjee, Biogenesis of reactive sulfur species for signaling by hydrogen sulfide oxidation pathways, *Nat Chem Biol* **11**(7) (**2015**) 457-464.
[119] R. Greiner, Z. Palinkas, K. Basell, D. Becher, H. Antelmann, P. Nagy, T.P. Dick, Polysulfides link H2S to protein thiol oxidation, *Antioxid Redox Signal* **19**(15) (**2013**) 1749-1765.
[120] G.K. Kolluru, X. Shen, C.G. Kevil, Reactive Sulfur Species: A New Redox Player in Cardiovascular Pathophysiology, *Arterioscler Thromb Vasc Biol* **40**(4) (**2020**) 874-884.
[121] Z.Z. Xie, Y. Liu, J.S. Bian, Hydrogen Sulfide and Cellular Redox Homeostasis, *Oxid Med Cell Longev* **2016** (**2016**) 6043038.
[122] D. Benchoam, E. Cuevasanta, M.N. Moller, B. Alvarez, Hydrogen Sulfide and Persulfides Oxidation by Biologically Relevant Oxidizing Species, *Antioxidants (Basel)* **8**(2) (**2019**) 48.
[123] E. Cuevasanta, M.N. Moller, B. Alvarez, Biological chemistry of hydrogen sulfide and persulfides, *Arch Biochem Biophys* **617** (**2017**) 9-25.
[124] G.H. Kelsall, I. Thompson, Redox chemistry of H2S oxidation in the British Gas Stretford Process Part I: Thermodynamics of sulphur-water systems at 298 K, *Journal of Applied Electrochemistry* **23** (**1993**) 279–286.
[125] N. Lau, M.D. Pluth, Reactive sulfur species (RSS): persulfides, polysulfides, potential, and problems, *Curr Opin Chem Biol* **49** (**2019**) 1-8.
[126] T.S. Bailey, M.D. Pluth, Reactions of isolated persulfides provide insights into the interplay between H2S and persulfide reactivity, *Free Radic Biol Med* **89** (**2015**) 662-667.

[127] H. Kimura, Signaling molecules: hydrogen sulfide and polysulfide, *Antioxid Redox Signal* **22**(5) (**2015**) 362-376.
[128] H. Kimura, Hydrogen Sulfide (H2S) and Polysulfide (H2Sn) Signaling: The First 25 Years, *Biomolecules* **11**(6) (**2021**) 896.
[129] T. Ubuka, Assay methods and biological roles of labile sulfur in animal tissues, *Journal of Chromatography B* **781**(1-2) (**2002**) 227-249.
[130] G.K. Kolluru, X. Shen, S.C. Bir, C.G. Kevil, Hydrogen sulfide chemical biology: pathophysiological roles and detection, *Nitric Oxide* **35** (**2013**) 5-20.
[131] X.M. Xu, S.G. Moller, Iron-sulfur cluster biogenesis systems and their crosstalk, *Chembiochem* **9**(15) (**2008**) 2355-2362.
[132] W.H. Orme-Johnson, Iron-sulfur proteins: structure and function, *Annual Review of Biochemistry* **42**(1) (**1973**) 159-204.
[133] H. Ye, T.A. Rouault, Human iron-sulfur cluster assembly, cellular iron homeostasis, and disease, *Biochemistry* **49**(24) (**2010**) 4945-4956.
[134] D.C. Johnson, D.R. Dean, A.D. Smith, M.K. Johnson, Structure, function, and formation of biological iron-sulfur clusters, *Annu Rev Biochem* **74** (**2005**) 247-281.
[135] Y. Ogasawara, K. Ishii, T. Togawa, S. Tanabe, Determination of Bound Sulfur in Serum by Gas Dialysis/High-Performance Liquid Chromatography, *Analytical Biochemistry* **215**(1) (**1993**) 73-81.
[136] P.M. May, D. Batka, G. Hefter, E. Konigsberger, D. Rowland, Goodbye to S(2-) in aqueous solution, *Chem Commun (Camb)* **54**(16) (**2018**) 1980-1983.
[137] L. Rydz, M. Wrobel, H. Jurkowska, Sulfur Administration in Fe-S Cluster Homeostasis, *Antioxidants (Basel)* **10**(11) (**2021**) 1738.
[138] B.D. Paul, S.H. Snyder, H(2)S signalling through protein sulfhydration and beyond, *Nat Rev Mol Cell Biol* **13**(8) (**2012**) 499-507.
[139] K. Ono, T. Akaike, T. Sawa, Y. Kumagai, D.A. Wink, D.J. Tantillo, A.J. Hobbs, P. Nagy, M. Xian, J. Lin, J.M. Fukuto, Redox chemistry and chemical biology of H2S, hydropersulfides, and derived species: implications of their possible biological activity and utility, *Free Radic Biol Med* **77** (**2014**) 82-94.
[140] P. Nagy, Mechanistic chemical perspective of hydrogen sulfide signaling, *Methods Enzymol* **554** (**2015**) 3-29.
[141] O. Kabil, R. Banerjee, Redox biochemistry of hydrogen sulfide, *J Biol Chem* **285**(29) (**2010**) 21903-21907.
[142] E.B. Getz, M. Xiao, T. Chakrabart, R. Cooke, P.R. Selvin, A Comparison between the Sulfhydryl Reductants Tris(2-carboxyethyl)phosphine and Dithiothreitol for Use in Protein Biochemistry, *Analytical Biochemistry* **273**(1) (**1999**) 73-80.
[143] J.A. Burns, J.C. Butler, J. Moran, G.M. Whitesides, Selective reduction of disulfides by tris(2-carboxyethyl)phosphine, *The Journal of Organic Chemistry* **56**(8) (**2002**) 2648-2650.
[144] S. Rajpal, P. Katikaneni, M. Deshotels, S. Pardue, J. Glawe, X. Shen, N. Akkus, K. Modi, R. Bhandari, P. Dominic, P. Reddy, G.K. Kolluru, C.G. Kevil, Total sulfane sulfur bioavailability reflects ethnic and gender disparities in cardiovascular disease, *Redox Biol* **15** (**2018**) 480-489.
[145] U. Hannestad, S. Margheri, B. Sörbo, A sensitive gas chromatographic method for determination of protein-associated sulfur, *Anal Biochem* **178**(2) (**1989**) 394-398.
[146] J.L. Wallace, R. Wang, Hydrogen sulfide-based therapeutics: exploiting a unique but ubiquitous gasotransmitter, *Nat Rev Drug Discov* **14**(5) (**2015**) 329-345.

[147] T. Ubuka, T. Abe, R. Kajikawa, K. Morino, Determination of hydrogen sulfide and acid-labile sulfur in animal tissues by gas chromatography and ion chromatography, *Journal of Chromatography B: Biomedical Sciences and Applications* **757**(1) (**2001**) 31-37.
[148] J. Furne, A. Saeed, M.D. Levitt, Whole tissue hydrogen sulfide concentrations are orders of magnitude lower than presently accepted values, *Am J Physiol Regul Integr Comp Physiol* **295**(5) (**2008**) 1479-1485.
[149] M.D. Levitt, M.S. Abdel-Rehim, J. Furne, Free and acid-labile hydrogen sulfide concentrations in mouse tissues: anomalously high free hydrogen sulfide in aortic tissue, *Antioxid Redox Signal* **15**(2) (**2011**) 373-378.
[150] S. Kage, T. Nagata, K. Kudo, Determination of thiosulfate in body fluids by GC and GC/MS, *Journal of analytical toxicology* **15**(3) (**1991**) 148-150.
[151] R.r. Hyšpler, A. Tichá, M. Indrová, Z. Zadák, L. Hyšplerová, J. Gasparič, J. Churáček, A simple, optimized method for the determination of sulphide in whole blood by GC–MS as a marker of bowel fermentation processes, *Journal of Chromatography B* **770**(1-2) (**2002**) 255-259.
[152] O. McCook, P. Radermacher, C. Volani, P. Asfar, A. Ignatius, J. Kemmler, P. Moller, C. Szabo, M. Whiteman, M.E. Wood, R. Wang, M. Georgieff, U. Wachter, H2S during circulatory shock: some unresolved questions, *Nitric Oxide* **41** (**2014**) 48-61.
[153] V. Vitvitsky, R. Banerjee, H2S analysis in biological samples using gas chromatography with sulfur chemiluminescence detection, *Methods Enzymol* **554** (**2015**) 111-123.
[154] A. Kovatsis, M. Tsougas, Determination of hydrogen sulfide (H2S) in environment by indirect atomic absorption spectroscopy, *Bulletin of Environmental Contamination and Toxicology volume* **15** (**1976**) 412–420.
[155] E.A. Guenther, K.S. Johnson, K.H. Coale, Direct Ultraviolet Spectrophotometric Determination of Total Sulfide and Iodide in Natural Waters, *Analytical Chemistry* **73**(14) (**2001**) 3481–3487.
[156] D. Amilan Jose, N. Sharma, R. Sakla, R. Kaushik, S. Gadiyaram, Fluorescent nanoprobes for the sensing of gasotransmitters hydrogen sulfide (H2S), nitric oxide (NO) and carbon monoxide (CO), *Methods* **168** (**2019**) 62-75.
[157] B. Chen, W. Li, C. Lv, M. Zhao, H. Jin, H. Jin, J. Du, L. Zhang, X. Tang, Fluorescent probe for highly selective and sensitive detection of hydrogen sulfide in living cells and cardiac tissues, *Analyst* **138**(3) (**2013**) 946-951.
[158] W. Feng, B.W. Dymock, Fluorescent Probes for H2S Detection and Quantification, *Handb Exp Pharmacol* **230** (**2015**) 291-323.
[159] M.C. Hartman, M.M. Dcona, A new, highly water-soluble, fluorescent turn-on chemodosimeter for direct measurement of hydrogen sulfide in biological fluids, *Analyst* **137**(21) (**2012**) 4910-4912.
[160] N. Kumar, V. Bhalla, M. Kumar, Recent developments of fluorescent probes for the detection of gasotransmitters (NO, CO and H2S), *Coordination Chemistry Reviews* **257**(15-16) (**2013**) 2335-2347.
[161] B. Li, H. Mei, M. Wang, X. Gu, J. Hao, X. Xie, K. Xu, A near-infrared fluorescent probe for imaging of endogenous hydrogen sulfide in living cells and mice, *Dyes and Pigments* **189** (**2021**) 109231.
[162] C. Liu, J. Pan, S. Li, Y. Zhao, L.Y. Wu, C.E. Berkman, A.R. Whorton, M. Xian, Capture and visualization of hydrogen sulfide by a fluorescent probe, *Angew Chem Int Ed Engl* **50**(44) (**2011**) 10327-10329.
[163] Y. Luo, C. Zhu, D. Du, Y. Lin, A review of optical probes based on nanomaterials for the detection of hydrogen sulfide in biosystems, *Anal Chim Acta* **1061** (**2019**) 1-12.
[164] B. Peng, W. Chen, C. Liu, E.W. Rosser, A. Pacheco, Y. Zhao, H.C. Aguilar, M. Xian, Fluorescent

probes based on nucleophilic substitution-cyclization for hydrogen sulfide detection and bioimaging, *Chemistry* **20**(4) (**2014**) 1010-1016.
[165] Y. Qian, J. Karpus, O. Kabil, S.Y. Zhang, H.L. Zhu, R. Banerjee, J. Zhao, C. He, Selective fluorescent probes for live-cell monitoring of sulphide, *Nat Commun* **2** (**2011**) 495.
[166] K. Shimamoto, K. Hanaoka, Fluorescent probes for hydrogen sulfide (H2S) and sulfane sulfur and their applications to biological studies, *Nitric Oxide* **46** (**2015**) 72-79.
[167] W. Sun, J. Fan, C. Hu, J. Cao, H. Zhang, X. Xiong, J. Wang, S. Cui, S. Sun, X. Peng, A two-photon fluorescent probe with near-infrared emission for hydrogen sulfide imaging in biosystems, *Chem Commun (Camb)* **49**(37) (**2013**) 3890-3892.
[168] J.K. Fogo, M. Popowsky, Spectrophotometric Determination of Hydrogen Sulfide, *Analytical Chemistry* **21**(6) (**1949**) 732-734.
[169] L.M. Siegel, A Direct Microdetermination for Sulfide, *Analytical Biochemistry* **11** (**1965**) 126-132.
[170] S.E. Sheppard, A.L. Geddes, Effect of Solvents upon the Absorption Spectra of Dyes. IV. Water as Solvent: A Common Pattern, *Journal of the American Chemical Society* **66**(12) (**1944**) 1995–2002.
[171] M. Ishigami, K. Hiraki, K. Umemura, Y. Ogasawara, K. Ishii, H. Kimura, A source of hydrogen sulfide and a mechanism of its release in the brain, *Antioxid Redox Signal* **11**(2) (**2009**) 205-214.
[172] R. Pomeroy, The Determination of Sulphides in Sewage, *Sewage Works Journal* **8**(4) (**1936**) 572-591.
[173] S.U. Khan, G.F. Morris, M. Hidiroglou, Rapid Estimation of Sulfide in Rumen and Blood., *Microchemical Journal* **25** (**1980**) 388-395.
[174] H. Lindell, P. Jäppinen, H. Savolainen, Determination of sulphide in blood with an ion-selective electrode by pre-concentration of trapped sulphide in sodium hydroxide solution, *Analyst* **113**(5) (**1988**) 839-840.
[175] M.D. Brown, J.R. Hall, M.H. Schoenfisch, A direct and selective electrochemical hydrogen sulfide sensor, *Anal Chim Acta* **1045** (**2019**) 67-76.
[176] J.A. Velazquez-Moyado, A. Navarrete, The detection and quantification, in vivo and in real time, of hydrogen sulfide in ethanol-induced lesions in rat stomachs using an ion sensitive electrode, *J Pharmacol Toxicol Methods* **89** (**2018**) 54-58.
[177] T. Xu, N. Scafa, L.P. Xu, S. Zhou, K. Abdullah Al-Ghanem, S. Mahboob, B. Fugetsu, X. Zhang, Electrochemical hydrogen sulfide biosensors, *Analyst* **141**(4) (**2016**) 1185-1195.
[178] T. Ditroi, A. Nagy, D. Martinelli, A. Rosta, V. Kozich, P. Nagy, Comprehensive analysis of how experimental parameters affect H2S measurements by the monobromobimane method, *Free Radic Biol Med* **136** (**2019**) 146-158.
[179] S. Koike, K. Kawamura, Y. Kimura, N. Shibuya, H. Kimura, Y. Ogasawara, Analysis of endogenous H2S and H2Sn in mouse brain by high-performance liquid chromatography with fluorescence and tandem mass spectrometric detection, *Free Radic Biol Med* **113** (**2017**) 355-362.
[180] X. Shen, M. Carlstrom, S. Borniquel, C. Jadert, C.G. Kevil, J.O. Lundberg, Microbial regulation of host hydrogen sulfide bioavailability and metabolism, *Free Radic Biol Med* **60** (**2013**) 195-200.
[181] X. Shen, G.K. Kolluru, S. Yuan, C.G. Kevil, Measurement of H2S in vivo and in vitro by the monobromobimane method, *Methods Enzymol* **554** (**2015**) 31-45.
[182] X. Shen, C.B. Pattillo, S. Pardue, S.C. Bir, R. Wang, C.G. Kevil, Measurement of plasma hydrogen sulfide in vivo and in vitro, *Free Radic Biol Med* **50**(9) (**2011**) 1021-1031.
[183] X. Shen, E.A. Peter, S. Bir, R. Wang, C.G. Kevil, Analytical measurement of discrete hydrogen

sulfide pools in biological specimens, *Free Radic Biol Med* **52**(11-12) (**2012**) 2276-2283.
[184] X.X. Tan, K.Q. Lian, X. Li, N. Li, W. Wang, W.J. Kang, H.M. Shi, Development of a derivatization method for the quantification of hydrogen sulfide and its application in vascular calcification rats, *J Chromatogr B Analyt Technol Biomed Life Sci* **1055-1056** (**2017**) 8-14.
[185] E.A. Wintner, T.L. Deckwerth, W. Langston, A. Bengtsson, D. Leviten, P. Hill, M.A. Insko, R. Dumpit, E. VandenEkart, C.F. Toombs, C. Szabo, A monobromobimane-based assay to measure the pharmacokinetic profile of reactive sulphide species in blood, *Br J Pharmacol* **160**(4) (**2010**) 941-957.
[186] X. Shen, S. Chakraborty, T.R. Dugas, C.G. Kevil, Hydrogen sulfide measurement using sulfide dibimane: critical evaluation with electrospray ion trap mass spectrometry, *Nitric Oxide* **41** (**2014**) 97-104.
[187] B. Tan, S. Jin, J. Sun, Z. Gu, X. Sun, Y. Zhu, K. Huo, Z. Cao, P. Yang, X. Xin, X. Liu, L. Pan, F. Qiu, J. Jiang, Y. Jia, F. Ye, Y. Xie, Y.Z. Zhu, New method for quantification of gasotransmitter hydrogen sulfide in biological matrices by LC-MS/MS, *Sci Rep* **7** (**2017**) 46278.
[188] Z. Fang, G. Yue, J. Wang, F. Luo, L. Guo, B. Qiu, Z. Lin, Chemiluminescent sensor for hydrogen sulfide in rat brain microdialysis based on target-induced horseradish peroxidase deactivation, *Analytical Methods* **11**(24) (**2019**) 3085-3089.
[189] C.K. Nicholson, J.P. Lambert, J.D. Molkentin, J. Sadoshima, J.W. Calvert, Thioredoxin 1 is essential for sodium sulfide-mediated cardioprotection in the setting of heart failure, *Arterioscler Thromb Vasc Biol* **33**(4) (**2013**) 744-751.
[190] R. Kaushik, A. Ghosh, A. Singh, D.A. Jose, Colorimetric sensor for the detection of H2S and its application in molecular half-subtractor, *Anal Chim Acta* **1040** (**2018**) 177-186.
[191] X. Hu, H. Li, X. Zhang, Z. Chen, R. Zhao, N. Hou, J. Liu, L. Xun, H. Liu, Developing Polysulfide-Sensitive GFPs for Real-Time Analysis of Polysulfides in Live Cells and Subcellular Organelles, *Anal Chem* **91**(6) (**2019**) 3893-3901.
[192] H. Li, H. Liu, Z. Chen, R. Zhao, Q. Wang, M. Ran, Y. Xia, X. Hu, J. Liu, M. Xian, L. Xun, Using resonance synchronous spectroscopy to characterize the reactivity and electrophilicity of biologically relevant sulfane sulfur, *Redox Biol* **24** (**2019**) 101179.
[193] V. Bogdandi, T. Ida, T.R. Sutton, C. Bianco, T. Ditroi, G. Koster, H.A. Henthorn, M. Minnion, J.P. Toscano, A. van der Vliet, M.D. Pluth, M. Feelisch, J.M. Fukuto, T. Akaike, P. Nagy, Speciation of reactive sulfur species and their reactions with alkylating agents: do we have any clue about what is present inside the cell?, *Br J Pharmacol* **176**(4) (**2019**) 646-670.
[194] N.S. Lawrence, J. Davis, R.G. Compton, Analytical strategies for the detection of sulfide: a review, *Talanta* **52**(5) (**2000**) 771-784.
[195] M.N. Hughes, M.N. Centelles, K.P. Moore, Making and working with hydrogen sulfide: The chemistry and generation of hydrogen sulfide in vitro and its measurement in vivo: a review, *Free Radic Biol Med* **47**(10) (**2009**) 1346-1353.
[196] K.R. Olson, Is hydrogen sulfide a circulating "gasotransmitter" in vertebrate blood?, *Biochim Biophys Acta* **1787**(7) (**2009**) 856-863.
[197] N.L. Whitfield, E.L. Kreimier, F.C. Verdial, N. Skovgaard, K.R. Olson, Reappraisal of H2S/sulfide concentration in vertebrate blood and its potential significance in ischemic preconditioning and vascular signaling, *Am J Physiol Regul Integr Comp Physiol* **294**(6) (**2008**) 1930-1937.
[198] K.R. Olson, E.R. DeLeon, F. Liu, Controversies and conundrums in hydrogen sulfide biology, *Nitric Oxide* **41** (**2014**) 11-26.
[199] R. Wedmann, S. Bertlein, I. Macinkovic, S. Boltz, J. Miljkovic, L.E. Munoz, M. Herrmann, M.R.

Filipovic, Working with "H2S": facts and apparent artifacts, *Nitric Oxide* **41** (**2014**) 85-96.
[200] J.E. Doeller, T.S. Isbell, G. Benavides, J. Koenitzer, H. Patel, R.P. Patel, J.R. Lancaster, Jr., V.M. Darley-Usmar, D.W. Kraus, Polarographic measurement of hydrogen sulfide production and consumption by mammalian tissues, *Anal Biochem* **341**(1) (**2005**) 40-51.
[201] M. Pose, K.M. Dillon, A. Denicola, B. Alvarez, J.B. Matson, M.N. Moller, E. Cuevasanta, Fluorescent detection of hydrogen sulfide (H2S) through the formation of pyrene excimers enhances H2S quantification in biochemical systems, *J Biol Chem* (**2022**) 102402.
[202] R. Kaushik, P. Kumar, A. Ghosh, N. Gupta, D. Kaur, S. Arora, D.A. Jose, Alizarin red S–zinc(ii) fluorescent ensemble for selective detection of hydrogen sulphide and assay with an H2S donor, *RSC Advances* **5**(97) (**2015**) 79309-79316.
[203] K. Shigetoshi, T. Nagata, K. Kimura, K.J.J.o.F.S. Kudo, Extractive alkylation and gas chromatographic analysis of sulfide, **33**(1) (**1988**) 217-222.
[204] L.R. Goodwin, D. Francom, F.P. Dieken, J.D. Taylor, M.W. Warenycia, R.J. Reiffenstein, G. Dowling, Determination of Sulfide in Brain Tissue by Gas Dialysis/Ion Chromatography: Postmortem Studies and Two Case Reports *Journal of Analytical Toxicology* **13**(2) (**1989**) 105-109.
[205] C.J. Richardson, E.A.M. Magee, J.H. Cummings, A new method for the determination of sulphide in gastrointestinal contents and whole blood by microdistillation and ion chromatography, *Clinica Chimica Acta* **293**(1-2) (**2000**) 115-125.
[206] R. Karunya, K.S. Jayaprakash, R. Gaikwad, P. Sajeesh, K. Ramshad, K.M. Muraleedharan, M. Dixit, P.R. Thangaraj, A.K. Sen, Rapid measurement of hydrogen sulphide in human blood plasma using a microfluidic method, *Sci Rep* **9**(1) (**2019**) 3258.
[207] A. Tangerman, Measurement and biological significance of the volatile sulfur compounds hydrogen sulfide, methanethiol and dimethyl sulfide in various biological matrices, *J Chromatogr B Analyt Technol Biomed Life Sci* **877**(28) (**2009**) 3366-3377.
[208] G. Alberti, V.M. Nurchi, L.R. Magnaghi, R. Biesuz, A portable, disposable, and low-cost optode for sulphide and thiol detection, *Analytical Methods* **11**(35) (**2019**) 4464-4470.
[209] Y. Zhou, F. Mazur, K. Liang, R. Chandrawati, Sensitivity and Selectivity Analysis of Fluorescent Probes for Hydrogen Sulfide Detection, *Chem Asian J* **17**(5) (**2022**) e202101399.
[210] L.A. Montoya, T.F. Pearce, R.J. Hansen, L.N. Zakharov, M.D. Pluth, Development of selective colorimetric probes for hydrogen sulfide based on nucleophilic aromatic substitution, *J Org Chem* **78**(13) (**2013**) 6550-6557.
[211] H. Peng, Y. Cheng, C. Dai, A.L. King, B.L. Predmore, D.J. Lefer, B. Wang, A fluorescent probe for fast and quantitative detection of hydrogen sulfide in blood, *Angew Chem Int Ed Engl* **50**(41) (**2011**) 9672-9675.
[212] L. Li, M. Bhatia, Y.Z. Zhu, Y.C. Zhu, R.D. Ramnath, Z.J. Wang, F.B. Anuar, M. Whiteman, M. Salto-Tellez, P.K. Moore, Hydrogen sulfide is a novel mediator of lipopolysaccharide-induced inflammation in the mouse, *FASEB J* **19**(9) (**2005**) 1196-1198.
[213] R.C. Fahey, G.L. Newton, R. Dorian, E.M. Kosower, Analysis of Biological Thiols, *Analytical Biochemistry* **111** (**1981**) 357-365.
[214] G.L. Newton, R. Dorian, R.C. Fahey, Analysis of biological thiols: derivatization with monobromobimane and separation by reverse-phase high-performance liquid chromatography, *Analytical Biochemistry* **114**(2) (**1981**) 383-387.
[215] M. Shea, S. Howell, HPLC Measurement of Exogenous thiosulfate, *Analytical Biochemistry* **140**(2) (**1984**) 589-594.

[216] I.A. Cotgreave, P. Moldéus, Methodologies for the application of monobromobimane to the simultaneous analysis of soluble and protein thiol components of biological systems, *Journal of Biochemical and Biophysical Methods* **13**(4-5) (**1986**) 231-249.
[217] E. M.Kosower, N. S.Kosower, Bromobimane Probes for Thiols, *Methods in Enzymology* **251** (**1995**) 133-148.
[218] G.L. Newton, R.C. Fahey, Determination of biothiols by bromobimane labeling and high-performance liquid chromatography, *Methods in Enzymology* **251** (**1995**) 148-166.
[219] F. Sardi, B. Manta, S. Portillo-Ledesma, B. Knoops, M.A. Comini, G. Ferrer-Sueta, Determination of acidity and nucleophilicity in thiols by reaction with monobromobimane and fluorescence detection, *Anal Biochem* **435**(1) (**2013**) 74-82.
[220] X.H. Ju, S. Tang, Y. Jia, J. Guo, Y. Ding, Z. Song, Y. Zhao, Determination and characterization of cysteine, glutathione and phytochelatins (PC(2)(-)(6)) in Lolium perenne L. exposed to Cd stress under ambient and elevated carbon dioxide using HPLC with fluorescence detection, *J Chromatogr B Analyt Technol Biomed Life Sci* **879**(20) (**2011**) 1717-1724.
[221] T. Togawa, M. Ogawa, M. Nawata, Y. Ogasawara, K. Kawanabe, S. Tanabe, High performance liquid chromatographic determination of bound sulfide and sulfite and thiosulfate at their low levels in human serum by pre-column fluorescence derivatization with monobromobimane, *Chemical and pharmaceutical bulletin* **40**(11) (**1992**) 3000-3004.
[222] X. Shen, C.B. Pattillo, S. Pardue, S.C. Bir, R. Wang, C.G. Kevil, Fluorescent Detection and Optimization of Hydrogen Sulfide in Blood, *Free Radical Biology and Medicine* **49** (**2010**).
[223] T. Ida, T. Sawa, H. Ihara, Y. Tsuchiya, Y. Watanabe, Y. Kumagai, M. Suematsu, H. Motohashi, S. Fujii, T. Matsunaga, M. Yamamoto, K. Ono, N.O. Devarie-Baez, M. Xian, J.M. Fukuto, T. Akaike, Reactive cysteine persulfides and S-polythiolation regulate oxidative stress and redox signaling, *Proc Natl Acad Sci U S A* **111**(21) (**2014**) 7606.
[224] L.A. Montoya, X. Shen, J.J. McDermott, C.G. Kevil, M.D. Pluth, Mechanistic investigations reveal that dibromobimane extrudes sulfur from biological sulfhydryl sources other than hydrogen sulfidedaggerElectronic supplementary information (ESI) available: Experimental details, pH stability data for BTE, NMR spectra. See DOI: 10.1039/c4sc01875cClick here for additional data file, *Chem Sci* **6**(1) (**2015**) 294-300.
[225] A. Baniya, S. Thapa, E. Borquist, D. Bailey, D. Wood, J. Glawe, C. Kevil, L. Weiss, Lab-on-a-chip for hydrogen sulphide detection—Part I: Sulphide separation from plasma sample, *Medical Devices & Sensors* **2**(3-4) (**2019**) 10045.
[226] H. Ibrahim, A. Serag, M.A. Farag, Emerging analytical tools for the detection of the third gasotransmitter H2S, a comprehensive review, *J Adv Res* **27** (**2021**) 137-153.
[227] H. Malaeb, I. Choucair, Z. Wang, X.S. Li, L. Li, W.C. Boyd, C. Hine, W.H.W. Tang, V. Gogonea, S.L. Hazen, Stable isotope dilution mass spectrometry quantification of hydrogen sulfide and thiols in biological matrices, *Redox Biol* **55** (**2022**) 102401.
[228] S. Yuan, R.P. Patel, C.G. Kevil, Working with nitric oxide and hydrogen sulfide in biological systems, *Am J Physiol Lung Cell Mol Physiol* **308**(5) (**2015**) 403-415.
[229] P. Dominic, J. Ahmad, R. Bhandari, S. Pardue, J. Solorzano, K. Jaisingh, M. Watts, S.R. Bailey, A.W. Orr, C.G. Kevil, G.K. Kolluru, Decreased availability of nitric oxide and hydrogen sulfide is a hallmark of COVID-19, *Redox Biol* **43** (**2021**) 101982.
[230] T. Morikawa, M. Kajimura, T. Nakamura, T. Hishiki, T. Nakanishi, Y. Yukutake, Y. Nagahata, M. Ishikawa, K. Hattori, T. Takenouchi, T. Takahashi, I. Ishii, K. Matsubara, Y. Kabe, S. Uchiyama, E.

Nagata, M.M. Gadalla, S.H. Snyder, M. Suematsu, Hypoxic regulation of the cerebral microcirculation is mediated by a carbon monoxide-sensitive hydrogen sulfide pathway, *Proc Natl Acad Sci U S A* **109**(4) (**2012**) 1293-1298.
[231] L.A. Lan, S.Y. Wu, X.G. Meng, J.J. Jiang, M.Y. Zheng, G.R. Fan, A simple liquid chromatography tandem mass spectrometric method for fast detection of hydrogen sulfide based on thiolysis of 7-nitro-2, 1, 3-benzoxadiazole ether, *J Chromatogr A* **1625** (**2020**) 461243.
[232] D.Y. Lee, W.C. Huang, T.J. Gu, G.D. Chang, Quantitative and comparative liquid chromatography-electrospray ionization-mass spectrometry analyses of hydrogen sulfide and thiol metabolites derivaitized with 2-iodoacetanilide isotopologues, *J Chromatogr A* **1552** (**2018**) 43-52.
[233] H.M. Xiao, X. Wang, Q.L. Liao, S. Zhao, W.H. Huang, Y.Q. Feng, Sensitive analysis of multiple low-molecular-weight thiols in a single human cervical cancer cell by chemical derivatization-liquid chromatography-mass spectrometry, *Analyst* **144**(22) (**2019**) 6578-6585.
[234] B. Roda, N. Zhang, L. Gambari, B. Grigolo, C. Eller-Vainicher, L. Gennari, A. Zappi, S. Giordani, V. Marassi, A. Zattoni, P. Reschiglian, F. Grassi, Optimization of a Monobromobimane (MBB) Derivatization and RP-HPLC-FLD Detection Method for Sulfur Species Measurement in Human Serum after Sulfur Inhalation Treatment, *Antioxidants (Basel)* **11**(5) (**2022**) 939.
[235] Q2(R1) Guideline-validation of analytical procedures: text and methodology, (**2005**).
[236] M.D. Hartle, M.D. Pluth, A practical guide to working with H2S at the interface of chemistry and biology, *Chem Soc Rev* **45**(22) (**2016**) 6108-6117.
[237] E.M. Kosower, B. Pazhenchevsky, H. Dodiuk, H. Kanety, D. Faust, Bimanes. 6. Reactive halogen derivatives of syn- and anti-1,5-diazabicyclo[3.3.0]octadienediones (9,10-dioxabimanes), *The Journal of Organic Chemistry* **46**(8) (**1981**) 1666–1673.
[238] J. Zhang, Q. Yan, J. Liu, X. Lu, Y. Zhu, J. Wang, S. Wang, Study of the interaction between 5-sulfosalicylic acid and bovine serum albumin by fluorescence spectroscopy, *Journal of Luminescence* **134** (**2013**) 747-753.
[239] J.M. Green, Peer Reviewed: A Practical Guide to Analytical Method Validation, *Analytical Chemistry* **68**(9) (**1996**) 305A–309A.
[240] P. Zoonen, R. Hoogerbrugge, S.M. Gort, H.J.v.d. Wiel, H.A.v.t. Klooster, Some practical examples of method validation in the analytical laboratory, *TrAC Trends in Analytical Chemistry* **18**(9-10) (**1999**) 584-593.
[241] R. Boqué, A. Maroto, J. Riu, F.X. Rius, Validation of Analytical Methods, *Grasas y Aceites* **53**(1) (**2002**) 128-143.
[242] R. Bhagat, R. Saudagar, A Review on Analytical method Development and Validation, *Journal of Drug Delivery and Therapeutics* **9**(3-s) (**2019**) 1064-1067.
[243] N.C. van de Merbel, Quantitative determination of endogenous compounds in biological samples using chromatographic techniques, *TrAC Trends in Analytical Chemistry* **27**(10) (**2008**) 924-933.
[244] J. Peris-Vicente, J. Esteve-Romero, S. Carda-Broch, Validation of Analytical Methods Based on Chromatographic Techniques: An Overview, Analytical Separation Science2015, pp. 1757-1808.
[245] W. Parys, M. Dołowy, A. Pyka-Pająk, Significance of Chromatographic Techniques in Pharmaceutical Analysis, *Processes* **10**(1) (**2022**).
[246] J. Wisniak, A. Polishuk, Analysis of residuals — a useful tool for phase equilibrium data analysis, *Fluid Phase Equilibria* **164**(1) (**1999**) 61-82.
[247] S. Weisberg, Applied Linear Regression. 2nd. ed. New York, NY: John Wiley & Sons., (**1985**).
[248] B.G. Tabachnick, L.S. Fidell, Experimental design using ANOVA, (**2007**).

[249] J.C. Watkins, An Introduction to the Science of Statistics., (**2016**) pp 403-408.
[250] S. Lee, D.K. Lee, What is the proper way to apply the multiple comparison test?, *Korean J Anesthesiol* **71**(5) (**2018**) 353-360.
[251] R.G. Brereton, Chemometrics for pattern recognition, John Wiley & Sons2009.
[252] S. Mani, H. Li, A. Untereiner, L. Wu, G. Yang, R.C. Austin, J.G. Dickhout, S. Lhotak, Q.H. Meng, R. Wang, Decreased endogenous production of hydrogen sulfide accelerates atherosclerosis, *Circulation* **127**(25) (**2013**) 2523-2534.
[253] K. Suzuki, M. Sagara, C. Aoki, S. Tanaka, Y. Aso, Clinical Implication of Plasma Hydrogen Sulfide Levels in Japanese Patients with Type 2 Diabetes, *Intern Med* **56**(1) (**2017**) 17-21.
[254] A. Longchamp, M.R. MacArthur, K. Trocha, J. Ganahl, C.G. Mann, P. Kip, W.W. King, G. Sharma, M. Tao, S.J. Mitchell, T. Ditroi, J. Yang, P. Nagy, C.K. Ozaki, C. Hine, J.R. Mitchell, Plasma Hydrogen Sulfide Is Positively Associated With Post-operative Survival in Patients Undergoing Surgical Revascularization, *Front Cardiovasc Med* **8** (**2021**) 750926.
[255] L. Gambari, G. Lisignoli, L. Cattini, C. Manferdini, A. Facchini, F. Grassi, Sodium hydrosulfide inhibits the differentiation of osteoclast progenitor cells via NRF2-dependent mechanism, *Pharmacol Res* **87** (**2014**) 99-112.
[256] L. Gambari, B. Grigolo, F. Grassi, Hydrogen Sulfide in Bone Tissue Regeneration and Repair: State of the Art and New Perspectives, *Int J Mol Sci* **20**(20) (**2019**) 5231.
[257] L. Gambari, E. Amore, R. Raggio, W. Bonani, M. Barone, G. Lisignoli, B. Grigolo, A. Motta, F. Grassi, Hydrogen sulfide-releasing silk fibroin scaffold for bone tissue engineering, *Mater Sci Eng C Mater Biol Appl* **102** (**2019**) 471-482.
[258] J. Ma, C. Shi, Z. Liu, B. Han, L. Guo, L. Zhu, T. Ye, Hydrogen sulfide is a novel regulator implicated in glucocorticoidsinhibited bone formation, *Aging (Albany NY)* **11**(18) (**2019**) 7537–7552.
[259] F. Grassi, A.M. Tyagi, J.W. Calvert, L. Gambari, L.D. Walker, M. Yu, J. Robinson, J.Y. Li, G. Lisignoli, C. Vaccaro, J. Adams, R. Pacifici, Hydrogen Sulfide Is a Novel Regulator of Bone Formation Implicated in the Bone Loss Induced by Estrogen Deficiency, *J Bone Miner Res* **31**(5) (**2016**) 949-963.
[260] E.F. Burguera, A. Vela-Anero, L. Gato-Calvo, C. Vaamonde-Garcia, R. Meijide-Failde, F.J. Blanco, Hydrogen sulfide biosynthesis is impaired in the osteoarthritic joint, *Int J Biometeorol* **64**(6) (**2020**) 997-1010.
[261] D. Mancardi, C. Penna, A. Merlino, P. Del Soldato, D.A. Wink, P. Pagliaro, Physiological and pharmacological features of the novel gasotransmitter: hydrogen sulfide, *Biochim Biophys Acta* **1787**(7) (**2009**) 864-872.
[262] G. Caliendo, G. Cirino, V. Santagada, J.L. Wallace, Synthesis and biological effects of hydrogen sulfide (H2S): development of H2S-releasing drugs as pharmaceuticals, *J Med Chem* **53**(17) (**2010**) 6275-6286.
[263] W. Guo, Z.Y. Cheng, Y.Z. Zhu, Hydrogen sulfide and translational medicine, *Acta Pharmacol Sin* **34**(10) (**2013**) 1284-1291.
[264] V. Calderone, A. Martelli, L. Testai, V. Citi, M.C. Breschi, Using hydrogen sulfide to design and develop drugs, *Expert Opin Drug Discov* **11**(2) (**2016**) 163-175.
[265] C.R. Powell, K.M. Dillon, J.B. Matson, A review of hydrogen sulfide (H2S) donors: Chemistry and potential therapeutic applications, *Biochem Pharmacol* **149** (**2018**) 110-123.
[266] E. Magli, E. Perissutti, V. Santagada, G. Caliendo, A. Corvino, G. Esposito, G. Esposito, F. Fiorino, M. Migliaccio, A. Scognamiglio, B. Severino, R. Sparaco, F. Frecentese, H2S Donors and Their Use in Medicinal Chemistry, *Biomolecules* **11**(12) (**2021**) 1899.

[267] C. Szabo, A. Papapetropoulos, International Union of Basic and Clinical Pharmacology. CII: Pharmacological Modulation of H2S Levels: H2S Donors and H2S Biosynthesis Inhibitors, *Pharmacol Rev* **69**(4) (**2017**) 497-564.
[268] A. Liguori, E. Petri, C. Gualandi, L.S. Dolci, V. Marassi, M. Petretta, A. Zattoni, B. Roda, B. Grigolo, E. Olivotto, F. Grassi, M.L. Focarete, Controlled Release of H2S from Biomimetic Silk Fibroin–PLGA Multilayer Electrospun Scaffolds, *Biomacromolecules* (**2023**).
[269] D. Profrock, A. Prange, Inductively coupled plasma-mass spectrometry (ICP-MS) for quantitative analysis in environmental and life sciences: a review of challenges, solutions, and trends, *Appl Spectrosc* **66**(8) (**2012**) 843-68.
[270] G. Paris, A.L. Sessions, A.V. Subhas, J.F. Adkins, MC-ICP-MS measurement of δ34S and Δ33S in small amounts of dissolved sulfate, *Chemical Geology* **345** (**2013**) 50-61.
[271] Y. Zakon, L. Halicz, F. Gelman, Isotope analysis of sulfur, bromine, and chlorine in individual anionic species by ion chromatography/multicollector-ICPMS, *Anal Chem* **86**(13) (**2014**) 6495-6500.